ABSTRACT

Title of Thesis**:**	**Mechanical Properties of Human Tooth Enamel: Patient Age and Spatial Distribution.**
Author:	Saejin Park, Master of Science, 2008
Thesis directed by:	Dr. Dwayne D. Arola, Associate Professor Department of Mechanical Engineering, UMBC

In this study the influence of aging on the mechanical behavior of human enamel was evaluated using 3rd molars from young (18≤age≤30 years) and old (55≤age) patients. The elastic modulus and hardness were quantified using nanoindentation as a function of distance from the Dentin Enamel Junction (DEJ) and within three different regions of the crown (i.e. cervical, cuspal and inter-cuspal enamel). The apparent fracture toughness of human enamel was estimated using the indentation fracture resistance test. The hardness, elastic modulus and apparent fracture toughness were then used in estimating the brittleness according to a model that accounts for the competing dissipative processes of deformation and fracture. The brittleness of human enamel was compared to that of selected dental restorative materials (i.e. porcelain, ceramic and micaceous glass ceramic (MGC)) that are used for crown replacement.

Results of the evaluation showed that the elastic modulus and hardness increased with distance from the DEJ in the all three regions examined, regardless of patient age. The largest increases with distance from the DEJ occurred within the cervical region of the old enamel. Overall, the results showed that there were no age-dependent differences in the properties of enamel near the DEJ. However, near the tooth's surface both the hardness ($p<0.025$) and elastic modulus ($p<0.0001$) were significantly greater in the old enamel. At

the surface of the tooth, the average elastic modulus of “old” enamel was nearly 20% greater than that of the enamel from young patients. The apparent fracture toughness of the young and old enamel ranged from 0.74 to 0.92 $MPa*m^{0.5}$ and from 0.67 to 0.88 $MPa*m^{0.5}$, respectively. The old enamel had significantly lower toughness than the young enamel at the outer surface. The average brittleness of the young and old enamel increased with distance from the DEJ. For the old enamel the average brittleness increased from approximately 300 μm^{-1} at the DEJ to nearly 900 μm^{-1} at the occlusal surface. While there was no significant difference between the two age groups at the DEJ, the brittleness of the old enamel was significantly greater (and up to four times higher) than that of the young enamel near the occlusal surface. The brittleness numbers for the restorative materials were up to 90% lower than that of the old enamel at the occlusal surface. Based on results of this study, it was concluded that the brittleness index could serve as a useful scale in the design of materials used for crown replacement, as well as a quantitative tool for characterizing degradation in the mechanical behavior of enamel.

Mechanical Properties of Human Tooth Enamel: Patient Age and Spatial Distribution

By

Saejin Park

Thesis submitted to the Faculty of the Graduate School
of the University of Maryland in partial fulfillment
of the requirement for the degree of
Master of Science
2008

DEDICATION

To my mother and my family for their constant support

throughout my studies

ACKNOWLEDGEMENT

First, I need to express my sincere appreciation to Dr. Dwayne Arola for giving me this opportunity to explore human tooth enamel. Without his advice and guidance, there is no doubt that this study could not have been achieved successfully. Out of all my academic activities, this research and his valuable advice provided a special experience and it gave me new insight as to how to interpret scientific matters. Also, I really appreciate Dr. Akhtar Khan and Dr. L.D. Timmie Topoleski who served as my dissertation committee and gave valuable lectures while I was attending UMBC. I would also like to thank George Quinn from NIST for freely passing on his expertise concerning the fracture toughness of brittle materials. I would like to thank Mr. Chuck Smithson and Ms. Cindy Lutz for their support, as well.

Also, I need to address all the LAMP members (Ahmad, Alpay, Balaji, Brian, Devendra, Heon and Juliana). Through numerous technical discussions and everyday interactions with them, I had the opportunity to broaden my understanding of engineering a great deal, which helped me to understand many physical phenomena that I had previously ignored unconsciously. Most importantly, I have to give my gratitude to my mother and family members Andy, Hyejin and Leah for their constant support and sacrifice, both physically and mentally, to complete my masters degree. Lastly, I deeply want to express my gratitude to God for everything that I was able to accomplish.

Table of Contents

List of Tables

List of Figures

Chapter 1

Introduction

The structure and mechanical properties of human tooth enamel have been topics of scientific interest for some time, due to its unique characteristics and the oral conditions that it survives. Despite the current level of understanding, there are many issues related to the structure and mechanical behavior of this tissue that remain and need to be addressed.

1.1 Human Dentition

The human tooth is a complex structure of critical importance to our daily routine and existence. Its primary functions are not only limited to mastication and the contribution to digestion of food, but also to play a critical role in proper speech and aesthetics. The human tooth is subject to cyclic loading, wear and friction within a moisturized environment over a finite period of life. It undergoes two stages to achieve its fulfilled shape and function, which are the primary teeth stage (or baby teeth) and permanent teeth stage, respectively. The primary teeth usually emerge in children at the age of two or three

years old. There are 10 primary teeth each in the mandibular (lower) and maxillary (upper) arches. These teeth are replaced by the permanent teeth between 12 to 15 years old. There are 16 permanent teeth each in the mandibular (lower) and maxillary (upper) arches. The 16 teeth in each arch are composed of six molars, four premolars, two canines, and four incisors based on their shapes, position, and functions (Figure 1-1).

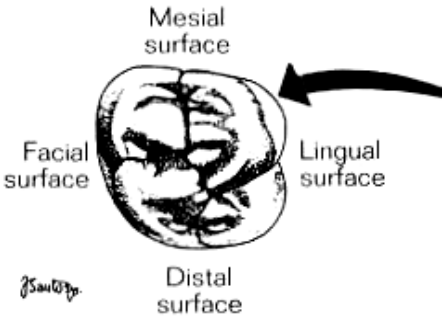

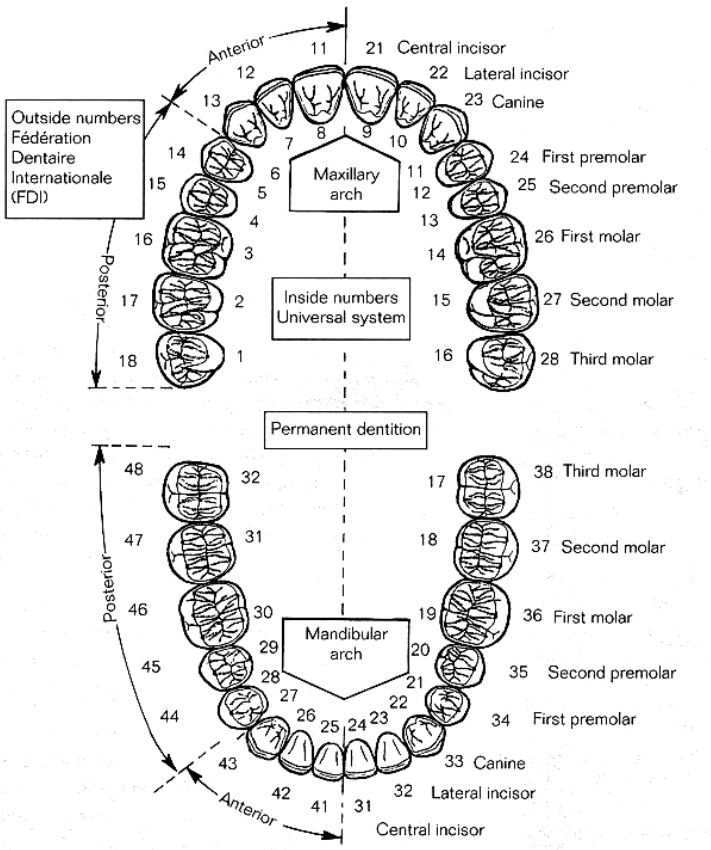

(a) **(b)**

Figure 1-1. Overview of the human dentition including the numbering system and corresponding nomenclature [Summitt *et al.*, 2001].

The geometry of a permanent tooth is described by five surfaces, which include the occlusal (top), facial, lingual, mesial and distal surfaces (Figure 1-1 a). The occlusal surface is actually the top surface (or biting surface) in posterior teeth. The facial surface is the outer surface facing toward the lip or cheeks and the lingual surface is the opposite side of the facial surface that is toward the tongue. The surface of the tooth that is facing

the midline is defined as the mesial surface, and the surface of the tooth that is facing away from the midline is called the distal surface.

1.2 The Microstructure of Human Teeth

Even though the teeth in each of the four aforementioned groups have their own shapes and functions, one thing common among all of them is that they are all comprised of the same constituents. The main components of the tooth include the enamel, dentin and pulp (or dental pulp) as shown in Figure 1-2. Enamel comprises the outermost shell of the tooth, and consists of hydroxyapatite crystals arranged in prismatic rods that are surrounded by an organic sheath. The main components of the enamel are approximately 96% inorganic (mineralized) substances by weight, with the remainder comprised of organic materials and water [Ten Cate, 1998]. Enamel is the hardest and most mineralized tissue in the human body and serves as a protective shell that covers the dentin and other components. Since it is located on the outer surface of the tooth and is the primary material involved in the mastication of food, the enamel is subjected to cyclic loading and may undergo progressive wear or even permanent scratching. Dentin resides beneath the enamel and serves as an elastic foundation as well as a protective enclosure for the pulp. Dentin occupies the majority of the human tooth by both weight and volume. Similar to enamel, dentin is composed of organic and inorganic substances, but in different ratios. Dentin is comprised of 65 ~ 70% mineralized materials (mainly calcium hydroxyl apatite), 20 ~ 25% organic materials (mainly collagen), with the remainder being water and other liquids [Ten Cate, 1998]. Dentin has three major structural forms, including the peritubular dentin, intertubular dentin and tubules. The dentin tubules extend outward from the pulp to the DEJ and it is believed that all nutrients are transferred through these tubules.

The pulp is a living soft, gelatinous tissue, which develops from the connective tissue of the dental papilla. It is surrounded by dentin and the main functions of the pulp are to provide all nutrients and water to the tooth and to keep the tooth in a hydrated state. Since both the nerves and blood supply pass through the pulp, it makes the tooth sensitive to both mechanical and thermal stimuli [Gartner 1999].

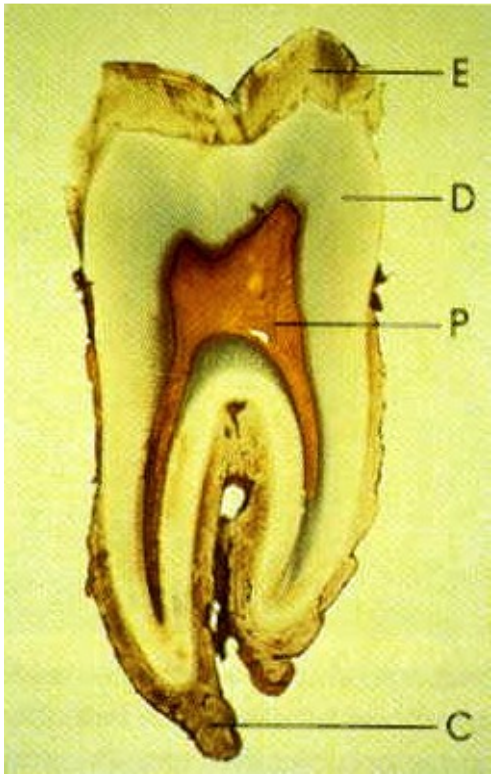

Figure 1-2. Overview of the longitudinally sectioned molar with nomenclatures [Ten Cate, 1998].

1.3 Caries and Restorative Dentistry

There are many diseases and oral conditions that can lead to a toothache, unattractive teeth or bad breath. According to modern dentistry, the majority of dental diseases are caused by bacteria that live in the mouth. Among these dental diseases, caries, which is commonly known as tooth decay, is the most common disease in or on the tooth. Many treatment

methods and restorative materials have been developed to treat tooth decay and to restore full oral function to the tooth (Figure 1-3). Bacteria that collect and survive on the surface of teeth secrete an acid that causes demineralization of the hard tissue, eventually, and tooth decay [Ten Cate, 1998]. The tooth decay usually emerges from the outer enamel surface, but sometimes it emerges from the pulp. More specifically, most tooth decay initiates in pits and grooves on occlusal surfaces of the posterior teeth. The only way for treating tooth decay is to remove the affected region in the tooth physically. In general, the average dentist removes decayed tissue by using high speed and low speed burs and using these burs introduces either flaws or micro cracks. Once flaws or micro cracks are induced, they may undergo propagation due to biting (cyclic loading) and the restored tooth may need further restorative treatment or complete extraction.

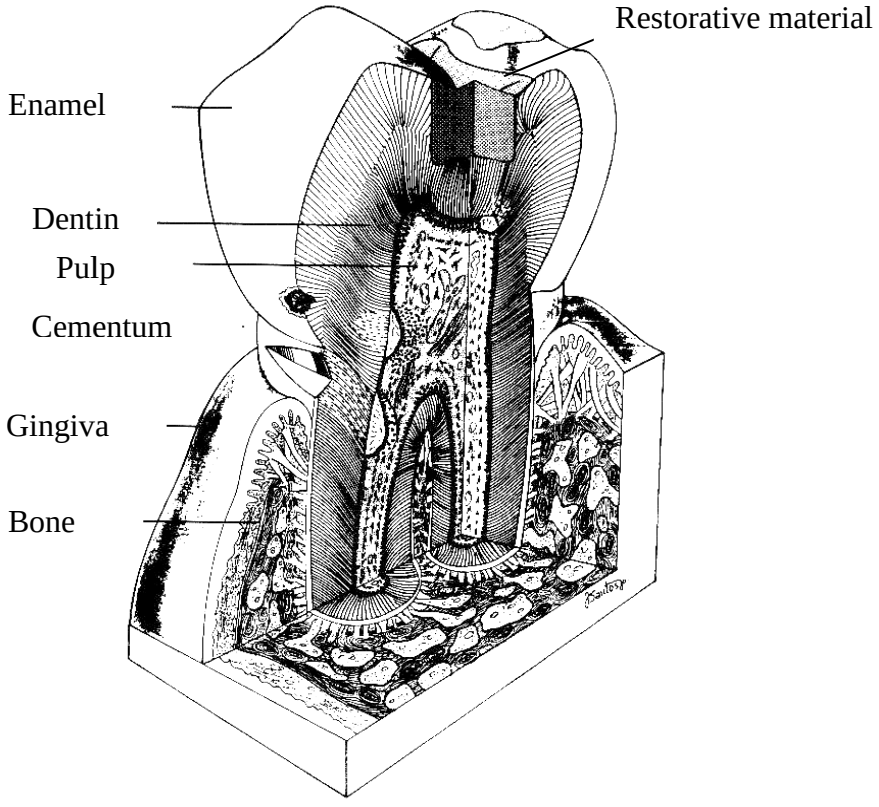

Figure 1-3. Primary tissues, and supporting structure of a restored human tooth [Summitt *et al.*, 2001].

From ancient history, humans have used several materials to replace decayed or damaged teeth, such as wood, gold and teeth or bones of animals. Today, there are two primary replacement materials available, including amalgam and composite resin materials (or polymers). These materials have advantages and disadvantages when used in restoring teeth. Traditionally, the amalgam alloy is the most commonly available restorative material. The amalgam alloy is mainly made by mixing liquid mercury with alloy particles of copper, silver, zinc, tin and other metallic materials [Craig 1996]. It has been used for around 150 years to replace teeth. Its main advantages are that it is easy to process into a prepared cavity, is relatively inexpensive, is durable, and has reasonable resistance to thermal or mechanical degradation posed by the oral environment. However, although amalgam has been used for long time and has numerous advantages, it brought about a health concern due to its mercury content. The primary drawback of amalgam alloys is its metallic color, which limits its application to either premolars or molars. Based on these drawbacks, nowadays composite resin materials have widely replaced amalgam alloys. As a matter of fact, natural resins from trees and other plants were widely used for dental applications a long time ago. Most current composite restoratives are synthetic materials (normally acrylic polymers). Its main constituents include a mixture of polymerized thermosetting resins and reinforcement particles [Craig 1996]. The most attractive advantage of the composite restoratives is aesthetics, as they match individual tooth color quite easily. Another advantage of composite materials is that they may be bonded to dentin and enamel, which provides reinforcement to the tooth; a feature not achieved with amalgam restorations. The main drawbacks of composite restoratives are high polymerization shrinkage and thermal property mismatch with the surrounding tooth structure [Robert, 1996]. This difference sometimes causes an interfacial gap to develop between the tooth and the restoratives, which may result in recurrent decay. Potentially,

high polymerization shrinkage and thermal property disparity between human tooth and the restorative materials may cause residual stress to develop. Figure 1-4 illustrates the potentially possible modes of fracture experienced by the teeth restored with resin composites. The shrinkage or contracting force in Figure 1.4 delineates the functional failure of human enamel in cuspal areas.

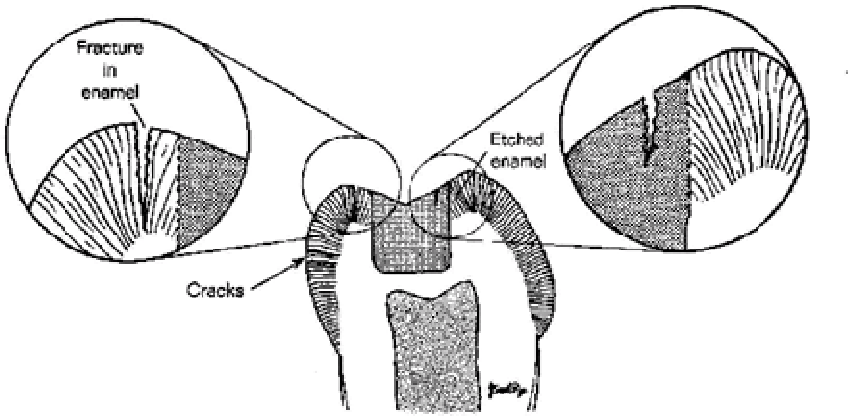

Figure 1-4. Polymerization shrinkage and thermal dimensional change cause cracks in either enamel or dentin as well as in the restoratives [Schwartz *et al*., 1996].

1.4 Restoratives Failures and Aging

As mentioned previously, most restorative dental materials have advantages and disadvantages and partial and full-coverage restorations (inlay/onlay or crowns) are mainly made out of ceramics. These ceramic materials are engineered to have elastic modulus, hardness and fracture toughness similar to that of enamel, but their mechanical properties are not exactly the same as that of the human tooth. Flaws (or micro cracks) induced during cavity preparation or the property disparity between human tooth enamel and the restorative dental materials can result in restored tooth failure or tooth fracture. Several examples of cracks and tooth fracture are presented in Figure 1-5 (a) and (b). In spite of tremendous advances in restorative materials, the failure of restored teeth is still one of the

major problems. Based on these problems, most dentists spend the majority of their clinical time repairing or replacing damaged restored teeth.

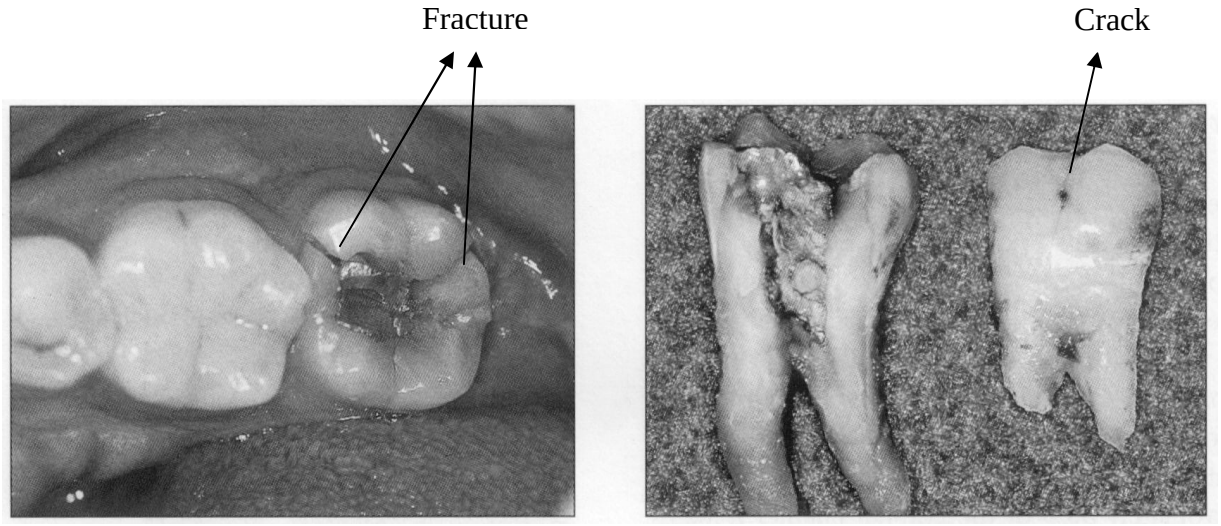

Figure 1-5. Typical cracks and tooth fracture in molars: initially, cracks or flaws were initiated during cavity preparation and they were propagated by biting (cyclic loading) [Schwartz, 1996].

A study by Moore and Stewart [1967] reported that most dentists in the United States expend approximately 40% of their clinical time repairing restorations. Similarly, Wilson *et al.* [1997] showed that over 60% of dental related clinicians in United Kingdom spend most of their clinical time repairing or replacing previously restored teeth. White *et al.* [1996] showed that more than 50% of restored teeth failed due to fracture or crack propagation. Also, several studies evaluated the longevity of restorations. Elderton [1976] reported that approximately half of amalgam restorations were failed within eight to ten years of their applications.

Restored teeth are normally replaced due to a number of factors, including recurring decay, debonding, bulk or cusp fracture, or marginal deterioration [Wilson *et al*., 1997]. Talim

and Gohil [1974] classified tooth fractures into four groups [Table 1-1]. In senior patients restored tooth fracture is not only one of the most common oral problems along with recurrent decay, but sometimes it also requires complete tooth extraction.

Table 1-1. Classification of tooth fracture types [Talim and Gohil, 1974].

Class	Types of Fractures
Class I	Fracture on Enamel
Class II	Fracture on Enamel and Dentin except Pulp
Class III	Fracture on Enamel, Dentin, and Pulp
Class IV	Fracture of Roots

There are largely two causes proposed as explanations for the primary cause of tooth fracture. That is, the removal of large tooth portions, such as the root canal treatment or large cavity preparation can reduce the structural integrity in a tooth. Tidmarsh [1976] verified the proportional relationship of the amount of main tooth structure removed to its mechanical deformation. From his research, it was found that the removal of a large portion of a tooth can cause considerable deformation or fracture under relatively small loads. Other research by Sedgley *et al*. [1992] demonstrated that the additional removal of tooth structures in order to repair the previously restored tooth leads to a greater susceptibility to tooth fracture. The second potential cause of tooth fracture is the different moisture and nutrient levels in a restored tooth, compared to that in a healthy tooth. It is well known that the pulp and dentin are the primary conduits for transferring all nutrients and water to tooth. If the pulp or dentin is damaged severely, for example removing large

portions of dentin and enamel, the tooth can no longer maintain the same levels of moisture and nutrient supply as a healthy tooth. Although the primary causes of restoration failure are not completely understood, some studies have investigated the contributions of physiological factors and function on the tooth failures. Arola *et al.* [2002] launched several studies, beginning with a study on cyclic crack growth in dentin and continuing with a study on restored tooth fractures, and evaluated the fatigue life of human dentin. His studies proved that subsurface flaws or cracks introduced during cavity preparations may causes restored tooth failure within five years. As life expectancies increase, people invest lots of time and money to maintain healthy oral conditions (Figure 1-6) and nowadays, implants and full coverage restorations are very popular and they are more common amongst seniors. Moreover, it is well known that the physical properties of most hard tissues undergo changes with aging.

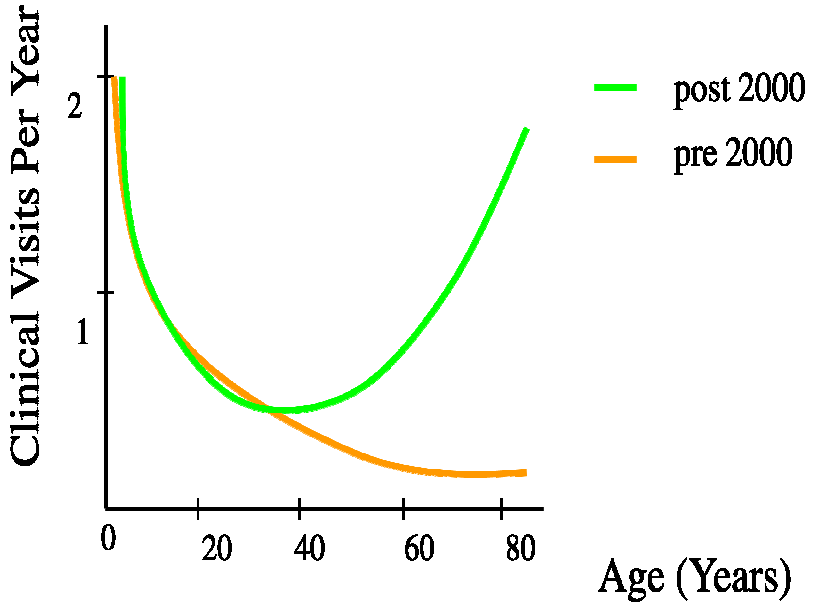

Figure 1-6. Increasing trends of the numbers of clinical visits in senior groups per year [Tinker, 2003; Berkey *et al.*, 2003].

Recently, numerous investigations have been conducted to evaluate the aging effects on the tooth tissues. For instance, in human dentin the mineral content increases with patient age due to the deposit of mineral salts with the tubule lumens [Ten Cate, 1998]. Arola and Reprogel [2005] evaluated the flexural modulus, energy to fracture and flexural strength in dentin as a function of age. They found that there was a significant reduction in strength and energy to fracture of dentin with patient age.

Unfortunately, very little knowledge has been obtained to explain the physical behavior of human enamel in terms of the aging effect. Since enamel is a very thin hard tissue - the maximum thickness is approximately 2 mm – there are inherent difficulties to evaluate the mechanical behaviors of this hard tissue. But, many studies have reported the physical properties of enamel using indentation techniques. He *et al*. [2007] evaluated the mechanical behavior of mature human enamel, including as sound, dehydrated, re-hydrated, dry and burnt. Also, Ge *et al*. [2004] reported the property variations in the prism (hydroxyapatite crystals) and the organic sheath within enamel by nanoindentation. Many other studies have investigated the mechanical properties of enamel. However, none of these studies considered the effects of aging on properties of enamel.

As previously mentioned, implants and full coverage restorations are very prevalent dental treatments for replacing or repairing restored teeth. They are found more commonly among senior patient groups due to the fact that the available tooth volume has been very limited by multiple restorations. Although these restored teeth may function properly themselves, the adjacent or opposing teeth may undergo functional failure by deformation or fracture through damage induced by contacting the engineered restorative materials. This mechanical disparity between aging enamel and the restorative materials could facilitate

catastrophic functional failures eventually. However, the degree of property disparity resulting from aging and its potential effects on the survival of human tooth enamel has not been studied.

1.5 Objectives

The overall objective of this research is to extend our current understanding of the mechanical properties of human tooth enamel. Many researchers have explored the mechanical properties of human tooth enamel, including elastic modulus, hardness and fracture toughness. However, most of these studies did not consider the effects of aging and spatial distribution. The current study addresses the importance of patient age and physiological processes on the mechanical behavior of enamel and its response to contact loads.

The specific aims of this research are to:

1) Evaluate the spatial distribution in the elastic modulus and hardness of human tooth enamel for young and old patients using nanoindentation approaches.

2) Evaluate the indentation size effects and indentation fracture resistance of young and old enamel using microindentation approaches.

3) Determine the brittleness of human enamel as a function of patient age and compare that with estimates of the brittleness for common dental materials used for replacement of enamel.

Chapter 2

Literature Survey

The failure of restored teeth due to fractures of the dental material or hard tissue has become one of the major oral health concerns in modern dentistry. To address this concern, the structure and mechanical behavior of human tooth enamel has been evaluated extensively to understand its functional limits. An understanding of the physical and mechanical behavior of enamel could provide crucial information needed to improve existing, or develop new dental restorative materials, as well as to help prevent catastrophic tooth failure.

2.1 Structure of Enamel

As described previously in Chapter 1, the tooth is composed of three primary tissues, including the enamel, dentin and pulp. Macroscopically, enamel comprises the outer shell and covers dentin, which serves as an elastic foundation. Enamel mainly consists of

carbonated hydroxyapatite crystals organized in a framework of prisms, and organic substances surrounding each prism (Figure 2-1). Overall, enamel is comprised of 96% mineralized material by weight, with the remaining 4% comprised of organic materials and bound water [Gartner, 1999]. Although enamel does not have uniform composition, its basic structure repeats in space over the entire volume as evident in Figure 2-1.

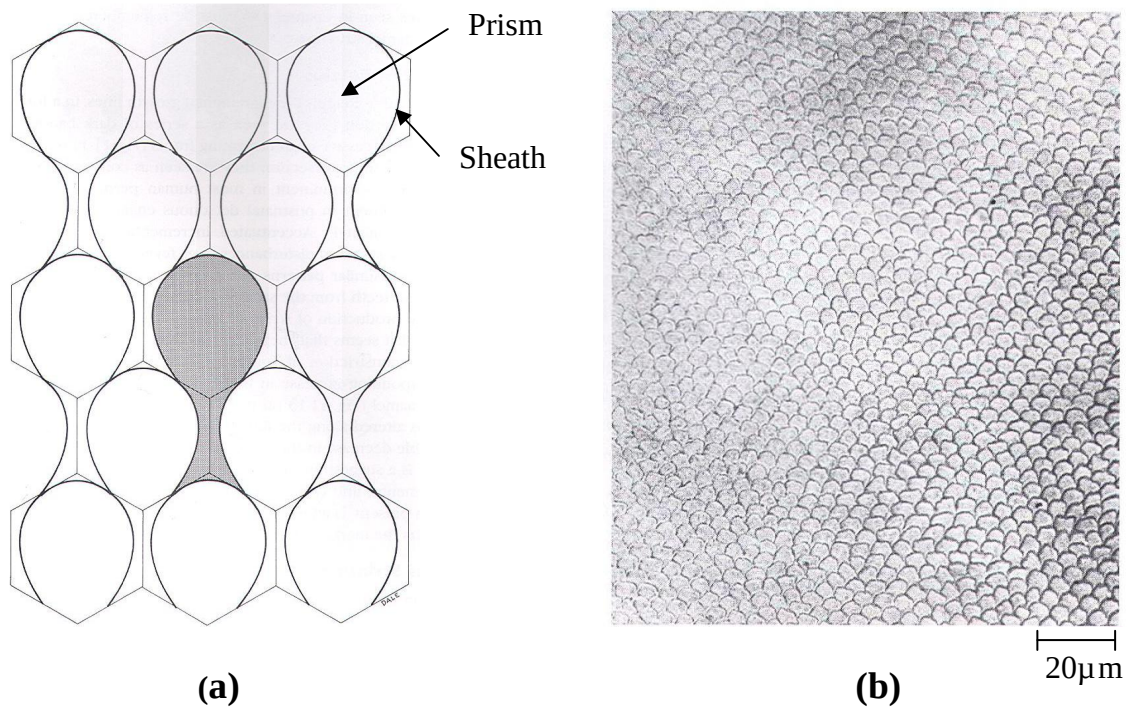

Figure 2-1. (a) Schematic drawing of prisms and the organic sheath that encases the prisms. (b) Image of enamel. Prism rods are clearly shown, which are surrounded by organic sheaths [Ten Cate, 1998].

There are two primary stages involved in the development of fully matured enamel, which includes secretion and maturation. In the secretion stage, a single and large cell process, called "Tomes' processes" is developed by the ameloblasts at their apical surface [Ten Cate, 1998]. This is a vital process for both prism (hydroxyapatite crystal) and organic sheath formation. Tomes' processes consist of two primary surfaces; that is, secretary and nonsecretary surfaces, respectively. Most prisms are formed in secretary surfaces, whereas

organic sheaths are developed in nonsecretary surfaces. After completing its secretary activities, the secretion stage is replaced by the maturation stage. There, the ameloblasts undergo continuous cytological changes in preparation for enamel maturation. During the maturation stage, matrix degradation occurs and compositional replacement by tissue fluid increases. Finally, most of the matrix (specifically the amelogenins) and the fluid are replaced gradually and the mineral content increases while ameloblasts continue to secrete proteins in this period to complete enamel formation [Ten Cate, 1998].

2.1.1 Enamel Rods

The primary component of enamel is the prismatic rods (or enamel prisms). The enamel prisms are comprised of *carbonated hydroxyapatite* crystallites, and have an effective diameter of approximately 4~5 μm [Gartner, 1999]. The hydroxyapatite crystals produced by ameloblasts form into the prismatic structure, which extends from the dentin-enamel junction (DEJ) to the occlusal surface. A schematic of their course is shown in Figure 2-2.

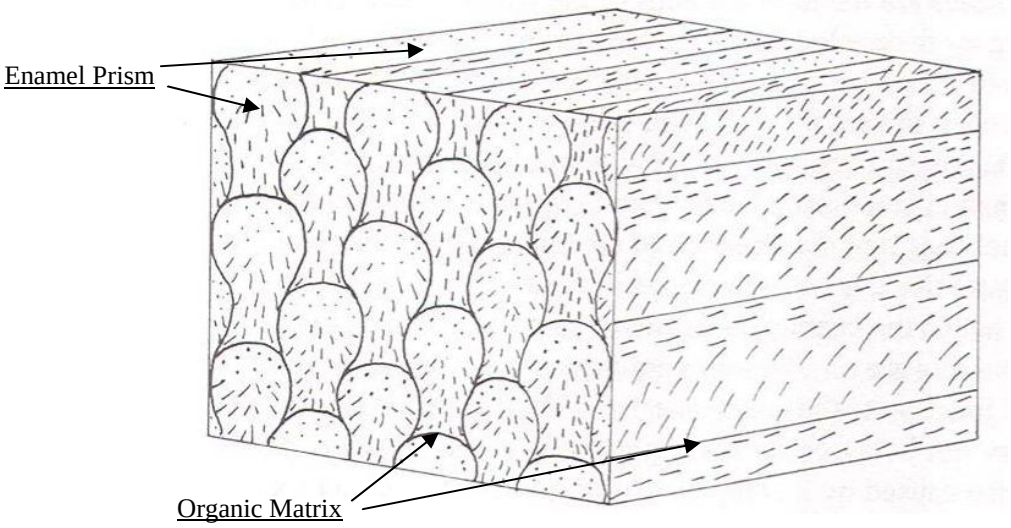

Figure 2-2. Structural morphology of enamel prism and organic matrix [Gartner, 1999].

Each prismatic rod is surrounded by organic material. The shape of the prism is similar to a 'keyhole or fish scale shape' [Gartner, 1999]. The prisms are tightly packed together and, although they extend nominally perpendicular to the dentin-enamel junction (DEJ), the prism arrangement is very complex and still not understood completely. Enamel prisms are parallel more or less, but they are tangled with each other or contorted in some regions as shown in Figure 2-3. It is understood that the path deviation of each prism at different levels in enamel results in a disarray of enamel rods [He *et al*., 2007]. The geometric structure of the enamel prisms is believed to prevent damage or failure under most loading conditions. Separated prismatic rods retard crack extension because this discontinuity creates distinct dimensional cleavage planes that will prevent crack propagation from advancing straight through the enamel, thereby enabling macro mechanical failure.

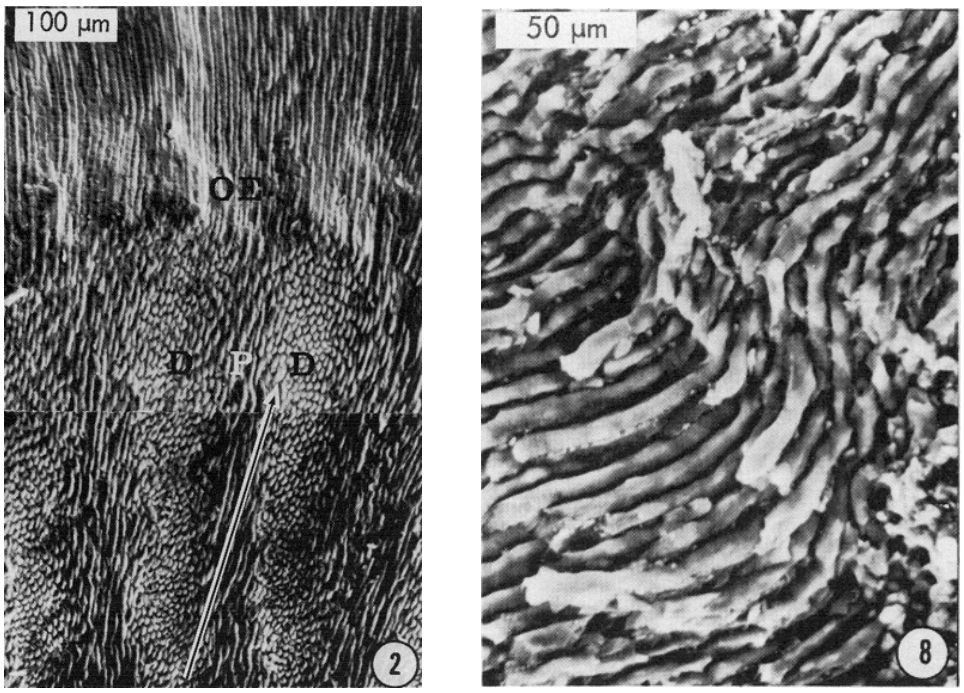

(a) **(b)**

Figure 2-3. SEM image of etched enamel: Clearly shown here are enamel prisms, which are tangled and contorted around each other [Ziedonis Skobe and Samuel Stern, 1980].

The organic sheath functions as an impact absorber and enables a small degree of relative movement between each rod. As such, the entanglement of prisms increases the structural integrity of enamel overall. Crack propagation could be retarded in enamel due to changes in the apparent loading direction with respect to the enamel prism orientation and the entwined ligaments [He, 2007]. Based on these features, many scientists are examining the importance of this structure and contributions of the interprismatic material on the mechanical behavior of enamel.

2.1.2 Organic Matrix (Organic Sheaths)

The organic sheath encircles each prism and is mainly comprised of proteins. These proteins consist of high molecular weight glycoproteins, enamelin, amelogenin, amelin and tuftelin [Gartner, 1999]. Even though the organic sheath and water are very minor parts of the enamel (typically less than 4% by weight), they play a key role in keeping the enamel hydrated. Recently, there has been some concentration on characterizing properties of the sheath. It is understood that the organic sheath behaves as a 'cement' to bond each prism and in 'load bearing' to transfer load between each prism. Another main characteristic of the organic sheath is its permeability, which enables water and ions to flow freely and to maintain the appropriate degree of compressibility and ionic conductivity [Waters, 1980].

2.1.3 Enamel Surface

Newly emerged teeth are coated by the primary enamel cuticle (or Nasmyth's membrane), which is a basal type lamina material produced by postameloblast [Ten Cate, 1998]. As the name implies, postameloblast is an ameloblast that completes two primary functions; secretion and mineralization for the formation and maturation of enamel structure. Due to

the friction of biting or brushing, the primary enamel cuticle is lost. However, the pellicle, which is made out of substances in saliva and food, is another constituent that covers the enamel. Similar to the primary enamel cuticle, the pellicle is worn off easily by brushing and flossing, otherwise it would turn into dental calculus [Gartner, 1999]. Several formations influence the characteristics of the enamel surface in erupted teeth, and among them the Striae of Retzuis and Perikymata are two primary formations that are of relevance in this regard.

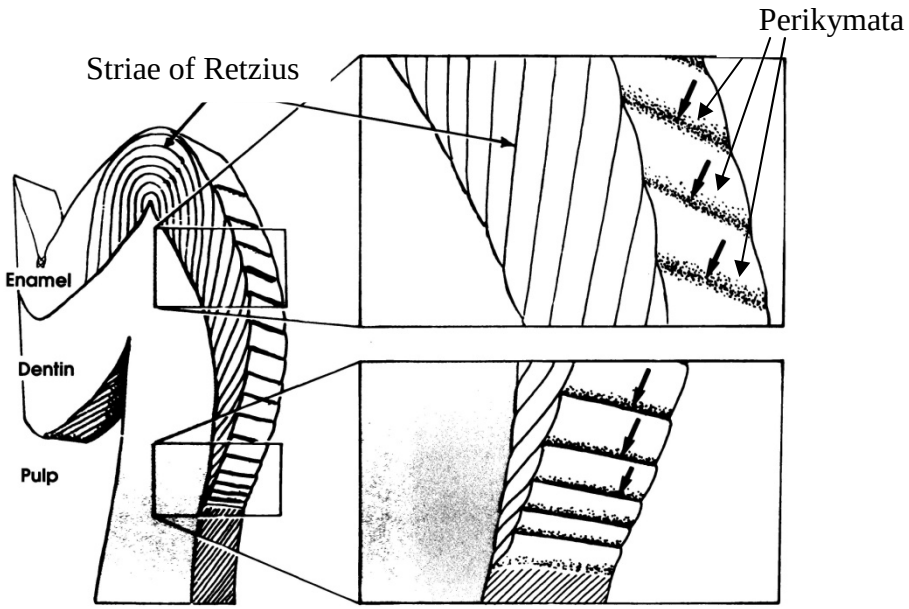

Figure 2-4. Schematic drawing of the striae of Retzius and surface Perikymata [Ten Cate, 1998].

The Striae of Retzius extends up to the enamel surface (Figure 2-4) and at the surface, each end of the Striae of Retzius is smoothed by Perikymata in shallow furrows [Gartner, 1999]. The Striae of Retzius is comprised of numerous series of rod segments and subsequent growth lines, which mostly run from the DEJ to the outer enamel surface. Their presence divides the enamel into compartments. Consequently, the Striae of Retzius may have the capability of arresting or minimizing mechanical failures by localizing damage within a module.

2.2 Mechanical Properties of Enamel

Due to its microstructure, enamel is a natural composite material. In general, a structural composite is a material system that is made of more than one component, which typically includes the reinforcement and the matrix, respectively. The reinforcement is usually either a high strength fiber or particle, such as carbon, glass or boron, while the matrix that is less stiff and weaker than the reinforcement. For example, in fiber reinforced plastics, the matrix is polymeric. Similar to common composites, the structure of enamel is akin to the structure of composite materials. That is, the prismatic rod serves as the primary reinforcement and the organic material surrounding the prism functions as the matrix. Also, unlike other calcified skeletal structures, fracture or damage of dental enamel is not repairable because it is a nonvital tissue.

The mechanical properties of enamel have been studied for almost a century as they are important to dentistry and provide inspiration for the design of engineering materials.

In describing the mechanical behavior of this hard tissue, the hardness, elastic modulus and fracture toughness have both physical significance and direct clinical relevance. Due to the limited volume of tissue available for examination, mechanical properties of enamel have been primarily evaluated using indentation methods. Also, in spite of tremendous work on enamel, the results of mechanical properties of enamel in the published literature are inconsistent. This may be attributed to the facts that enamel has a very complex structure and the properties are a function of location. Also, different testing methodologies, loading type, prism orientation, or physiology may be other factors that cause this inconsistency.

2.2.1 Hardness

Hardness represents a measure of a material's resistance to permanent deformation or "penetration" under a contact load. Therefore, it is one of the fundamental properties used in characterizing enamel. A material's hardness is usually measured by a characteristic of indentation shape, such as diagonal length of indentation or indentation depth under the applied load. Many testing methods have been proposed to measure the hardness of enamel. Overall, the indentation method is the most effective way to measure the hardness of enamel due to the limited sample size requirements. In the nanoindetation test, the hardness is defined as the ratio of the indent load and the contact area while applying the maximum load, whereas the hardness in microindentation testing is a measurement of the ratio of the indent load and the surface area after unloading. Consequently, the estimated hardness from the nanoindentation and microindentation tests is technically different. That is, in microindentation testing the hardness is measured after unloading and this hardness measurement includes the material's elastic recovery ability during the unloading process. In general, the hardness from the microindentation test is higher than that from the nanoindentation test, especially in polymeric materials. However, in brittle materials, such as enamel, the difference in hardness values between the microindentation and nanoindentation test would be expected to be minor since its elastic recovery in strain is very small.

2.2.2 Elastic Modulus

The elastic modulus (or Young's modulus) is defined as a measurement of the apparent stiffness of a material. The elastic modulus describes a material's resistance to deform elastically and quantifies the ratio of the magnitude of stress responsible for a

corresponding degree of deformation. Before the advent of micro-or nanoindentation tests, the macroindentation test was the primary method used to evaluate the elastic modulus of enamel. Today most experiments are being conducted by the micro or nanoindentation tests.

Macro-scale tests, such as compression, acoustic impedance, or 4 point bending tests, have been employed to evaluate the elastic modulus of enamel. Many macro-scale tests were commonly conducted until the mid of 1900's, but the overall values were very inconsistent. For example, Stanford *et al*. [1958] reported that the range of the elastic modulus of enamel is between 9 to 47.5 GPa under the compressive test, whereas Tyldeslsy [1959] performed four point bending tests to evaluate this property and reported that it ranges from 125 to 150 GPa. The overall range in reported elastic modulus of enamel from macro-scale tests is roughly 9 to 150 GPa, depending on location in enamel, testing method and applied load. Table 2-1 provides a summary of the test results for the elastic modulus of human enamel on the macro-scale. It should be recognized that most macro-scale testing arrangements are inadequate for geometrically small specimens, including enamel. Yet, it was inevitable that macro-scale tests were employed during these early investigations due to the limitation of contemporary technology. Some of the macro-scale tests have preferred assuming that the tensile behavior of enamel is equal to the compressive behavior [Stanford *et al*. 1958]. Moreover, these papers did not consider the potential size effect, which could play an important role in the evaluation of mechanical properties, especially in a brittle material, or one that is naturally inhomogeneous.

Table 2-1. Elastic modulus of enamel by different macro-scale testing methods.

Group(s)	Tooth	Pism orientation	Test method (Load or depth)	Elastic Modulus (GPa)
Stanford et al., (1958)		Variable	Compressive	47.5
		Cross section		30.3
		Occlusal surface		8.96
Stanford et al., (1958)	Canine	Variable	Compressive	47.5±5.5
		Cross section		33±2.1
		Variable (cusp)		20±6.2
Craig et al., (1961)	Molar	Variable	Compressive	46.2±4.8
		Cross section		32.4±4.1
		Occlusal surface		9.65±3.45
		Occlusal surface		84.1±6.2
		Cross section		77.9±54.8
Tyldeslsy [1959]	Molar		4 point bending	131±16
Reich et al. [1967]		Occlusal surface	Acoustic impednace	76.5
Staines et al., (1981)		Occlusal surface	Spherical indentation (Up to 800N)	83±8

Many investigations have been conducted using either standard indentation or microindentation tests, including the Vickers, Brinell, Rockwell and Knoop hardness tests, to evaluate the hardness of enamel. The microindentation test is an appropriate method for small specimens and is a relatively easy method for measuring the mechanical properties (hardness and potentially the elastic modulus). However, the main drawbacks of both macro and micro indentation tests are that they require measuring indentations using optical devices, which means that measuring the indentation size is subjective and depends on how the indentation size is measured or who measures it. Consequently, results by the microindentation test for enamel may vary due to the above reasons. The microindentation test has mainly been employed to evaluate the hardness of enamel although Mahoney *et al*., [2000] and Xu *et al*., [1998] measured both the hardness and elastic modulus of enamel

from the microindentation test. Results of these studies are listed in Table 2-2. In comparison, a far greater number of evaluations on enamel have been conducted using nanoindentation.

Table 2-2. Elastic modulus and hardness of enamel by different testing schemes in micro and nano-scale (1993 – 2000).

Group(s)	Tooth	Pism Orientation	Test method (Load or depth)	Elastic Modulus (GPa)	Hardness (GPa)
Xu et al. (1998)		Occlusal surface	Standard Vickers indentation (2 - 50N)		
		Occlusal surface	Modified Vickers indentation (1.9N)	94±5	
		Cross section		80±4	
Willems et al. (1993)		Occlusal surface	Nanoindentation (10mN)	90.59±16.13	
Poolthong (1998)		Cross section	Nanoindentation (50 & 150 mN)		
		Buccal side		90.79±2.2	
		Cusp tip		83.83±6.3	
Marshall et al. (2000)		Cross section	AFM indentation (Up to 14mN)	63.55±1.46	
		DEJ			
Fong et al. (2000)		Occlusal surface	Nanoindentation (0.3 & 2.5mN)	98.3±5.9	
		Cross section		95.6±4.9	
		Occlusal surface		87.5±2.1	
		Cross section		72.7±4.4	
Mahoney et al. (2000)	Molar	Cross section	Nanoindentation (50 & 150 mN)	80.4±7.7	
Marshall et al. (2000)	Molar	Cross section	Nanoindentation (30mN)	62.09 - 65.02	3.38 - 3.63
Habelitz et al. (2001)		Head of rod	Nanoindentation (1.5mN)	88.0±8.6	
		Tail of rod		80.3±7.2	
		Interrod		86.4±11.7	
Cuy et al. (2000)		Cross section	Nanoindentation (Depth: 400 & 800nm)	47 ~ 120	
		Outer enamel		>115	
		DEJ		<70	

The nanoindentation test is a relatively new (within this decade) testing methodology for characterizing the mechanical properties of materials. In general, it is most commonly employed in measurements of the elastic modulus and hardness of the substrate. However,

it is also used in examining creep and stress relaxation behavior, dynamic response of the material and spatial dependence in properties over selected regions of analysis. As of late, most studies on the mechanical behavior of enamel are being conducted by nanoindentation. The main advantage employing the nanoindentation test is sensitivity. In the nanoindentation test, the indentation depth and applied load can be controlled very precisely, even at the nanoscale. Therefore, it is possible to evaluate the physical properties of each rod and organic sheath separately if desired. Overall, the variation in elastic modulus determined using the nanoindentation method is far smaller than that found using macro and microscopic scale tests. Nevertheless, variation is still a consideration and may be attributed to the degree of sample polishing, testing location, applied load, geometry of the indenter, machine calibration or prism orientation. A review of the properties of enamel determined using nanoindentation is listed in Tables 2-2 and 2-3.

Table 2-3. Elastic modulus and hardness of enamel by different testing schemes in micro and nano-scale (2002 – 2008).

Group(s)	Tooth	Pism Orientation	Test method (Load or depth)	Elastic Modulus (GPa)	Hardness (GPa)
Habelitz et al. (2002)		Cross section	Nanoindentation (0.75 & 1.5mN)	74±4 ~ 80±9.1	
Barbour et al. (2003)		Occlusal surface	Nanoindentation (3mN) (5mN) (7mN)	99.6±1.8 101.9±1.6 105.2±1.3	
Cui et al. (2005)	Molar	prism sheath	Nanoindentation (1mN) (0.3mN)	83.4±7.1 39.5±4.1	4.3±0.8 1.1±0.3
Ge et al. (2005)		Occlusal surface Rod Interrod	Nanoindentation (1mN)	 83.4±7.1 39.5±4.1	
He et al. (2006)		Occlusal surface Cross section	Nanoindentation (1 - 450mN)	60 - 100 40 - 80	5±0.45 4.5±0.45
Braly et al. (2007)	Molar	Occlusal surface Cross section	Nanoindentation (Depth: 200nm)	120 - 130	6.0 - 7.0
Zhou and Hsiung (2007)		Occlusal surface	Nanoindentation (Depth: 100 - 2000nm)	104~70	
He et al. (2007)	Premolar	Occlusal surface Sound Dehydrated Re-hydrated Dry Burnt	Nanoindentation (10 - 250mN)	 95 - 115 115 85 - 105 110 - 120 115	 4.49±0.15 5.01±0.25 4.15±0.10 4.78±0.13 5.94±0.34
Low et al. (2008)	Adult canine Baby canine	Occlusal surface Cross section Occlusal surface	Vickers indentation (2 - 100N)		2.2 -3.9 0.2 - 3.0

2.2.3 Factors Contributing to the Elastic Modulus and Hardness of Enamel

Tables 2-2 and 2-3 summarized the elastic modulus and hardness of enamel reported from studies that employed micro or nanoindentation tests. While it is beyond the scope of the present study to provide a full description of all studies on the elastic modulus and

hardness, among them, specific ones are of larger importance. Note the estimated hardness values from the micro and nanoindentation tests are technically different. As explained in Section 2.2.1, in nanoindentation testing hardness is measured while the indentation tip is contacting a sample, whereas hardness in microindentation testing is measured after the indentation tip is removed. That is, the measured hardness from the microindentation test does include the deformation that a material undergoes during elastic recovery. The elastic deformation, but the measured hardness in the nanoindentation test does not include the deformation associated with elastic recovery. Therefore, the estimated hardness values in the nanoindentation and microindentation tests could be different due to the above reason even though both tests may be conducted under the same conditions, including applied load, tip geometry and testing temperature. Nevertheless, due to the relatively high elastic modulus of enamel and its apparent brittleness, the measured hardness values of the microindentation and nanoindentation tests are not significantly different as evident in Tables 2-2 and 2-3.

Spears [1997] reported that the hardness and elastic modulus of enamel is largely dependent on the mineral content. The elastic modulus increased 93 to 113 GPa as the crystalline fraction increases from 0.81 to 0.99. Xu *et al*. [1998] measured the hardness and elastic modulus of enamel by the indentation method in the enamel occlusal surface and the enamel axial surface to examine the influence of the prism orientation and the tooth to tooth variation. They reported that the elastic modulus ranges from 78 to 100 GPa and hardness of enamel ranges from 3 to 4 GPa. They concluded that these variations are attributed to the location of evaluation and prism orientation. Habelitz *et al*. [2001] measured the mean values of the elastic modulus and hardness parallel and perpendicular to the enamel rods; the mean elastic modulus and mean hardness were 72.7 ± 4.5 GPa and

3.3 ± 0.3 GPa in a direction parallel to the enamel rods, while in a perpendicular direction to the enamel rods, the mean elastic modulus and mean hardness were 87.5 ± 2.2 GPa and 3.9 ± 0.3 GPa, respectively. Interestingly, Ge *et al*. [2005] reported that there is significant difference in the mechanical properties between the prisms and organic sheaths. The hardness and elastic modulus of the prisms were found to be 4.3 ± 0.8 GPa and 83.4 ± 7.1 GPa, respectively, whereas in organic sheaths they were 1.1 ± 0.3 GPa and 39.5 ± 4.1 GPa, respectively. These results imply that changes in the content of the interprismatic material could have important effects on the global properties.

Another interesting focus of studies performed on enamel concerns the influence of hydration and chemical variation on the mechanical behavior. He *et al*. [2007] investigated the importance of environment on the mechanical behavior of human enamel and found that there are statistically significant differences in mechanical properties of teeth treated using different methods. They treated teeth by performing ethanol dehydration, water re-hydration, desiccation at room temperature and heating up to 300˚C (i.e. burnt). In the burnt enamel, the elastic modulus and hardness were approximately 115 and 6 GPa, respectively, whereas they were around 95 and 4 GPa in the re-hydrated enamel, respectively. The differences were attributed to the relative contribution of the organic sheath to the mechanical response. Earlier, Cuy [2002] conducted a nanoindenatation test to understand the importance of enamel structure on the mechanical behavior. He concluded that mechanical properties are dependent on changes in the chemical content and microstructure across the thickness from the DEJ to the outer surface. His research showed that at the enamel surface, the hardness and elastic modulus are approximately 6 GPa and 115 GPa, respectively, and near the DEJ they are less than 3 GPa and 70 GPa, respectively. Although many papers concluded that the prism direction is one of the

primary factors contributing to variation in the elastic modulus and hardness of enamel, a recent study by Braly *et al*. [2007] reported that the enamel rod direction is not a significant factor. In their study, the difference between properties parallel and perpendicular to the prisms is less than 3%.

2.2.4 Fracture Toughness

Fracture toughness (or resistance to fracture) is a property that delineates a material's ability to resist the propagation of cracks under a particular state of stress. Very few studies have reported on the fracture toughness of enamel, primarily due to its limited size and its inherently complex structure. The most common approach in evaluating the fracture toughness of enamel is the indentation method, and this choice is largely attributed to the limited tissue available for examination. But there are recognized complications. The main complications of evaluations on the fracture toughness of enamel are the prism orientation and its anisotropic structure (Figure 2-5).

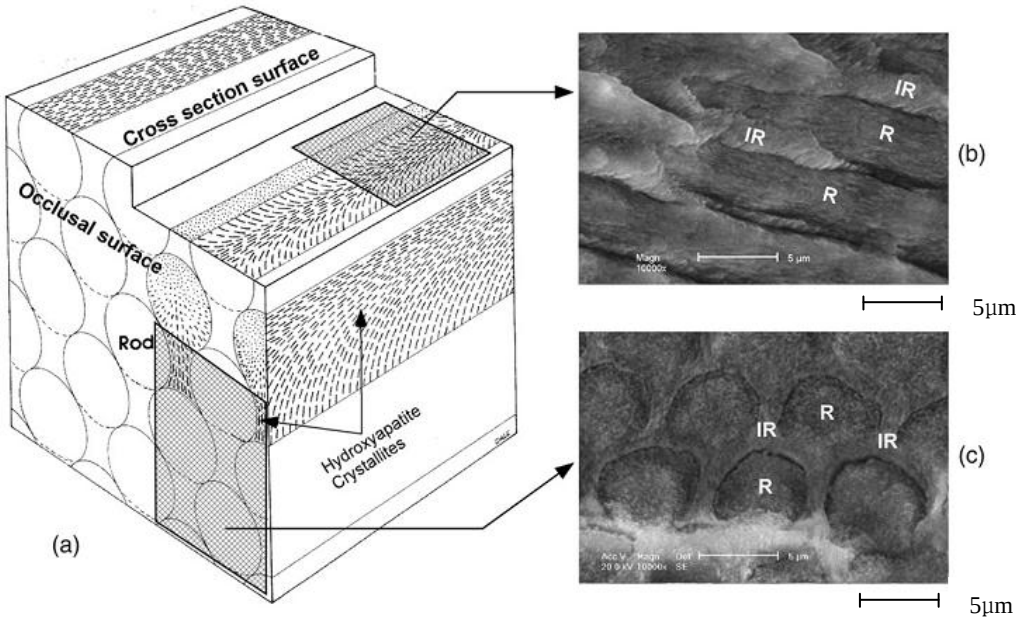

Figure2-5. (a) The hierarchical structure of enamel [Eisenmann, 1998] and SEM images of cross sectional surface (b) and occlusal surface (c) [He *et al*., 2007].

In general, the fracture toughness, K_c of a material estimated using the indentation approach is defined according to

$$K_{Ic} \text{ or } K_c = c*f(P, E, H, c, d) \quad (2\text{-}1)$$

where c is a constant that accounts for the crack configuration, P is an applied load, E is the elastic modulus, H is the hardness, c is a crack length, and d is a parameter of dimension associated with the indentation. For example, it could be the diagonal length for a Vickers indentation. As seen in Figure 2-5, the prism orientation can have a critical effect on the propagation of cracks in enamel. If the indentation is made on the occlusal surface, the cracks would extend from each indentation corner in a direction perpendicular to the axis of the prisms. On the other hand, if the indentation is introduced on a sectioned surface, cracks may be introduced that are oriented both parallel and perpendicular to the prism orientation. Natural cracks in enamel that develop *in vivo* proceed parallel along the enamel prisms and not perpendicular. Therefore, the structural anisotropy is expected to contribute to mechanical anisotropy in evaluations of toughness.

Another issue in estimating the fracture toughness by the indentation approach is recognizing the damage zone resulting from the indentation. There are two primary types of crack configurations resulting from indentations, which include the radial/median crack and Palmqvist crack configurations as shown in Figure 2-6. In the radial/median crack configuration, the fractured zone caused by the indentation is a semi circle (Figure 2-6 (a)) and its radius is a sum of the crack length (c) and half the diagonal length (L/2). On the other hand, in the Palmqvist crack development, the fractured zone resulting from an indentation is limited to the indentation periphery (Figure 2-6 (b)). Therefore, in identifying an appropriate model to estimate the indentation fracture toughness of enamel,

the first step is to identify the crack type that develops. Unfortunately, in most reported studies on enamel there was not a clear explanation of the crack configuration observed and why particular equations were adopted for estimation of the apparent fracture toughness.

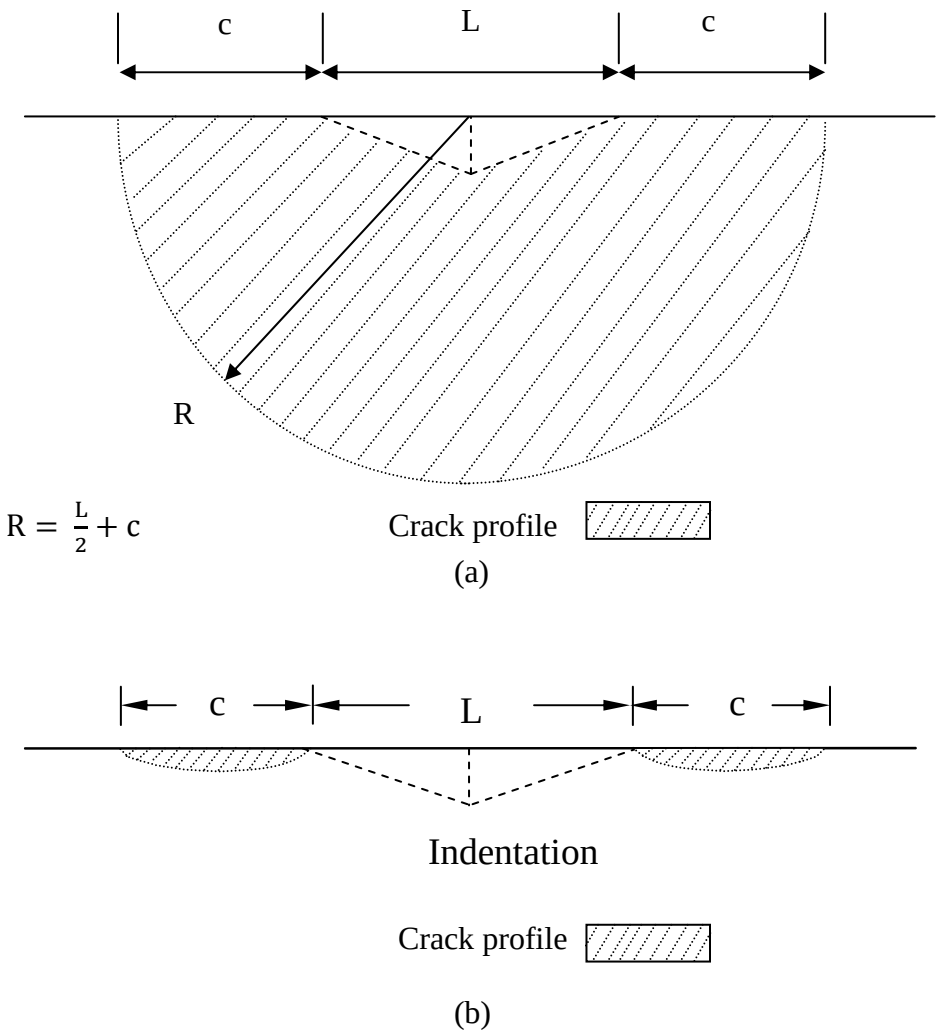

Figure 2-6. Two types of crack configurations from a side view of a Vickers indentation; Radial crack (a) and Palmqvist crack configuration (b).

Hassan *et al*. [1981] reported the first study on the fracture toughness of enamel under different loading conditions. They reported that it ranges from 0.7 to 1.15 MPa*$m^{1/2}$ under 300g indentation load and it ranges from 0.68 to 1.27 MPa*$m^{1/2}$ under 500g load. They

concluded that although the variation in fracture toughness is not fully understood, some of the variation is caused by contributions from the chemical content and the toughening mechanism promoted by the micro structure.

Xu *et al*. [1998] examined the fracture toughness of human enamel and the energy absorbed under indentation within the occlusal surface and axial sections of enamel. They summarized the overall fracture toughness of enamel ranged from .4 to 1.25 MPa*$m^{1/2}$. Imbeni *et al*. [2005] measured fracture toughness of enamel from the DEJ to the outer surface of enamel and found that the fracture toughness decreased from 3.4 in the DEJ to 0.6 MPa*$m^{1/2}$ close to the outer surface of enamel.

A summary of all reported studies on the fracture toughness of enamel is listed in Table 2-4.

Table 2-4. Fracture toughness of enamel estimating using the indentation approach.

Group(s)	Tooth	Pism Orientation	Test method (Load or depth)	Fracture Toughness (MPa*m^0.5)
Hassan et al. (1981)	Incisors & molars	Top surface	Vickers indentation (300g and 500g)	0.7 - 1.27
Xu et al. (1998)	Molar	Top surface	Vickers Indentation (2 - 50N)	0.77±0.05
		Cross section		0.52±0.06
		45˚ tilted rod		1.3±0.18
Marshall et al. (2000)	Molar	Cross section	Nanoindentation (30mN)	0.6 - 0.7
White et al. (2001)		Top surface	Vickers Indentation	1.3±0.3
		Cross section		0.9±0.22
Imbeni et al. (2005)	Molar	Cross section	Vickers indentation (3 and 5N)	~1.3
		Occlusal surface		~0.7
Low et al. (2008)	Adult Canine	Occlusal surface	Vickers indentation (2 - 100N)	1.5
		Cross section		
	Baby Canine	Occlusal surface		1.25

The overall fracture toughness of enamel ranges from approximately 0.5 to 1.5 MPa*$m^{1/2}$. It is believed that the prism orientation, applied load (dependency of indentation size effect), toughening mechanisms and spatial variations in structure of enamel lead to these variations in measured fracture toughness. One outstanding drawback of the studies presented in Table 2-4 is that there was little emphasis placed on understanding if there were spatial variations in the toughness.

2.3 Aging of Enamel

Similar to other hard tissues in the human body, it is assumed that the overall structure and properties of enamel could change with aging. Young enamel is highly permeable to water, ions and various molecular substances normally present in saliva. These substances flow freely through the intercrystal spaces, but it is not clearly understood how and if the property changes take place in enamel with age. In general, there are natural changes in the mineral content of hard tissues with aging. For example, in human dentin the mineral content increases with patient age due to deposition of mineral salts with the tubule lumens [Ten Cate, 1998]. This process has prompted studies focused on changes in the structure and chemistry of dentin and their effects on the corresponding mechanical behavior. Recent studies have shown that there is a significant reduction in the fatigue strength and fracture toughness of dentin with patient age, both of which increase the potential for tooth fracture [Kinney *et al*., 2005; Arola and Reprogel, 20005; Bajaj *et al*., 2006].

Despite the aforementioned changes in properties of dentin with age, no study has examined the influence of aging on the mechanical properties of human enamel. Therefore, one of the objectives in this study is to determine if the mechanical properties of enamel

are dependent on patient age and if there are unique property changes within specific regions of the tooth. In comparison to the efforts directed towards dentin and bone, there is little available literature on aging of enamel. One thing that has been distinguished is that as enamel ages, the hydroxyapatite crystals increase in size, thus reducing the space available for exchange of materials [Robinson *et al*. 1995]. Consequently, interprismatic protein (organic sheath) size decreases and this causes the permeability of enamel to decrease with age, suggesting that the topical application of fluoride, which can replace hydroxyl groups in the apatite lattice structure, is more beneficial in the young than in the older individual. Therefore, one of the most significant age related alterations of enamel is the reduction in its permeability [Bertacci *et al*. 2007].

2.4 Brittleness of Materials

Many theories and equations have been introduced to quantify the brittleness of a material. Table 2-5 provides a list of some parameters used to quantify or characterize the degree of brittleness of engineering materials. Even though hardness, elastic modulus and fracture toughness are important and fundamental indices used to characterize the mechanical behavior of a material, they do not provide a clear description of the material's brittleness. Specifically, they do not address the propensity for inception of flaws and cracks under contact loads, or characterize a material's ability to resist the initiation of fracture processes through either elastic or inelastic deformation. Thus, evaluating brittleness of enamel can serve as a useful scale in the design of materials used for crown replacement, as well as a quantitative tool for characterizing degradation in the mechanical behavior of enamel.

Table 2-5. Some parameters used to quantify the degree of brittleness [Quinn and Quinn, 1997]

Author(s)	Parameter	Comment
Irwin	K_{Ic}	Critical stress intensity factor, Mode I
Griffith	γ_f	Fracture surface energy $\gamma_f = K_{Ic}^2(1-\nu^2)/2E$ (plane strain)
Irwin	G_{IC}	Critical strain energy release rate, $G_{Ic}=2\gamma_f$
Kelly et al.	σ/τ	Compares theoretical cleavage strength, σ to theoretical shear strength τ in single crystals
Rice and Thomson	$\mu b/\gamma_f$	Shear modulusμ time Burger's vector, b, divided by fracture surface energy γ_f. Determines whether a crack in a single crystal is atomically sharp or blunt due to dislocation generation when stress is applied
Gogosti	$X=(\sigma_u^2/2E)\int \sigma d\varepsilon$	The area under the stress-strain curve up to failure if the material were completely elastic normalized by the actual area under the stress-strain curve to failure, X is equal to 1 for linearly elastic brittle ceramics.
Lawn et al.	$H^2/G_{Ic}E$ or H^2/K_{Ic}^2	G_{Ic} is the strain energy release rate. When expressed in terms of E and K_{Ic}, this index of brittleness is similar to the next index
Puttick	$E\gamma_f/\sigma_y^2$ or K_{Ic}^2/σ_y^2	σ_y is the yield stress, i.e. the ratio of the surface energy associated with fracture to the volume strain energy If σ_y is proportional to H, then Puttick's index is the inverse of the Lawn index
Lawn and Marshall	H/K_{Ic}	Vickers hardness divided by stress intensity. This is the square root of the index listed above; developed for convenient comparison rather than a theoretical basis
Mouginot	$A_t \propto E\gamma_f/H^2$	Brittleness is determined by the size, of a flat punch needed to induce brittle behavior rather than plastic deformation
Quinn and Quinn	$B=EH_c/K_{Ic}^2$	Ratio of indentation work to fracture energy; this can be related to the onset of extensive fracture via a critical length
Sehgal	c/d	Ratio of crack length, c, to indent size, d, for Vickers indents at a specified load; empirically related to H/K_{Ic}

Note that by virtue of fracture toughness, including fracture surface energy, critical stress intensity and critical strain energy release rates, brittleness of a material could be expressed more quantitatively, compared to the equations that have been proposed before. However, note that fracture toughness does not characterize the brittleness of a material completely as it quantifies a material's inherent resistance to the propagation of a crack, but not the resistance to the initiation of a crack.

2.4.1 The Brittleness Number

Brittleness describes the relative propensity for a material to undergo fracture rather than elastic or inelastic deformation. As such, it would be expected that the brittleness of a material should be related to its hardness, elastic modulus and fracture toughness. What follows is a theoretical treatment of brittleness in terms of the aforementioned properties, which was developed by Quinn and Quinn [1997].

In general, the hardness is defined as the ratio of the applied load to the contact (sometimes, projected) area and is expressed as

$$H = \alpha \frac{P}{d^2} \tag{2-2}$$

where P is the applied load, α is an indenter constant, and d is the diagonal length of the indentation. Note that the hardness is a function of the applied load, therefore the hardness value can be either constant or varied, depending on the material's property. Consequently, the hardness vs. the load plot does not necessarily align with the Meyer law, which is defined as

$$P = Cd^n \tag{2-3}$$

where C is a constant, and d is the diagonal length, and n is the logarithmic number representing the hardness-load equation in the Meyer law. If Eqn. 2-2 and 2-3 are combined and n =2, then a new equation is obtained for the hardness as

$$H = C * \alpha \tag{2-4}$$

where the hardness is now independent of the applied load. Specifically, if n=2, the hardness is constant regardless of the applied load, while the hardness decreases as the applied load increases if n<2. Since the Meyer law does not predict a transition point to

constant hardness, a power series expansion was proposed by Bückle [1965] and Mitsche [1948], which was later modified by Fröhlich *et al*. [1977] and Li and Bradt [1992] as

$$P=a_1d+a_2d^2 \tag{2-5}$$

Eqn. 2-5 can be rewritten by dividing by d^2 on both sides and if P/d^2 is replaced by H, then the hardness can be a function of constants, a_1, a_2, and the diagonal length of indentation, d, which is represented as

$$\frac{P}{d^2} = \frac{a_1}{d} + a_2 \tag{2-6}$$

and

$$H = \frac{a_1'}{d} + a_2' \tag{2-7}$$

Note that the hardness, H in Eqn. 2-7 is the transition hardness so that the hardness value is independent of load. Therefore, a_1' and a_2' are new constants that account for the transition hardness. By multiplying both sides of Eqn. 2-6 by d^3, it can be rewritten as

$$Pd=a_1d^2+a_2d^3 \tag{2-8}$$

In Eqn. 2-8, the term, Pd represents the external work done by the indenter, and the terms a_1d^2 and a_2d^3 are related to the energy consumed for the new indented area, including that associated with fracture and cracks, and the energy for creating permanent deformation (or the volume energy component), respectively. In brittle materials, the hardness generally decreases and then becomes constant as the applied load increases beyond a critical value. That point where the hardness value reaches a stable or constant state is called a 'Transition point' [Quinn *et al*. 1997]. At a transition point, the critical ratio, $ß_c$ is defined as the ratio of the energy consumed for the new indented area to the total external work

done by the indenter. This critical ratio, ß$_c$ can be represented using Eqn. 2-8 as

$$\beta_c = \frac{a_1 d_c^2}{P_c d_c} \quad \text{or } \beta_c = \frac{a_1/d_c}{P_c/d_c^{\,2}} = \frac{(a_1^{'}/d_c)}{H_c} \tag{2-9}$$

where H_c is the hardness at d_c and a_1, $a_1^{'}$ are constants, and P_c is the applied load.

The constant, a_1 is related to the energy consumed for the new indented area, therefore it is proportional to thermodynamic surface free energy (γ_s) and effective fracture surface energy (γ_f). Considering thermodynamic surface free energy (γ_s) and effective fracture surface energy (γ_f), Eqn. 2-9 can be converted to

$$\beta_c = \frac{A(\gamma_f/d_c)}{H_c} \tag{2-10}$$

where A is a constant.

The fracture toughness for plane strain is represented in terms of the fracture surface energy as

$$K_{Ic} = \left[\frac{2E\gamma_f}{(1-\nu^2)}\right]^{1/2} \tag{2-11}$$

Combining Eqn. 2-10 and 2-11, the critical ratio of ß$_c$ is re-expressed as a function of the fracture toughness (K_{Ic}) as

$$\beta_c = \frac{A^{'}(K_{Ic}^2/d_c)}{H_c E} \tag{2-12}$$

where $A^{'}$ is a new constant pertaining to constant, A and Poisson's ratio, ν. Rearranging Eqn. 2-12, solving for d_c, and inverting provides

$$\frac{1}{d_c} = \frac{\beta_c}{A'}\left(\frac{H_c E}{K_{Ic}^2}\right) \tag{2-13}$$

Now, the combination in the bracket is considered as a new parameter for characterizing the brittleness of a material. Since the numerator, H_c*E delineates the combined deformation energy and the denominator, K_{Ic}^2 represents the fracture energy, this ratio of the deformation and fracture energy describes the material's brittleness in a very quantitative manner. Therefore, the Brittleness Number (B) quantifies a material's relative resistance to deformation and fracture and is defined by

$$B \equiv \left(\frac{H_c E}{K_{Ic}^2}\right) \tag{2-14}$$

where H_c is the "transition point hardness" or constant hardness of the material and E and K_{Ic} are the elastic modulus and indentation fracture toughness, respectively.

The brittleness index is a quantitative interpretation of the competing dissipative processes of deformation and fracture and has been used as a practical measure for characterizing the brittle behavior of engineering ceramics. Materials with high B value are most apt to fracture rather than undergo elastic or inelastic deformation, whereas materials with low B would be more likely to deform elastically or dissipate energy through inelastic deformation. Table 2-6 shows the mechanical properties of some characteristically brittle materials. From this table, it is found that the fracture toughness of a material is not necessarily proportional to its brittleness. For example, the fracture toughness of Al_2O_3 AD999 and α-SiC are 4 and 3 $MPam^{-1/2}$, respectively, while their brittleness numbers are 439 and 1290 μm^{-1}, respectively. The α-SiC is generally regarded as far more brittle than the Al_2O_3 and the brittleness number captures this phenomenon more appropriately than the K_{Ic} alone.

Table 2-6. Material properties of some brittle materials [Quinn *et al*. 1997].

Material	ρ (Mgm^{-3})	E (GPa)	K_{Ic} ($MPam^{-0.5}$)	Vickers hardness HV_c (GPa)	d_c (μm)	P_c (N)	B (μm^{-1})
Al_2O_3 AD999, Coors sintered	3.96	386	4	18.2	45.9	20.7	439
Pyroceram 9603, Corning	2.64	134	2.4	6.8	125	57.3	157
α-SiC Carborundum sintered	3.11	410	3	22.6	20.2	5	1023
Si_3N_4 NC132, Norton hot pressed	3.23	320	4.6	15.4	78.9	51.7	233
Si_3N_4 NBD200, Norton hot isopressed	3.16	320	5.4	14.9	120	116	163
Si_3N_4 NT154, Norton hot isopressed	3.23	315	5.8	14.9	114	105	140
α-SiC Carborundum sintered	3.16	430	3	27	14.5	3.1	1290
ALON, Army Research Laboratory aluminum oxynitride spinel	3.61	320	2.75	14.6	31.1	7.6	618

2.4.2 Brittleness of Enamel and Dental Materials

Although numerous papers have been published on the mechanical properties of enamel, they have ignored the potential importance of brittleness on the characteristics of clinical function. Also, despite the innate relevance of this physical description to the performance of dental materials, a quantitative measure of brittleness has not been adopted for characterizing their mechanical behavior. As shown in Table 2-6, Quinn *et al*. [2003] computed the brittleness numbers of common engineering ceramics. A similar evaluation of dental materials used for crown replacement and a comparison with the brittleness of enamel would be valuable and could provide new insight. However, no study has been

performed to estimate the brittleness of enamel. As such, changes in brittleness with age in this hard tissue have not been characterized. If there is a difference in the brittleness of enamel with respect to age and location, it may provide valuable information in designing dental restorative materials as well as understanding the aging effect on enamel.

2.5 Summary

Functional failure of restored teeth is a major concern in modern dentistry. Fractures are an even greater concern now, especially with the rise in number of elderly patients. Many studies have been conducted to facilitate the design and development of new dental restorative materials, which are generally designed to mimic the properties of natural enamel. Although numerous papers have quantified the mechanical properties of enamel, no study has considered the potential changes in mechanical properties of enamel that are associated with aging. Also, while enamel is considered to be brittle, the brittleness with respect to restorative materials that it contacts has not been considered. Consequently, a better understanding of the brittleness of enamel and the property changes in enamel with regard to aging is needed. This information serves to address potential oral health problems in seniors related to mechanical failure of tooth structure as well as to provide critical information that facilitates the design of improved dental restoratives.

Chapter 3

Materials and Methods

The primary goal of this study was to quantify spatial variations in the mechanical behavior of human tooth enamel and to identify differences related to age of the patient. To achieve this goal, both nanoindentation and microindentation test methods were used and performed on enamel specimens that were prepared from human teeth.

3.1 Materials

Human third molars were obtained from participating clinics within the state of Maryland according to an approved protocol issued by the Institutional Review Board (IRB) of the University of Maryland, Baltimore County. Both the age and gender of the patient were

obtained with each tooth. The teeth were placed in Hank's balanced salt solution (HBSS) immediately after extraction to minimize changes in properties with storage [Habelitz *et al*., 2002]. At receipt the molars were divided by age into "young" (18≤age≤ 30) and "old" (55≤age) age groups, which were defined according to a classification used previously in evaluation of human dentin and not based on expectations regarding the properties of enamel [Arola and Reprogel, 2005; Bajaj *et al*., 2006]. The average age and standard deviation of the young and old groups were 23±4 years and 73±15 years, respectively. Fully erupted 3rd molars were used to avoid the influence of cuspal wear on the enamel thickness, and the potential for differences in properties due to large loads transmitted near the cusps. The teeth were cast in a polyester resin foundation and sectioned using a programmable slicer/grinder (K.O. Lee Model S3818EL, Aberdeen, SD) with diamond impregnated slicing wheels (#320 mesh abrasives) and continuous water-based coolant (Figure 3-1).

(a) **(b)**

Figure 3-1. Setup for primary sectioning of a human molar. Primary sections were along the axis of the root. a) mounted for sectioning, b) after slicing.

3.2 Nanoindentation Testing

3.2.1 Specimen Preparation

A total of 14 teeth were used, including 7 each for the young and old age groups. A single longitudinal slice was made in the bucco-lingual plane approximately equidistant from the mesial and distal surfaces. One of the two halves (Figure 3-2(a)) was then mounted in a cold-cured epoxy resin, which consists of an epoxy resin and a hardener (Epofix resin, HQ and Epofix hardener, HQ, Struers). The epoxy resin and hardener were mixed with the weight ratio of 8 g epoxy to 1g of hardener. The mixed epoxy resin and sectioned tooth were placed into a container (Figure 3-2 (b)). Once the epoxy hardened (approximately 20 hours), the specimen underwent an abrasive and preliminary polishing process using silicon carbide abrasive papers with successively smaller particle sizes.

(a)

(b)

(c)

Figure 3-2. Details of the specimen preparation process for nanoindentation. (a) Longitudinally sectioned human molar. (b) Longitudinally sectioned human molar embedded in epoxy. (c) Sample after completion of the polishing protocol.

The initial process was started by using #800 grit silicon carbide abrasive paper. Thereafter, #1200, 2400, and 4000 mesh number papers were used successively for both preliminary polishing and for minimizing scratches on the surface. Further polishing was achieved by using diamond particle suspensions (Buehler) of 9, 3, and 0.04 µm particle diameters with the corresponding polishing cloth discs. Figure 3-2 (c) shows the final sample after the polishing process has been completed. In the nanoindentation test, the surface roughness is a significant factor that can influence the elastic modulus and hardness measurement.

Therefore, it was essential to measure the average surface roughness before conducting the experiment to insure adequate surface quality had been obtained. The average surface roughness (Ra) resulting from the preparation was characterized after polishing using scanning probe microscopy (SPM) in contact mode. The surface roughness was measured over a single selected area of 50 x 50 μm^2 in selected specimens and found to be 0.01 µm ± 0.003µm. After completion of polishing, the specimens were bonded to a ferro-magnetic base using a cyanoacrylate adhesive for mounting them on the nanoindenter stage (Figure 3-3). The specimens were maintained at room temperature (22°C) in HBSS until evaluation and the surface was maintained hydrated during testing.

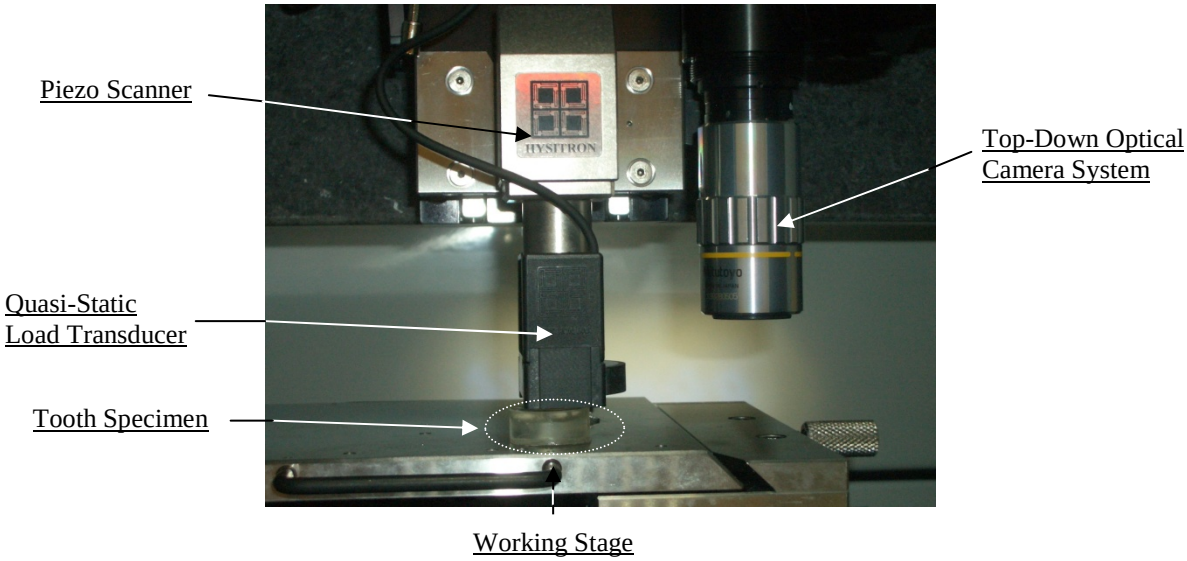

Figure 3-3. The nanoindentation setup and the sample mounted on the x-y stage for conducting the nanoindentation test. The resin-mounted sample is circled for clarity.

3.2.2 Testing Protocols and Apparatus

Indentations were introduced in the prepared enamel surfaces using an automated nanoindenter (Hysitron Triboindenter, Minneapolis, MN) and a 3-sided Berkovich diamond indenter with a 50 nm tip radius (Figure 3-3). A standard load/unload procedure was used with a rate of loading and unloading of 1 mN/sec, and a maximum load of 5 mN held for 5 seconds. At this indentation load the average depth and edge length of the indentations were approximately 190 nm and 2 µm, respectively. Both the elastic modulus and hardness were evaluated as a function of distance from the DEJ along 6 different paths and within 3 different regions of each tooth. Indentations were made on the sectioned polished surface along the buccal and lingual aspects of the cervical regions (A, F), at the buccal and lingual cusps (B, E), and within the intercuspal region (C, D) as described in Figure 3-4 (a). All six paths (A through F) were defined as being parallel to the enamel prism, beginning at the DEJ and continuing to the outer surface of the tooth (Figure 3-4 (a)). Indents were introduced at 9 different equidistant sites along each path and four

indents were introduced at each site according to a square array. The first site was located 20 µm from the DEJ, followed by increments of equidistant spacing over the defined path (Figure 3-4 (b)). The last set of four indents was placed within 50 µm of the outer surface of the tooth (Figure 3-4 (b)). Through the aforementioned procedures, 36 indents were made along each path and a total of over 200 (6x9x4=216) indents were introduced in the enamel of each tooth.

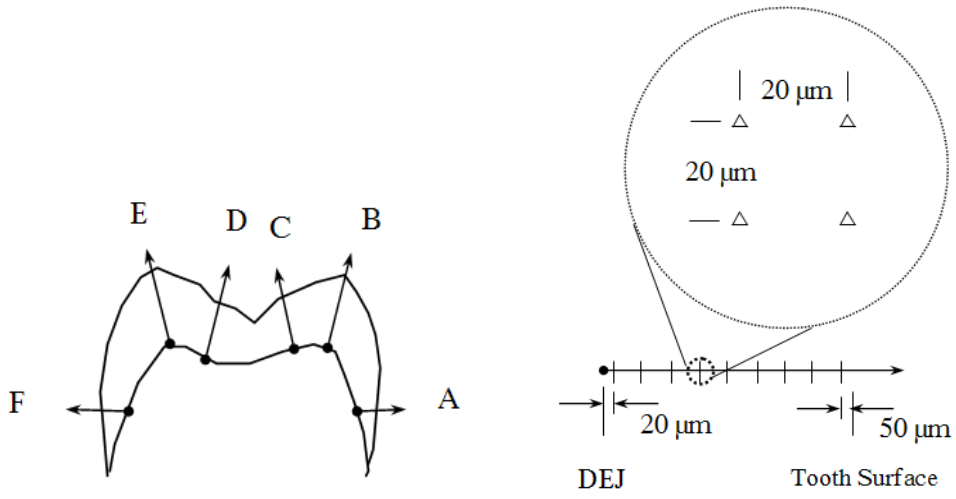

Figure 3-4. Schematic diagram of a sectioned tooth and the six different paths of evaluation. (a) Evaluation paths A and F (Cervical), B and E (Cuspal) and C and D (Inter-Cuspal) were consistent for each of the 14 teeth evaluated. (b) Each path has 9 indentation sites and each indentation site has four indents with 20 µm interval.

By virtue of the sectioning process and specimen orientation the indentations were essentially perpendicular to the enamel prism axis. However, as the prisms are rarely directed entirely straight from the DEJ to the outer surface, there is potential for small error (i.e. ±10˚) in the relative orientation between the indentation and prism axis. A study performed by Braly *et al*., [2007] reported that the differences in the elastic modulus and hardness due to different prism orientations is very small, and found to be approximately 2%. The distances from the DEJ to the enamel surface in the cervical (A, F: ≈ 0.5 mm),

cuspal (B, E ≈ 2 mm), and inter-cuspal regions (C, D ≈ 1.5 mm) were quite different. Therefore, the incremental distance between the 9 sites ranged from less than 100 to over 200 µm apart and depended on the enamel thickness within that region. Due to differences in distance from the DEJ to the tooth's outer surface within the three regions of evaluation, the spatial property distributions were evaluated as a function of absolute distance, and also as a function of normalized distance from the DEJ. The normalized distance was established by dividing the distance of measurement from the DEJ by the total distance from the DEJ to the enamel surface along that path of evaluation. Normalization enabled the property distributions to be compared objectively over a distance ranging from 0 to 1 along each path of evaluation in each tooth, despite differences in the enamel thickness within the three unique regions.

The hardness and elastic modulus were computed for every indentation using the standard approach [Oliver and Pharr, 1992]. It is important to highlight that the modulus reported here is often regarded as the "reduced" elastic modulus. Based on analytical treatments performed by Oliver and Pharr [1992], the "reduced modulus", E_r is defined as

$$\frac{1}{E_r} = \frac{(1-\nu_s^2)}{E_s} + \frac{(1-\nu_i^2)}{E_i} \tag{3-1}$$

where E_s and E_i are the elastic modulus of the specimen and indenter and ν_s and ν_i are the Poisson's ratio of the specimen and indenter, respectively. The elastic modulus, (E_i) and the Poisson's ratio, (ν_i) of a diamond indenter are 1141 GPa and 0.07, respectively. The Poisson's ratio of enamel is approximately 0.28 [Waters, 1980]. If these values are substituted for the corresponding parameters, Eqn. 1 becomes

$$\frac{1}{E_r} = \frac{0.9216}{E_s} + 0.000872 \tag{3-2}$$

which indicates that in investigations on enamel

$$\frac{1}{E_r} \approx \frac{1}{E_s} \quad \text{or} \quad E_r \approx E_s \tag{3-3}$$

Note that with this approach that the elastic modulus is within less than 10% of the reduced elastic modulus. The "reduced" elastic modulus was determined for each indentation according to

$$E_r = \frac{S * \sqrt{\pi}}{2 * \sqrt{A}} \tag{3-4}$$

where S is the stiffness and A is the surface area. The stiffness is estimated from the indentation load (P) and depth (h) response during elastic recovery according to

$$S = \frac{\Delta P}{\Delta h} \tag{3-5}$$

The hardness was determined from the ratio of the applied load to the indentation surface area and is defined as

$$H = \frac{P_{max}}{A} \tag{3-6}$$

where P_{max} is the maximum applied load and A is a surface area at the maximum load.

A calibration of the 3- sided Berkovich indenter was performed prior to testing to obtain the tip area function on a fused quartz crystal, which is suggested as a reference sample.

Through this process the surface area (A) for the indentation was estimated directly from the indentation depth.

3.2.3 Data Analysis

Each indentation provided an indentation force displacement response as shown in Figure 3-5. Note that the unloading section was used to calculate the elastic modulus since the materials undergo elastic recovery during the unloading process.

It is important to highlight that the total indentation depth (h) that occurs during the indentation is described by

$$h=h_s+h_c \tag{3-7}$$

where h_s is the surface displacement at the periphery of the indented area due to the peak load, and h_c is the contact depth when the indenter is impressing the surface at peak load.

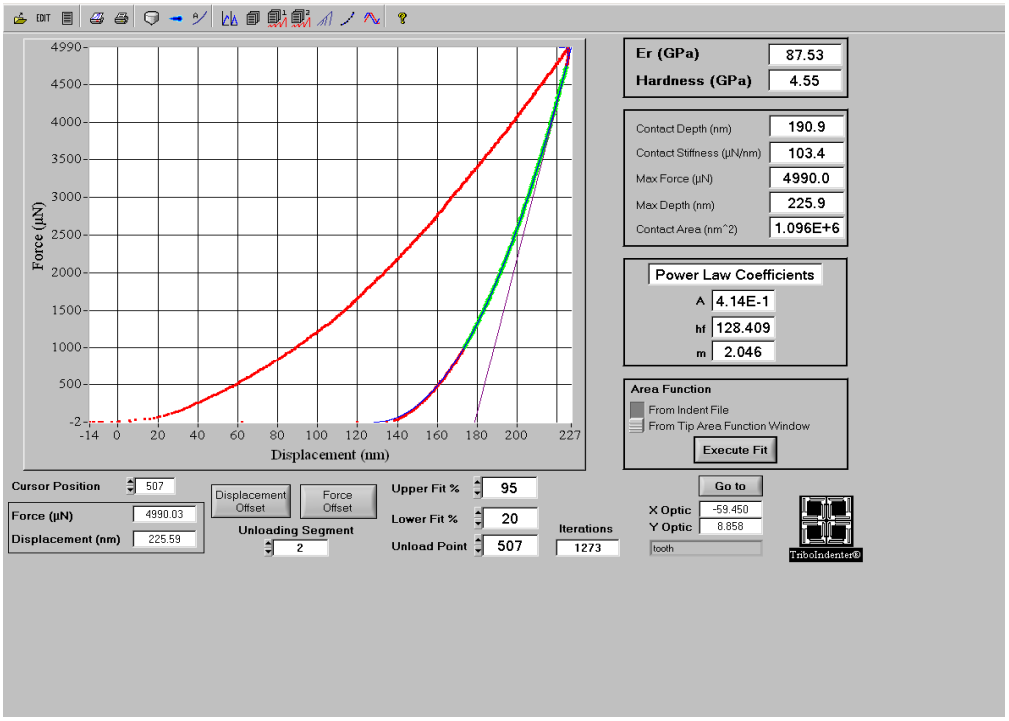

Figure 3-5. A typical load/unload history obtained from an indentation routine on enamel. The elastic modulus and hardness were calculated automatically by the software and are evident in the upper right-hand corner of the screen capture.

These components of displacements are shown schematically in Figure 3-6, as well as h_f, which is the final displacement after elastic recovery of the deformed material and removal of the indentation load. Due to the measurement of hardness under the applied load (Eqn. 3-6), hardness measurements from nanoindentation are different from those performed using microindentation. Microindentation measurements of hardness are obtained after the indent load has been removed, which indicates that they include the effects of inelastic deformation only due to the process of elastic recovery.

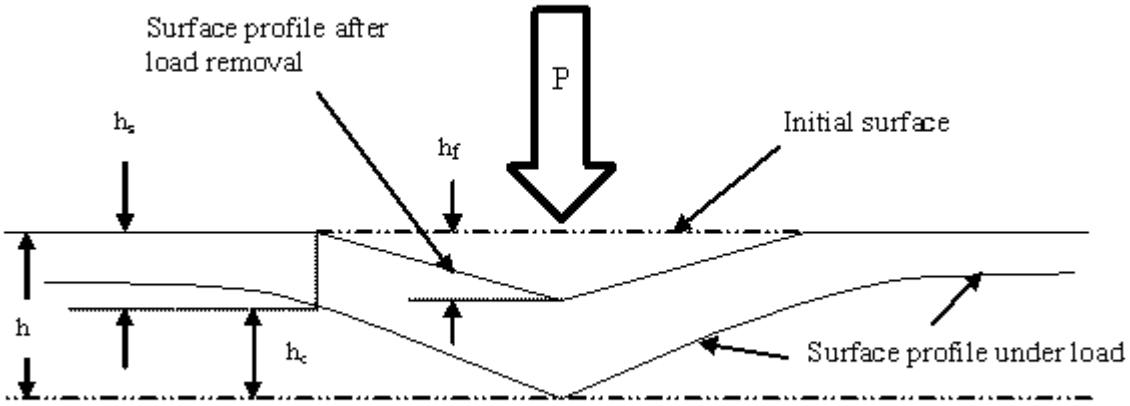

Figure 3-6. A schematic drawing of an indenter and surface. The surface profile and final indentation depth are displaced after load is removed [Oliver and Pharr, 1992].

As such, hardness obtained by nanoindentation and microindentation are not expected to be equivalent, even if measured at the same load. Special conditions may result in agreement between these two methods of testing as described in Chapter 2.

Using cumulative results for the teeth in each age group, the average hardness and elastic modulus of the young and old enamel were determined. All data was processed using commercial software to evaluate trends and to develop plots of the spatial variations. The property distributions were quantified for each age group as a function of absolute and normalized distance from the DEJ including all paths, as well as separately for the three specific regions of evaluation (cervical, cuspal, and inter-cuspal regions). A comparison of these distributions was conducted within each age group and between the two age groups as well. Significant differences in properties at each measurement site were identified using an ANOVA ($p \leq 0.05$) and a comparison of property gradients was conducted using a two-sample Wilcoxon test ($p \leq 0.05$).

3.3 The Microindentation Test

Microindentation tests were performed to obtain information that could not be determined from nanoindentation testing. Specifically, the microindentation test permitted an evaluation of enamel over a far larger range in the indentation load.

3.3.1 Specimen Preparation

A total of 20 teeth, including 10 from each age group, were tested using the microindentation approach. Ten teeth were used for an evaluation of indentation size effects (ISE) and the rest of the remaining 10 teeth were tested for evaluating the apparent fracture toughness and brittleness numbers. To examine the indentation size effects on enamel, selected teeth were sectioned bucco-lingually and samples were prepared using the same procedures outlined in Section 3.2.1. An evaluation of indentation fracture resistance was conducted on the occlusal surface of the enamel. To conduct these measurements, the

tooth was sectioned bucco-lingually and secondary sections were made from initial bucco-lingual sections to extract beams from beneath the cusps as shown in Figure 3-7. The beams were mounted in the epoxy resin with the prisms oriented nominally perpendicular to the polished surface. Polishing was performed using procedures similar to those used for preparation of specimens for the nanoindentation tests. The specimens were polished using silicon carbide abrasive paper with successively smaller particle sizes (mesh sizes of #800, 1200, 2400, and 4000). After that, the specimens were further polished using diamond particle suspensions with the corresponding discs as explained in Section 3.2.1.

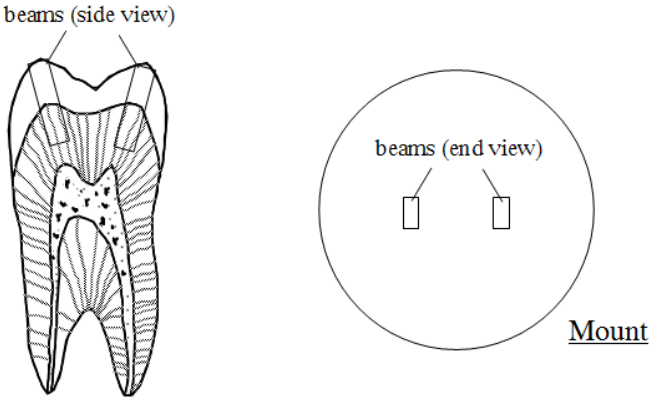

Figure 3-7. Schematic drawing of a sectioned tooth used for the indentation fracture toughness (IFT) evaluation using the microindentation approach. The cuspal beams were mounted in cold-cured epoxy such that the occlusal surface faced outward and the enamel prisms were oriented perpendicular to the testing surface.

In the study of Indentation Fracture Toughness (IFT), there are two primary crack configurations that may develop as outlined in the literature, namely the radial crack and the Palmqvist crack configuration. Estimation of toughness or fracture resistance is dependent on geometric features of the crack, and assumes one of the two different configurations. Therefore, recognizing the crack configuration that developed in enamel was required prior to performing an indentation fracture toughness evaluation. To identify

the crack configuration, several indentations were introduced and the surface was then polished until 3 µm was removed from the original layer as shown in Figure 3-8. Then the surface and crack shape were examined. After removal of the material no surface cracks were evident about the periphery of the indentation. Thus, the crack could not have a radial crack configuration because the crack should remain evident from the indentation corners. Therefore, the complementary subsurface evaluation distinguished that the crack introduced by indentation in enamel exhibited a Palmqvist crack configuration.

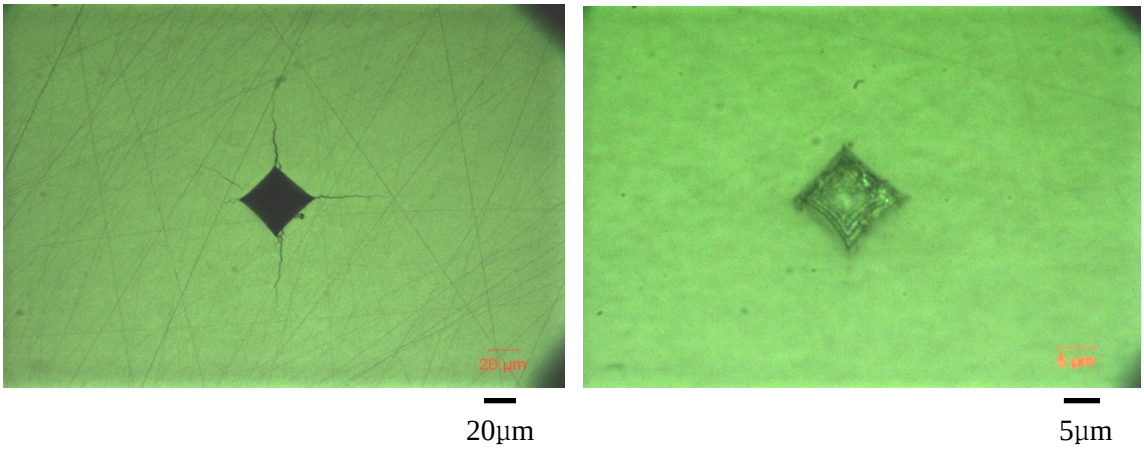

Figure 3-8. Experiment for verifying the crack configuration in enamel. (a) an indentation in enamel. (b) the indentation surface after removal of 3µm of material clearly defined the crack in enamel as a Palmqvist configuration.

3.3.2 Testing Protocols and Apparatus

Microindentation testing of the enamel, including both the ISE and IFT components of evaluation, was performed using a semi-automated Leitz Miniload II Microhardness Tester (Ernst Leitz, Wetzlar, Germany) with a Vickers diamond indenter. Note that the specimens were maintained hydrated with HBSS solution during testing. The system is shown in Figure 3-9 (a) and is located in the Ceramics Division of the National Institute of Standards

and Technology in Gaithersburg, MD. The indentation diagonal length and crack lengths were measured using a Leitz microscope (Ernst Leitz, Wetzlar, Germany) shown in Figure 3-9 (b).

(a) **(b)**

Figure 3-9. Leitz II microhardness tester (a) and Leitz Microscope (b) for evaluating the fracture toughness and brittleness numbers.

3.3.2.1 The Indentation Size Effects (ISE) Test

In some materials the hardness is a function of the indentation load. To determine the load dependence in hardness of enamel, indentations were introduced in 10 teeth specimens at three different locations, namely at distance no more than 100 μm from the DEJ (inner enamel), midway between the DEJ and occlusal surface (middle enamel), and at a distance no more than 100 μm from the occlusal surface (outer enamel) as schematically shown in Figure 3-10. Within each region, indents were made at loads of 0.1, 0.25, 0.5, 1.0, 2.0, 3.0

and 5.0 N. Ten indents were made at each load level in each tooth. The Vicker's hardness (HV) was estimated from the indent diagonals in accordance with the ASTM standard C1327 by the indent load divided by the contact area. The hardness distribution was plotted in terms of indentation load to identify the transition point hardness (HV_c).

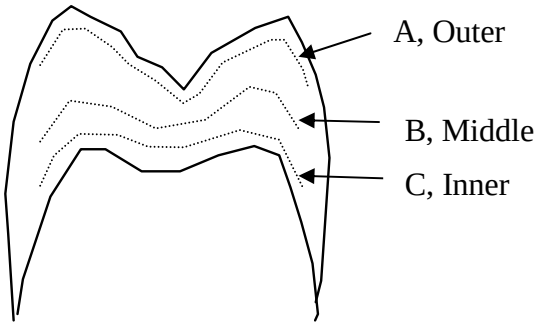

Figure 3-10. A schematic drawing of the locations examined for the Indentation Size Effects (ISE). Indents were introduced in three different regions, namely A, B, and C. Note that the dashed lines A and C are approximately 100 μm away from the occlusal surface and the DEJ, respectively, and the middle line, C is at the midpoint of the DEJ and occlusal surface.

3.3.2.2 Indentation Fracture Testing

The excised beams of enamel mounted in epoxy were used in evaluating the indentation fracture resistance or apparent fracture toughness ($K_{c(app)}$) through measurement of indentation crack lengths. A total of 5 indents were made on the polished surface of each beam using a 3 N load, which exceeded the critical load (2 N) corresponding to the transition point hardness. The diagonal lengths and average crack lengths emanating from the indentation corners (Figure 3-11) were measured for each indentation. Then, the surface was polished to remove approximately 200 μm of material and the indentation process was repeated. Sequential polishing and measurement was continued until reaching the DEJ. At an indentation load of 3 N the diagonal length and depth of the indentation are

approximately 40 µm and 5.7 µm, respectively. Therefore, there was no residual indentation damage remaining in the surface after polishing that could interfere with the subsequent indentation response.

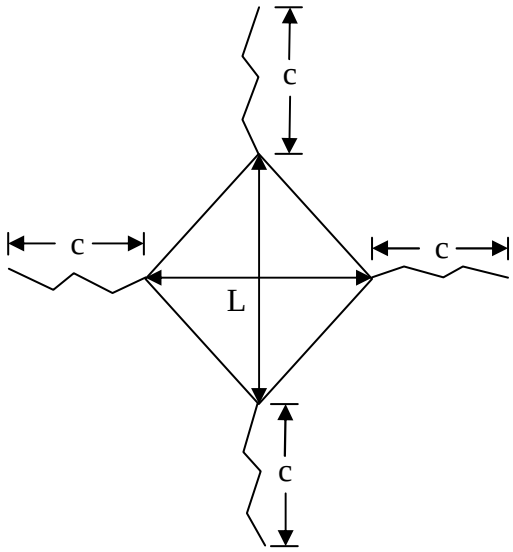

(a) Top view

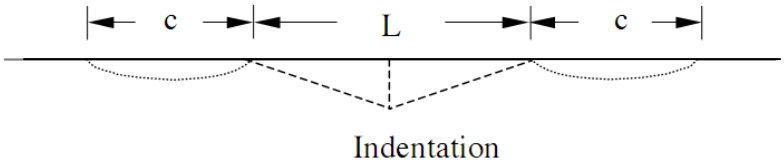

(b) Side view

Figure 3-11. Schematic drawing of a Palmqvist crack configuration found in enamel.

An important consideration in estimating the indentation fracture toughness is the range between the ratio of crack length (c) to the indent diagonal length (L). The ratio of the crack length to indent diagonal length, (c/L) was measured using the result of indents and it was found that it ranged from $0.125 \leq c/L \leq 1.25$. Therefore, considering a Palmqvist crack

configuration and the range of c/L, the most appropriate equation for estimating the apparent fracture toughness ($K_{c(app)}$) of enamel was presented by Niihara *et al*., [1982]. The apparent fracture toughness ($K_{c(app)}$) was estimated for each indentation according to

$$K_c = 0.0084 * \left(\frac{E}{HV_c}\right)^{2/5} * \left(\frac{2P}{L}\right)\frac{1}{c^{1/2}} \quad (3\text{-}8)$$

where E and HV_c are the elastic modulus and the transition point hardness, respectively, and P, L, and c are the indentation load (kg), average diagonal length (m) and crack length (m), respectively.

Due to the anisotropic structure of the enamel that is associated with the prisms, crack propagation varies according to the prism orientation. This appeared to influence the characteristics of cracks resulting from the indentations. Also, there were some complex crack networks that formed in the enamel specimens (Figure 3-12). There is no standard for measuring the crack length in the indentation test or for restricting (or accepting) cracks that develop.

In this study, many conditions were considered to acquire the most appropriate and/or most representative crack length measurement for indentations. After preliminary assessments, there were three criteria considered for measuring crack lengths. The first criterion (Criterion I) restricted measurements to indentations with one primary crack from each corner, the crack orientation angle is within 20 degrees from the diagonal length direction (Figure 3-13), and the ratio of the crack length and diagonal length falls within the range defined by Eqn. 3-8. Therefore, if the crack length did not satisfy the given ratio constraints ($0.125 \leq c/L \leq 1.25$), the crack was excluded from the evaluation, but the indent and the remaining cracks were included. For example, if an indent has only three primary

cracks, c_1, c_2, and c_3 from each of the three corners (not four cracks from each of the four corners), only three cracks were considered. In this case, the average crack length (c_{ave}) was calculated by $c_{ave}=(c_1+c_2+c_3)/3$ and the average diagonal length (L_{ave}) was $L_{ave}=(L_1+L_2)/2$. In general, only two cracks per every 10 indents (each indent has four cracks) were excluded. The second criterion (Criterion II) involved measuring the longest crack from each indent. In this criterion, only the longest crack was selected among all cracks generated from an indentation. The crack orientation was still within 20 degrees, but the ratio of the crack length and diagonal length were not considered. Therefore, it would be expected that this criterion provides insight toward understanding the worst fracture scenario of human enamel. The third criterion (Criterion III) included the consideration of all cracks regardless of orientation and length as shown in Figure 3-13 and included them in the estimate of fracture resistance. In all conditions, including each of the three criteria, the crack length (c) was measured from the tip of the indentation diagonal to the end of the crack tip (Figure 3-11). As explained previously, indentations were introduced from the outer surface of the enamel to the DEJ in order to examine the indentation fracture toughness spatial distribution. After the completion of all indentation tests, the indentation fracture toughness was estimated and compared according to the three criteria described. However, Criterion III was eliminated due to difficulty in measuring cracks uniformly since some cracks were interwoven with each other due to the enamel's structure as evident in Figure 3-12. Measuring crack lengths according to Criterion III was highly influenced by the different testers; the final crack lengths were significantly different among those who measured them. Therefore, Criterion III was not carried out through the entire investigation since it was impossible to obtain a consistent and completely objective evaluation.

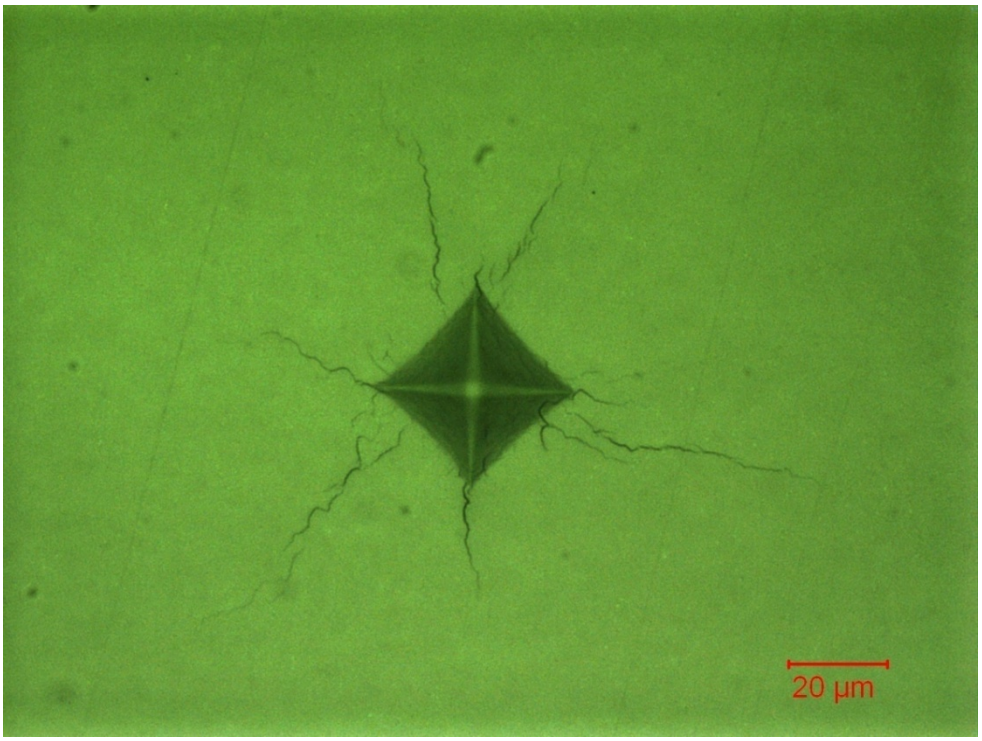

Figure 3-12. A typical example of crack propagation that caused inconsistency when following Criterion III. Consistency in the measurement of crack lengths by different testers was not achieved. As a result, the measured crack lengths varied, depending on who measured them.

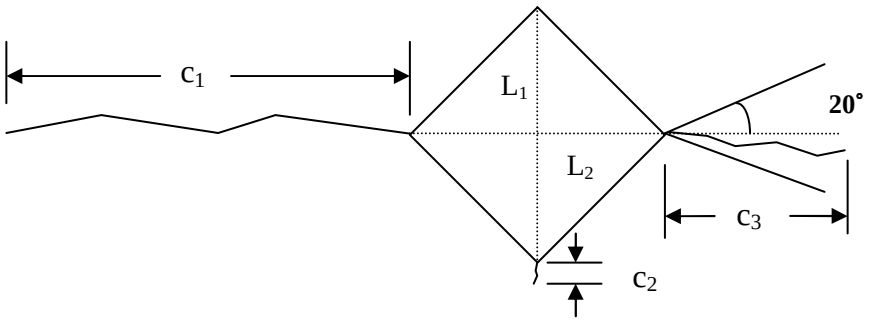

Figure 3-13. A schematic diagram of potential cracks in enamel. Note the crack lengths c_1 and c_2 were excluded in Criterion I, since they do not conform to the given ratio constraints ($0.125 \leq c/L \leq 1.25$) even though their crack orientation angles are less than 20˚ from the diagonal length (dotted line). On the other hand, in Criterion II c_1 was selected. All cracks (c_1, c_2 and c_3) were measured in Criterion III regardless of their angle and the ratio of the crack length to the diagonal length.

It is important to emphasize that quantities computed using Eqn. 3-8 are regarded herein as the "apparent" fracture toughness in recognition of concerns raised in using indentation tests to estimate the fracture toughness of materials [Quinn and Bradt, 2007]. Specifically, the indentation fracture resistance is not a direct measure of the fracture toughness. There are a number of concerns related to the crack geometry, the apparent mode of extension and nonuniformity in cracks extending from the indentation corners as described earlier. However, indentation tests are used for estimating the fracture toughness of materials, particularly when the volume of material available precludes the use of standardized methods of evaluation. In light of these concerns, the results are often termed the indentation fracture resistance (IFR) rather than fracture toughness and as such the values reported herein are termed the "apparent fracture toughness".

3.3.3 Brittleness of the Enamel and Dental Materials

The brittleness (B) of the enamel was estimated in terms of the brittleness number according to

$$B = \left(\frac{H_c * E}{K_c^2}\right) \tag{3-9}$$

where H_c is the "transition point hardness" or constant hardness of the material and E and K_c are the elastic modulus and apparent fracture toughness, respectively [Quinn and Quinn, 1997]. Note that the elastic modulus and hardness values used in Eqn. 3-9 were measured using either conventional methods or nanoindentation testing.

In addition, brittleness numbers for selected restorative dental materials (mainly crown materials), including Micaceous Glass Ceramics, Feldspathic Porcelains and Dissimilars,

were also estimated according to Eqn. 3-9. The properties were not all evaluated using indentation techniques in the interest of time. Values were obtained from the literature. The brittleness of these materials provided valuable information for comparison and clinical relevance.

3.3.4 Data Analysis

After measuring the primary mechanical properties (E, HV_c and $K_{c(app)}$) of the enamel, the brittleness of the enamel was estimated according to Eqn. 3-9 within the inner, middle, and outer enamel and as a function of distance from the DEJ. Comparisons of the mechanical properties were conducted using a t-test or an analysis of variance where appropriate. Significance was defined as $p \leq 0.05$.

Chapter 4

Results

Micro and nano indentation experiments were performed to evaluate the mechanical properties of human tooth enamel as a function of patient age and location in the crown of the tooth. The mechanical properties that were quantified include the elastic modulus, hardness, fracture toughness and brittleness numbers.

4.1 Nanoindentation Results

The nanoindentation tests were conducted to evaluate the elastic modulus and hardness of enamel. For a maximum load of 5 mN, the average indentation depth and edge length were approximately 190 nm and 2 µm, respectively. Figure 4-1 shows a typical indentation in the enamel. It was found that the indentation sizes varied with testing location, particularly when comparing indentations made in the inner (DEJ), middle, and outer surface of the enamel; the overall indentation size in the outer enamel was smaller than that near the DEJ.

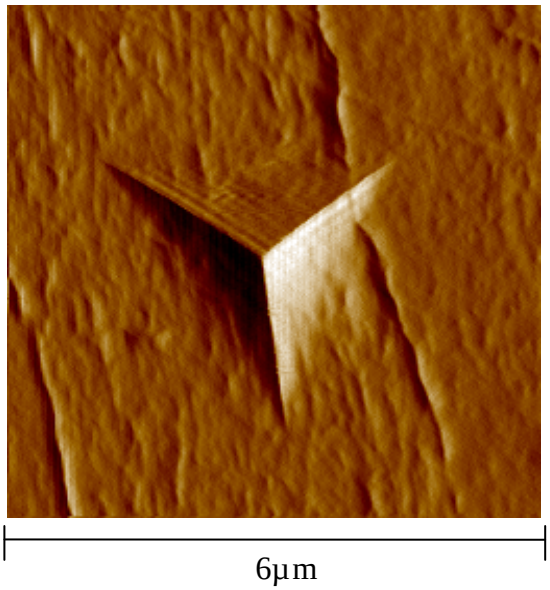

Figure 4-1. A typical Berkovich indentation in enamel by nanoindentation testing. The indentation depth and edge length is approximately 190 nm and 2 µm, respectively.

The elastic modulus and hardness were measured from the load vs. load-line displacement history as shown in Figure 4-2. Specifically, as described in Chapter 3 the hardness was determined from the maximum load and the surface area of the indent at the maximum load, whereas the elastic modulus was determined by the unloading history. Conventionally, a restricted portion between 20% and 95% of the unloading curve is used to determine the slope. According to an assessment of all indentations performed, the average elastic modulus of enamel from the young and old molars was 84.4 ± 4.4 GPa and 91.1 ± 6.5 GPa, respectively. The average hardness of enamel from the young and old molars was 4.0 ± 0.3 GPa and 4.0 ± 0.5 GPa, respectively. The elastic modulus and hardness measurements of all tested specimens are listed in Appendix A. Overall, there was no significant difference ($p>0.05$) between the average properties determined for the young and old age groups.

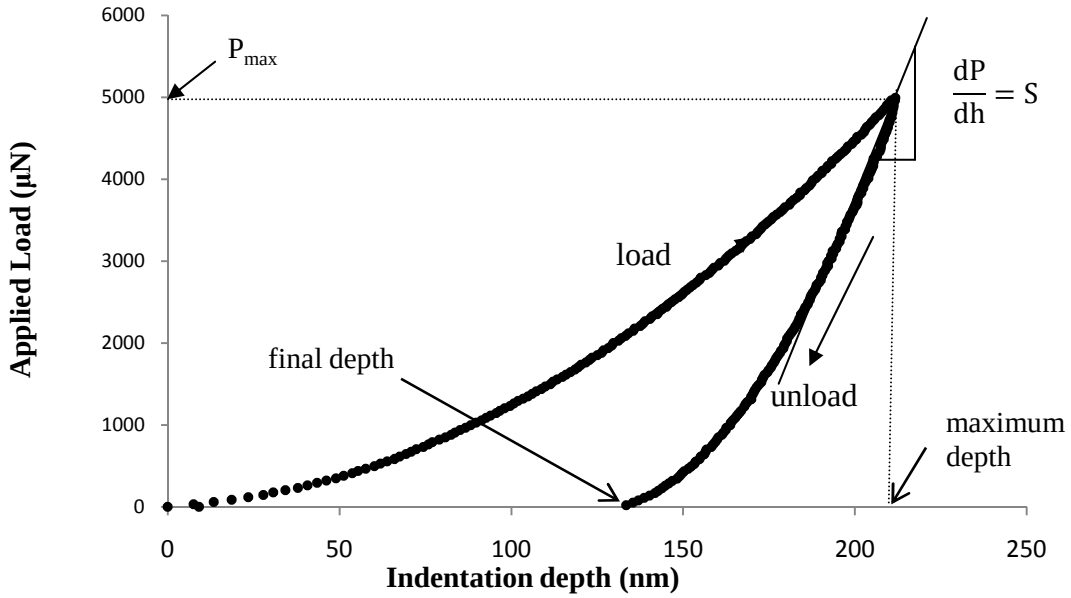

Figure 4-2. Load-indentation depth curve for the enamel from the nanoindentation test. Note that the unloading section was used to estimate the elastic modulus, and hardness was measured based on the maximum load [Oliver and Pharr, 1992].

Figure 4-3 (a) and (b) present the elastic modulus and hardness of the cervical, cuspal and inter-cuspal regions of the young and old enamel in terms of the normalized distance from the DEJ, respectively. The average elastic modulus and hardness of enamel within each of the three regions (i.e. cervical, cuspal and inter-cuspal regions) were not significantly different within or between the two age groups. Namely, the elastic modulus and hardness from the DEJ to the outer surface in the three distinct regions exhibited a very similar trend that was independent of age. However, in both the young and old age groups there was a distinct influence of distance from the DEJ in all three regions (Figure 4-3). Note that the larger variation in properties of the young enamel near the outer surface in comparison to that of the old enamel. Also, note that the slight reduction in the average elastic modulus and hardness of the young enamel near the outer surface. Both properties of the old enamel increased uniformly throughout the enamel thickness.

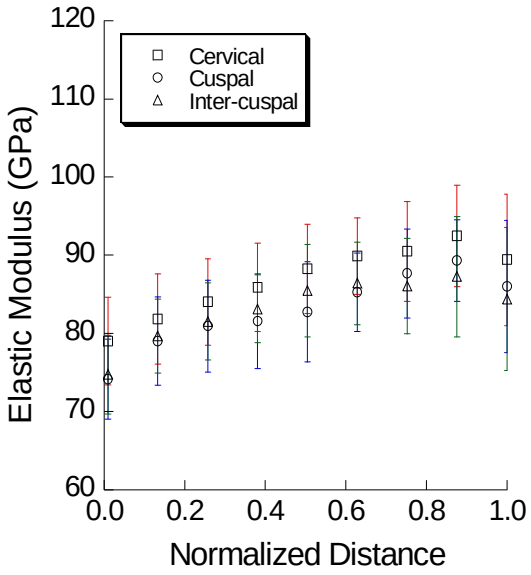

(a) young enamel, normalized distance

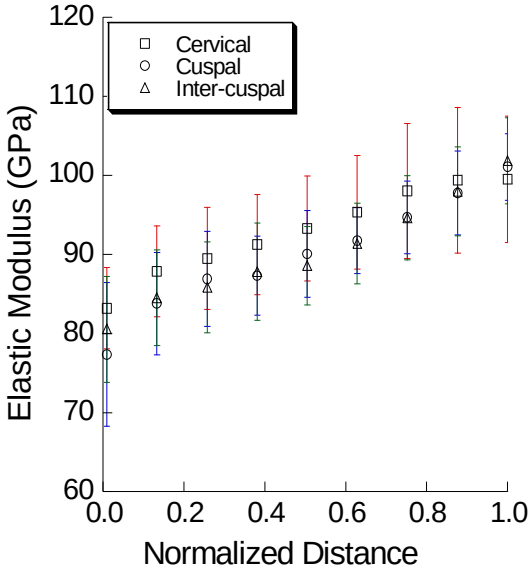

(b) old enamel, normalized distance

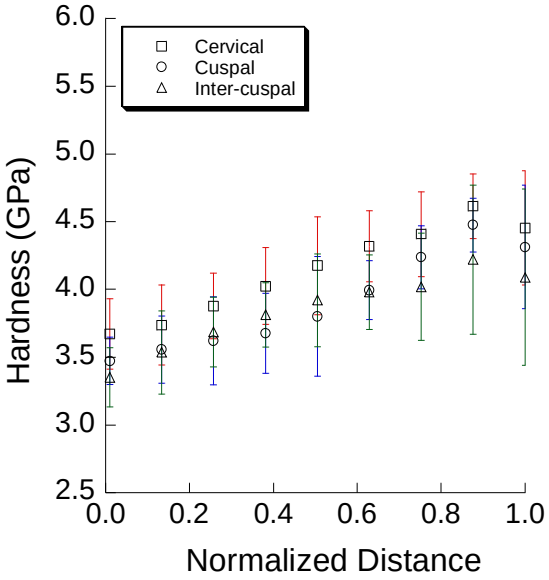

(c) young enamel, normalized distance

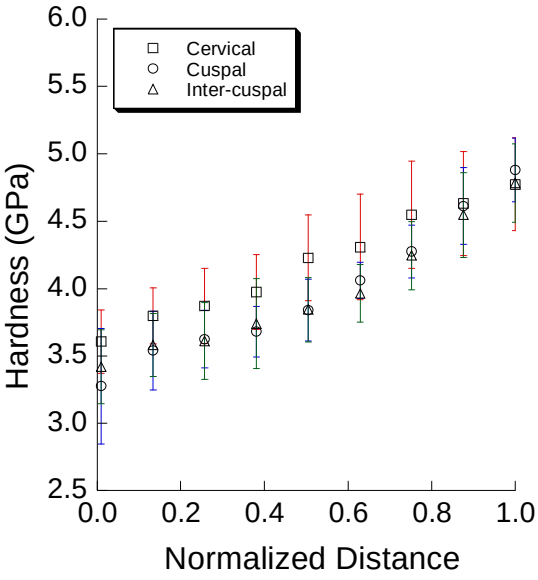

(d) old enamel, normalized distance

Figure 4-3. The elastic modulus and hardness of the three regions (i.e. cervical, cuspal and inter-cuspal regions) of the young and old age groups. Note that these properties were evaluated in terms of the normalized distance from the DEJ to the occlusal surface of the enamel.

The elastic modulus distributions in the enamel of a young (22-year-old female) and old molar (57-year-old male) are presented in terms of the absolute and normalized distance in Figure 4-4. Specifically, the elastic modulus distributions for the selected teeth are shown in terms of the absolute distance in Figures 4-4 (a) and (b), respectively, and in terms of the normalized distance from the DEJ in Figure 4-4 (c) and (d), respectively. In general, there was an increase in the elastic modulus along all distinct paths (A-F), and for all teeth, regardless of age. However, the increase of the elastic modulus with absolute distance in the old molars appeared linear in all regions of the evaluation (Fig. 4-4 (b)) in comparison to the largely non-linear distributions for the young enamel. Within the cervical, cuspal and inter-cuspal regions of the old enamel, the increase in elastic modulus with absolute distance from the DEJ was 15, 9 and 10 GPa/mm, respectively. The increase within the cervical region of the old enamel was relatively larger than that within the cuspal and inter-cuspal regions, but the differences were not significant ($p = 0.273$). Similar to the elastic modulus distributions presented in Figure 4-4, the change in hardness with the distance from the DEJ is shown for the selected teeth (22 year-old female and 57 year-old male) in Figure 4-5. Specifically, the variation in hardness with absolute distance from the DEJ is shown for a young and old molar in Figure 4-5 (a) and 4-5 (b), respectively. The hardness is presented for these two molars in terms of the normalized distance in Figure 4-5 (c) and 4-5 (d), respectively.

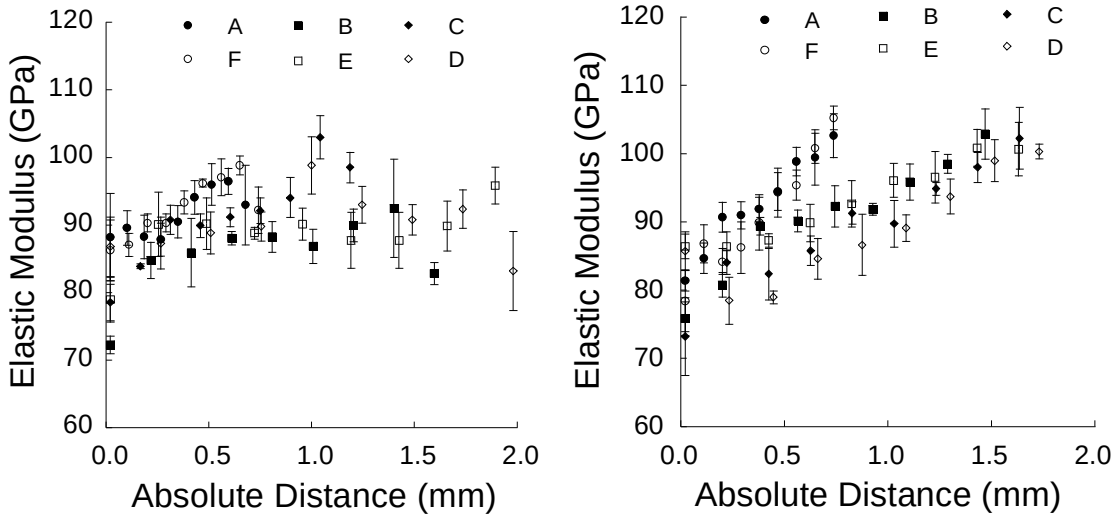

(a) young enamel, absolute distribution (b) old enamel, absolute distribution

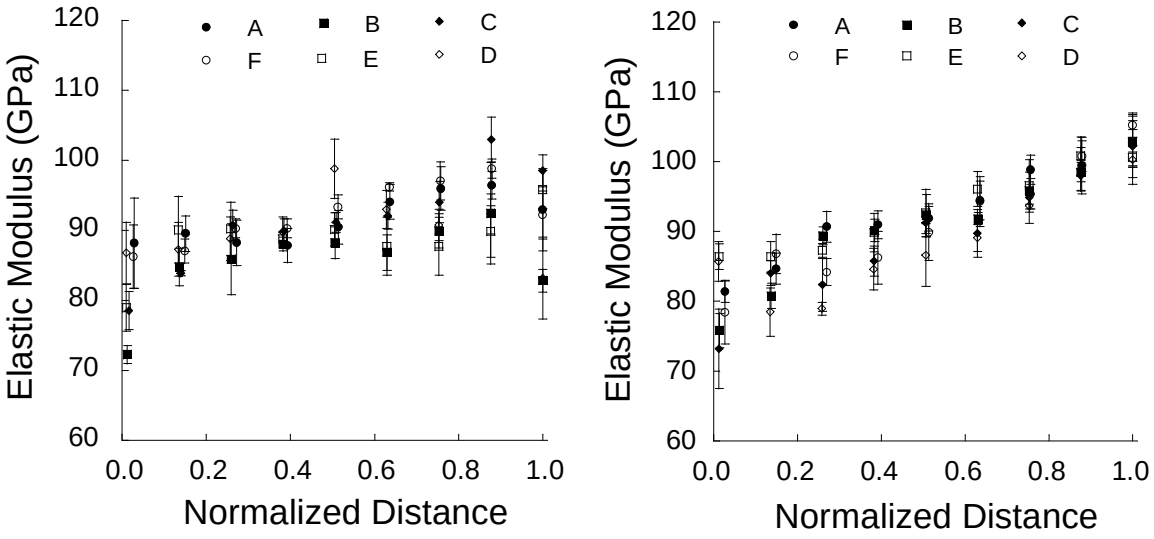

(c) young enamel, normalized distribution (d) old enamel, normalized distribution

Figure 4-4. The spatial distribution of the elastic modulus for enamel from selected young (22-year-old female) and old (57-year-old male) molars. The circular, square, and diamond points correspond to properties within the cervical, cuspal and inter-cuspal region, respectively.

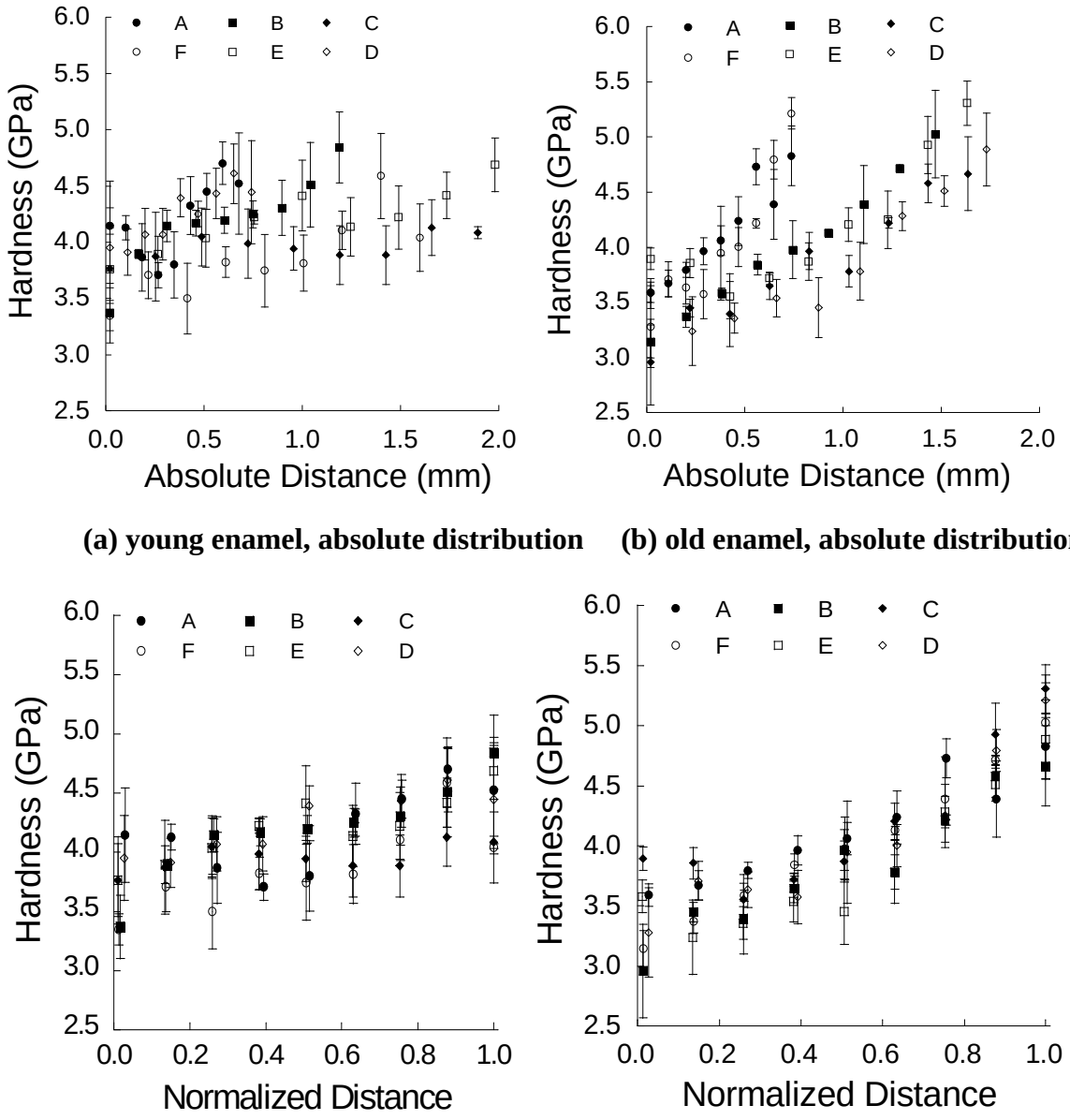

(a) young enamel, absolute distribution **(b) old enamel, absolute distribution**

(c) young enamel, normalized distribution **(d) old enamel, normalized distribution**

Figure 4-5. The spatial distribution of the hardness for enamel from selected young (22 year old female) and old (57 year old male) molars. The circular, square, and diamond points correspond to properties within the cervical, cuspal, and inter-cuspal regions, respectively.

Analogous to the trends in the elastic modulus, there was generally an increase in hardness with the distance from the DEJ for all paths (A-F), and for all examined teeth. The increases in the old enamel were largest and primarily linearly distributed in comparison to those of the young enamel, which appeared to exhibit non-linear trends with distance.

Within the cervical, cuspal and inter-cuspal regions of the old enamel, the increase in hardness with absolute distance from the DEJ was approximately 1.0, 0.7 and 0.7 GPa/mm, respectively. The differences in property gradients within these regions were very distinct as shown in Figure 4-5, but not significant ($p = 0.095$).

As evident in Figures 4-4 (c), (d) and 4-5 (c), (d), the properties of enamel within each of the three regions of evaluation exhibited consistent spatial distributions when represented in terms of normalized distance from the DEJ. Therefore, the properties obtained within each of the six unique paths of evaluation were combined for all teeth in each age group to obtain a cumulative description for the properties as a function of normalized distance from the DEJ. The combined elastic modulus and hardness distributions for the young and old enamel are shown with respect to normalized distance in Figure 4-6 (a) and 4-6 (b), respectively. The property distributions represented in this figure are based on the results of all seven teeth for each age group. According to the ANOVA, the elastic modulus of the old enamel was significantly greater ($0.0001 \leq p \leq 0.025$) than that of the young enamel from nearly mid-span to the occlusal surface; the level of significance increased with proximity to the tooth's surface. It was found that the old enamel is significantly harder than the young enamel at the tooth's surface only ($p < 0.025$). A power analysis was conducted with the elastic modulus and hardness data using means obtained for the young and old groups at each of the nine positions. When examining the elastic modulus, sufficient power ($p \geq 0.8$) existed for identifying significant differences at all nine positions of evaluation. For hardness, the difference in means relative to the variability showed that there was sufficient power to avoid type II errors at the tooth's surface only. As evident in Figure 4-6, the level of significance appeared to be limited by variation in properties of the young enamel. The magnitude of property variation decreased towards the tooth's surface in the old enamel,

whereas the property variations increased with proximity to the tooth's surface in young enamel.

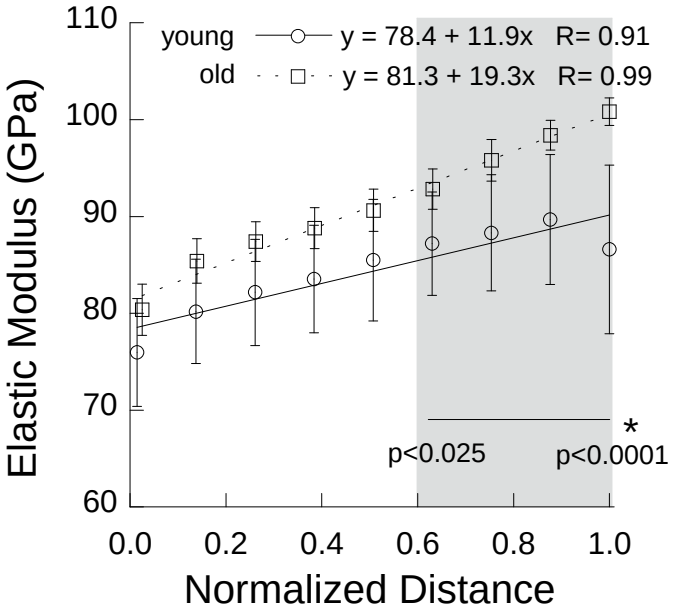

(a) distribution in elastic modulus with normalized distance

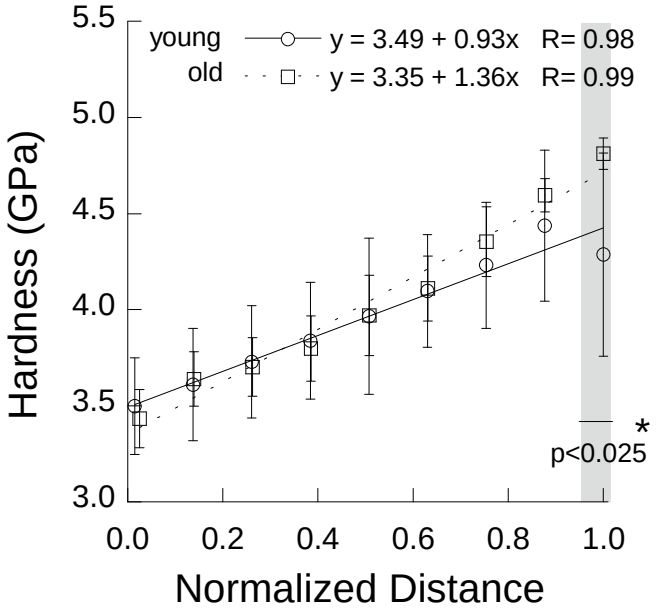

(b) distribution in hardness with normalized distance

Figure 4-6. Elastic modulus and hardness distributions of enamel for all teeth from the two age groups. *The highlighted area indicates a region of significant difference with level identified by the p-value.

4.2 Indentation Size Effects (ISE)

There were two components of microindentation testing. The first phase of testing was conducted to examine whether the hardness of enamel exhibits indentation size effects (ISE). The second component of microindentation was used to estimate the apparent fracture toughness. Vickers hardness tests were performed on the inner, middle and outer enamel as described in Chapter 3. The hardness obtained within these three regions for a selected young molar are plotted in terms of the indentation load in Figure 4-7 (a). Consistent with results of nanoindentation testing, the hardness increased from the inner to the middle enamel, and the largest hardness was found at the occlusal surface. However, the effect of indentation load was far greater. There was a 50% reduction in the hardness from loads of 0.1 to 5 N (Figure 4-7). Each of the three regions exhibited a prominent indentation size effect and a transition in hardness to a constant value (HV_c) that was essentially load independent beyond an indentation load of approximately 2 N. Microcracks and flaws were evident along the indentation periphery for loads between 0.25 and 2 N, whereas fully formed cracks were developed at the indentation corners at loads greater than 2 N. While difficult to estimate objectively, the degree of microcracking appeared to be most extensive in the occlusal region of both age groups, and particularly in the old enamel. The indentation damage findings are overlayed with the measured hardness in Figure 4-7 (a) and convey that the reduction in hardness is associated with the development of microcracking. The transition point hardness was accompanied by peripheral cracks concentrated at the indentation corners. Though the HV_c of the inner, middle and outer regions was significantly different ($p<0.01$), there was no significant difference in the values from corresponding regions between the young and old enamel. Regardless of age, the inner and outer enamel possessed the smallest and largest transition

point hardness, respectively (Fig. 4-7 (a)).

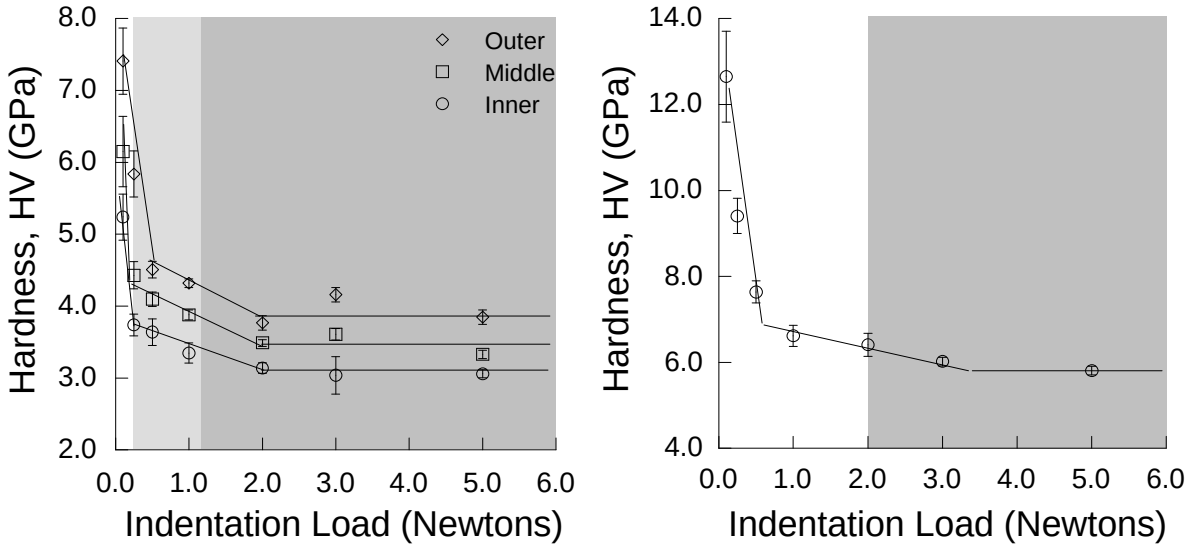

(a) **(b)**

Figure 4-7. Indentation size effect diagrams for enamel and a selected crown material. a) human enamel (patient age = 23). The highlighted region indicates the load range in which microcracks (light grey) were evident at the indentation periphery and well-defined cracks (grey) were evident at the indentation corners. b) porcelain veneer on an alumina foundation. The highlighted region indicates the load range in which well-defined cracks were evident at the indentation corners. There was no evidence of microcracking at smaller loads.

The hardness distribution with indentation loads for a fined grained incisal Leucite porcelain veneer is plotted in Figure 4-7 (b). This material also exhibited indentation size effects with higher hardness at low loads and transition hardness (HV_c) beyond a load of approximately 3 N. An overlay of the damage analysis revealed that the transition point hardness is associated with the development of cracks at the indentation corners. In contrast to the enamel, microcracking was not observed at lower loads. While the trend in hardness for the porcelain veneer is very similar to that of the enamel in overall behavior (Figure 4-7), the physical response of the enamel appeared to be more sensitive to loads than the porcelain veneer. Specifically, the enamel exhibited three unique aspects of

indentation load response, including inelastic deformation (between 0 and 0.2 N), inelastic deformation and microcracking (between 0.2 and 2 N), and fully developed cracks beyond loads of 2 N. On the other hand, the porcelain veneer exhibited only two different aspects; namely inelastic deformation for loads between 0 to 0.5 N and fully developed cracks for loads beyond 0.5 N.

4.3 Indentation Fracture Resistance

The indentation fracture resistance or "apparent fracture toughness" was also evaluated using microindentation testing. Results of the indentation size effects (ISE) analysis showed that a load beyond 2 N should be used to initiate well-developed cracks. Therefore, a load of 3 N was chosen for the evaluation of fracture resistance. Examples of indentations with cracks in different locations (inner and outer) of the young and old enamel are shown in Figure 4-8. Indentations made within the young and old enamel near the DEJ are presented in Figure 4-8 (a) and 4-8 (b), respectively, and indentations made within the young and old enamel near the occlusal surface are presented in Figure 4-8 (c) and 4-8 (d), respectively. The indentation sizes were different in the three regions (i.e. inner, middle and outer enamel), as expected according to the indentation size effects evaluation. The indentations in the inner region were relatively larger than the other two regions, but not significantly different and appeared to be influenced by the degree of cracking. The longest cracks resulting at the indentation diagonals were found in the outer region of both the young and old enamel. In the inner region, the crack lengths were smaller and in some indentations, only microcracks developed about the indentations rather than well-defined cracks as shown in Figure 4-9.

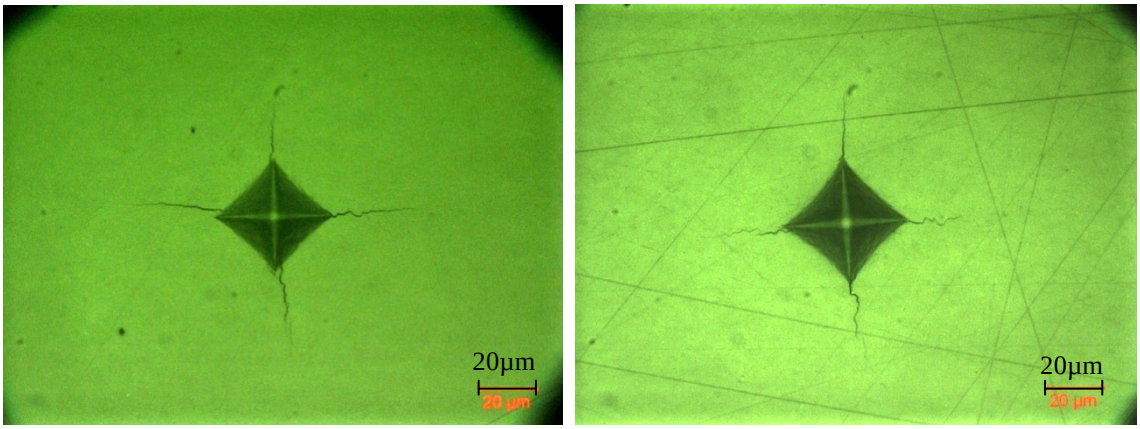

(a) young enamel, DEJ region **(b) old enamel, DEJ region**

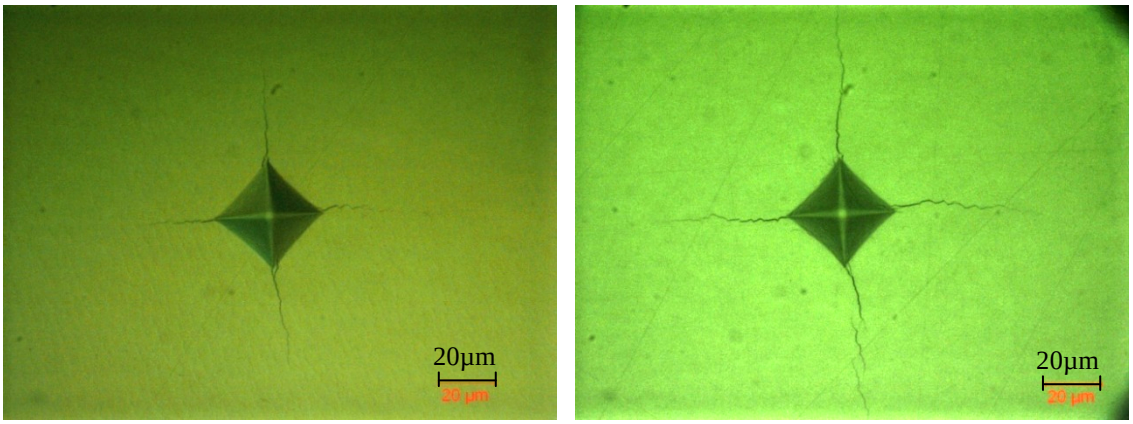

(c) young enamel, occlusal region **(d) old enamel, occlusal region**

Figure 4-8. Typical indentations and the development of cracks at the indentation corners in the young and old enamel.

Based on the aforementioned mechanical properties (E, HV_c) and estimated crack lengths, the indentation fracture toughness of the young and old enamel were estimated according to Eqn 3-8 within the inner, middle, and outer enamel and with respect to distance from the DEJ to the outer surface of the enamel. To achieve a more continuous and detailed description of indentation fracture toughness over the enamel thickness, the hardness measurements obtained from microindentation at the three distinct locations were replaced by the spatial hardness distribution in cuspal regions of the enamel obtained using nanoindentation (Figure 4-10).

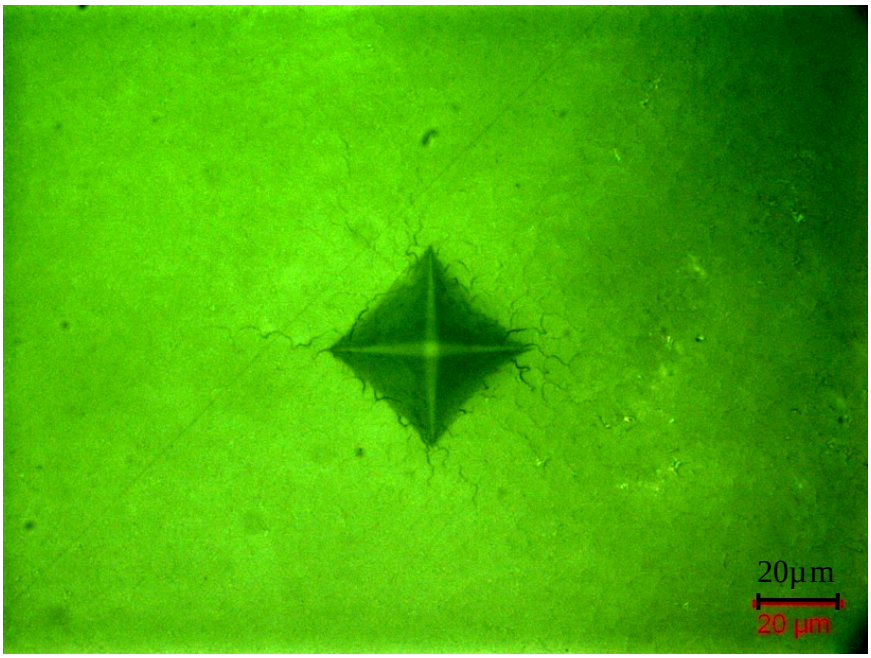

Figure 4-9. An indentation in the DEJ region (68 year-old male). Some indentations in the DEJ region generated only microcracks and flaws rather than primary cracks that were normally found in the middle and outer regions. Note that the microcracks developed about the entire indentation periphery.

Nanoindenation and microindentation measures of hardness are not exactly the same. Technically, hardness obtained from nanoindenation is determined by the indentation load divided by the contact area under the applied load, thereby accounting for both elastic and inelastic deformation. On the other hand, hardness obtained from microindentation is defined by the indentation load divided by the contact area after load removal, which accounts for inelastic deformation only due to elastic recovery after unloading. Nanoindentation and microindentation hardness measurements would tend to exhibit the closest agreement when a large degree of the elastic energy is dissipated by fracture, which occurs in the measurement of HV_c, especially if the material is brittle. The enamel is regarded as a brittle material based on its high mineral content. A comparison of the hardness between microindentation and nanoindentation testing is presented in Table 4-1.

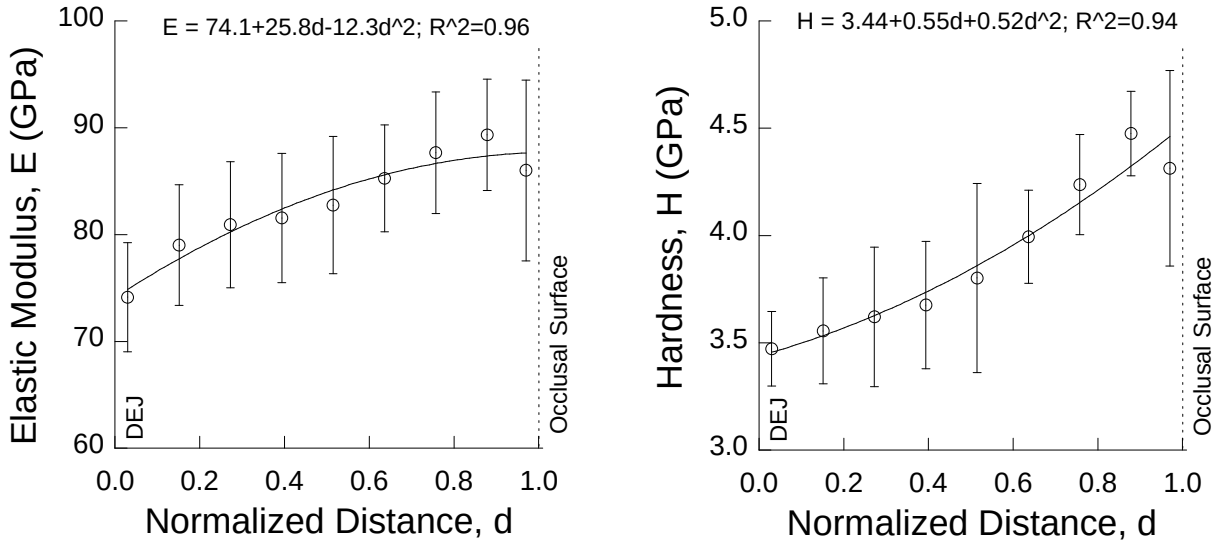

a) elastic modulus **b) hardness**

Figure 4-10. Property distributions of the young cuspal enamel determined using nanoindentation. The normalized distance ranges from 0 (at the DEJ) to 1 (at the occlusal surface).

The spatial trends in hardness are the same for the two approaches. It was found that within the three specific regions the hardness obtained from nanoindentation and the HV_c obtained using Vickers indentations are within approximately 15% of each other; the average difference is 9%.

Table 4-1. Comparison of hardness from microindentation and nanoindentation. Note HV_c and H_{nano} are Vickers hardness and nanoindentation hardness, respectively. % diff was calculated by % diff= $|HV_c - H_{nano}|*100/H_{nano}$.

	Young			Old		
	Inner	**Middle**	**Outer**	**Inner**	**Middle**	**Outer**
HV_c (Gpa)	3.28	3.58	4.08	3.12	3.40	4.01
H_{nano} (Gpa)	3.51	3.80	4.38	3.41	3.83	4.74
% Diff	***6.5***	***5.8***	***6.8***	***8.5***	***11.2***	***15.4***

Therefore, after replacing the transition point hardness (HV_c) with the hardness distribution obtained from nanoindentation, the apparent fracture toughness of the young and old enamel was estimated as a function of distance from the DEJ. The distributions in apparent fracture toughness of the young and old enamel are plotted in terms of normalized

distance from the DEJ in Figures 4-11 (a) and (b), respectively.

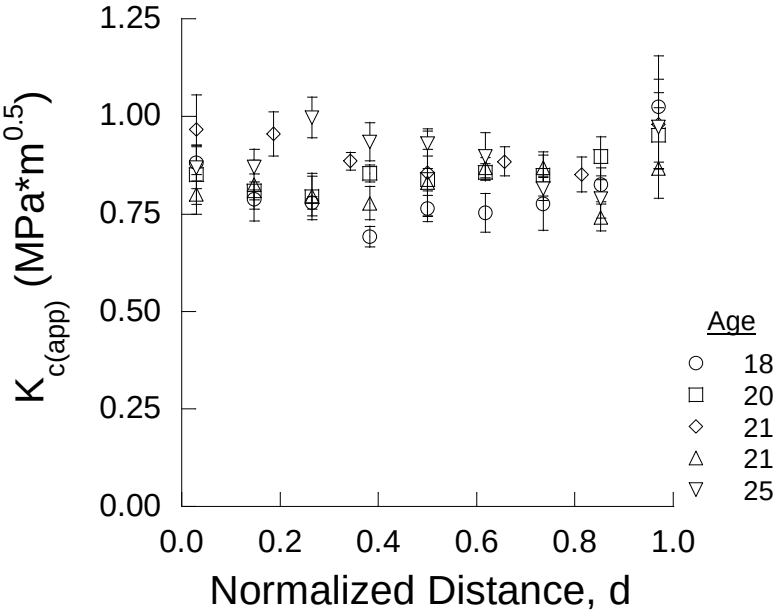

(a) young enamel

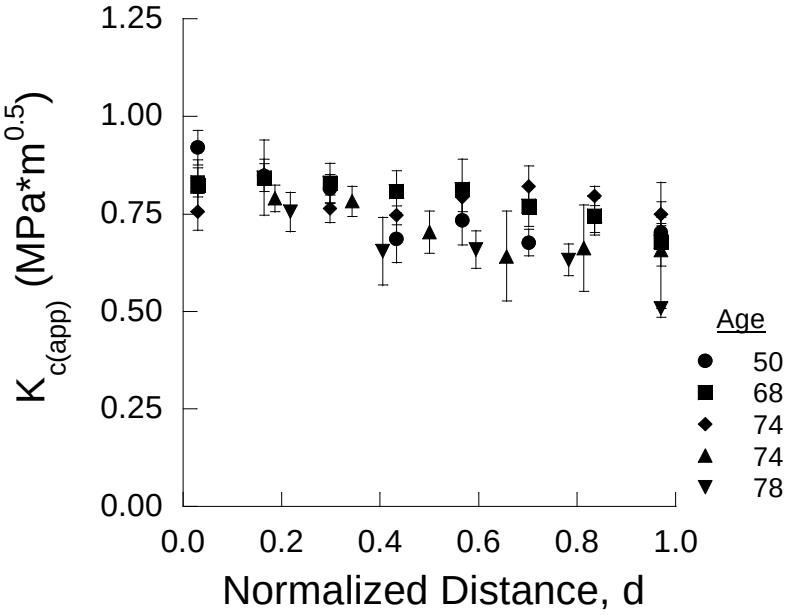

(b) old enamel

Figure 4-11. The apparent fracture toughness distribution of the young and old enamel obtained from indentation fracture resistance testing (Criterion I).

There was no distinct trend in $K_{c(app)}$ of the young enamel with distance from the DEJ (Figure 4-11(a)); the average $K_{c(app)}$ of the young enamel was 0.83 ±0.09 MPa•$m^{0.5}$. In contrast, there was a decrease in the average $K_{c(app)}$ of the old enamel from the DEJ (0.88 MPa•$m^{0.5}$) to the occlusal surface (0.67 MPa•$m^{0.5}$) as evident in Figure 4-11(b). The difference in $K_{c(app)}$ between the two age groups was significant at the occlusal surface ($p < 0.001$), but not within the inner or middle regions.

As mentioned in Chapter 3, three different criteria were considered when measuring crack lengths. For the purpose of comparison, the apparent fracture toughness of the enamel was also calculated choosing the longest crack length (Criterion II) as shown in Figure 4-12.

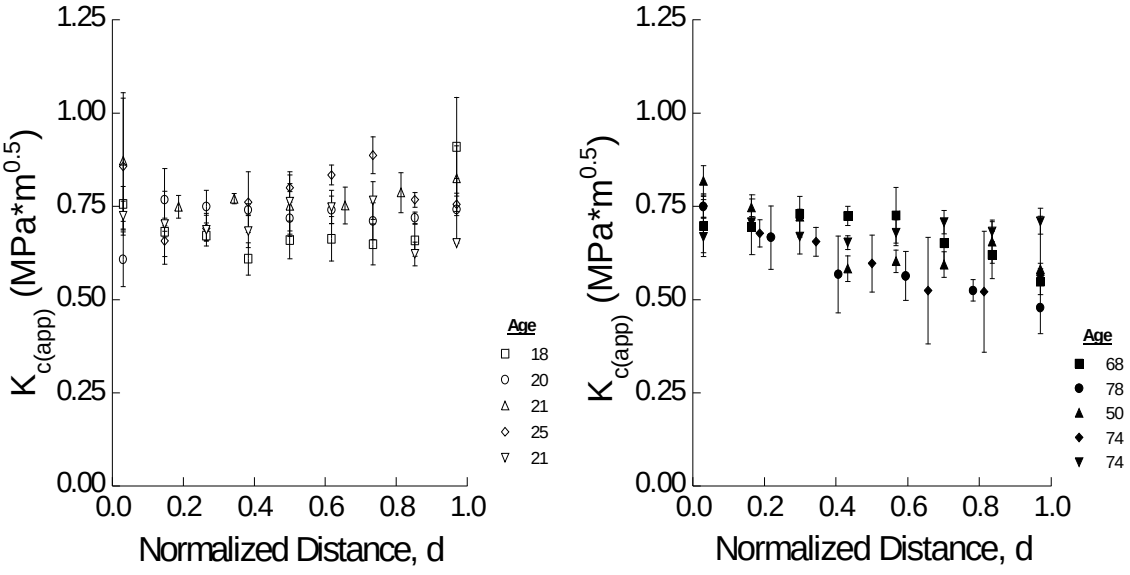

(a) young enamel **(b) old enamel**

Figure 4-12. The apparent fracture toughness distribution of the young and old enamel obtained from the longest crack extension (Criterion II).

As expected, the apparent fracture toughness values obtained using Criterion II were lower than those from Criterion I; the average $K_{c(app)}$ of the young and old enamel was 0.74

±0.072 MPa•$m^{0.5}$ and 0.65 ±0.08 MPa•$m^{0.5}$, respectively. Although these results were lower than those obtained from Criterion I, the overall trends of both age groups were very similar and there were no significant differences in results obtained using the two measures.

4.4 Brittleness

The brittleness of the enamel was estimated according to Eqn. 3-9 using the elastic modulus and hardness from nanoindentation testing and the apparent fracture toughness estimated using results from the indentation fracture resistance test. Results are presented in Figure 4-13. There is an increase in the brittleness from the DEJ towards the occlusal surface, irrespective of patient age.

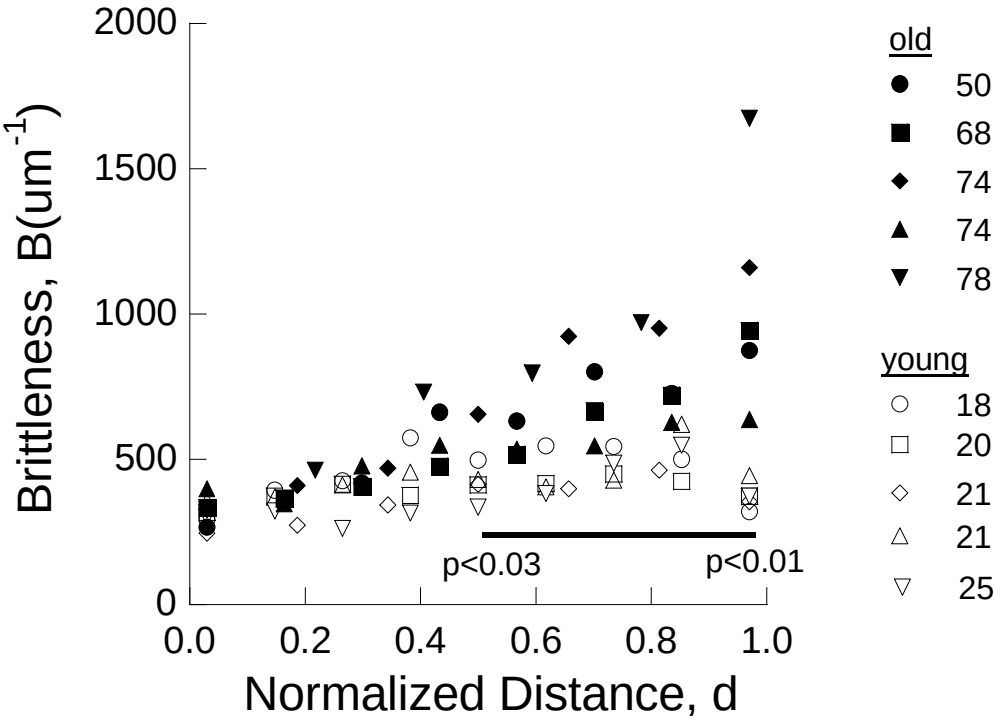

Figure 4-13. Brittleness distribution for the young and old enamel with respect to the distance from the DEJ to the occlusal surface.

Nevertheless, the average brittleness of the old enamel is over 100% greater than that of the young enamel at the occlusal surface. Using the hardness estimated from nanoindentation testing, the average brittleness of the young and old enamel at the occlusal surface was 407 and 1058 μm^{-1}, respectively. The average brittleness of the old enamel is nearly three times higher than that of the young enamel, and the values are significantly different ($p \leq 0.005$). If hardness values obtained using microindentation testing are employed, the average brittleness of the young and old enamel at the same region were estimated as 393 and 897 μm^{-1}, respectively. Average values for the brittleness of enamel within the three regions of evaluation (i.e. inner, middle and outer surface of the enamel) are presented in Table 4-2. Note that the brittleness numbers for enamel are presented for estimates using both microindentation and nanoindentation. Results for the same mechanical properties of the selected dental materials, including the micaceous glass ceramics, feldspathic porcelains and dissimilar are listed in this table as well. Brittleness numbers of the dental materials were computed using these properties published in the dental literature. In general, the brittleness of the dental materials was lower than that of the young and old enamel, except for the Leucite Empress, Finesse and the glass-infused alumina as evident in the table. The feldspathic porcelains exhibited the largest brittleness among the dental materials with values ranging from approximately 200 to 400 μm^{-1}. Yet, its brittleness is still less than half the brittleness numbers estimated for the outer surface region of the old enamel. According to the brittleness index, it was found that enamel is the most brittle material of those studied and the disparity in brittleness between the enamel and restorative materials increases with patient age.

Table 4-2. Mechanical properties of the enamel and selected restorative materials obtained from the indentation analyses. Values presented represent the mean. Note [a] from Quinn et al, [2003], [b] values for the enamel were obtained using indentation and represent apparent toughness ($K_{c(app)}$), and [m], [n] are brittleness numbers measured using hardness values from microindentation and nanoindentation testing, respectively.

Material	HV_c (GPa)	E (GPa)	K_c (MPa*$m^{0.5}$)[b]	B (μm^{-1})
Human Enamel (young)				
Inner	3.1	75	0.88	305^m, 335^n
Middle	3.5	82	0.88	375^m, 416^n
Outer	4.1	87	0.95	393^m, 407^n
Human Enamel (old)				
Inner	3.0	79	0.88	313^m, 348^n
Middle	3.4	90	0.73	582^m, 647^n
Outer	4.0	100	0.67	897^m, 1056^n
Micaceous Glass Ceramics[a]				
Fine (d=1.1 µm)	4.2	71	1.04	271
Medium-fine (d=1.8 µm)	3.6	70	1.18	180
Medium (d=3.7 µm)	3.4	68	1.31	135
Coarse (d=10 µm)	2.7	50	1.65	49
Cmacor glass (d=15 µm)	1.8	64	1.50	51
Feldspathic Porcelains[a]				
Leucite Body	5.6	67	1.14	288
Leucite Incisal	5.3	65	1.26	216
Leucite Finesse	5.6	70	0.99	402
Leucite Empress	5.6	67	1.03	353
Nepheline syenite	6.3	70	1.19	310
Dissimilars[a]				
Zirconia	13.9	210	4.90	122
Glass-infused alumina	11.7	250	3.10	304
Glass-ceramic	5.5	104	2.80	73

Chapter 5

Discussion

The elastic modulus and hardness of the young and old enamel were quantified using the nanoindentation method as a function of distance from the dentin-enamel junction (DEJ) and within three different regions of the crown (i.e. cervical, cuspal, and inter-cuspal). Furthermore, the apparent fracture toughness and brittleness of the enamel in both age groups were investigated with respect to the distance from the DEJ using measurements obtained from both microindentation and nanoindentation. Results from this study showed that both location and patient age are important to the mechanical behavior of enamel and should be considered in future evaluations of the mechanical behavior of this hard tissue.

5.1 Elastic Modulus and Hardness

The average elastic modulus of the young and old enamel obtained from results of nanoindentation were found to be 84.4 ± 4.4 GPa and 91.1 ± 6.5 GPa, respectively. Similarly, the average hardness of these two age groups was 4.0 ± 0.3 GPa and 4.0 ± 0.5 GPa, respectively. Results obtained from this study exhibited good agreement with results of previous studies (Table 2-2 and 2-3), although most previous studies did not specify the patient age. Also consistent with earlier investigations, both properties increased with distance from the DEJ. Cuy *et al*., [2002] analyzed the mechanical properties of human enamel using nanoindentation mapping. Their results showed that the elastic modulus and hardness of the enamel were dependent on distance from the DEJ. Near the DEJ the elastic modulus and hardness were reported to be approximately 70 GPa and 3 GPa, respectively, whereas at the occlusal surface they were approximately 115 GPa and 6 GPa, respectively. They reported that these variations are attributed to the changes in chemistry and microstructure and concluded that the chemical composition is the most critical factor that influences the mechanical properties of human enamel.

Spatial variations in the mechanical properties of enamel could be attributed to a number of factors, the most likely of which are the potential differences in crystallography and chemical composition. The hydroxyapatite crystals of outer enamel are considered more densely packed and tightly arranged than those within the inner enamel [Shore *et al*., 1995]. Also, enamel exhibits tubules near the DEJ, which would reduce the effective volume fraction of mineralized tissue in this region and contribute to the comparatively lower hardness and elastic modulus [Ichijo *et al*., 1993]. Yet, the largest contributions to spatial variations in properties are expected to be the chemical composition and corresponding

level of mineralization. There is a natural reduction in the interprismatic organic matrix with maturation and that physical space is replaced with mineral. Indeed, the elastic modulus and hardness of the young and old enamel at the occlusal surface were significantly different; for the old enamel the average elastic modulus and hardness at the occlusal surface were greater than 100 and 4.7 GPa, respectively. For the young enamel they were approximately 85 and 4.3 GPa, respectively. It is believed that this difference may be related to the influence of fluoride and the development of fluorapatites. Lester and Boyde [1986] investigated the influence of fluoride on human teeth and concluded that prolonged exposure to fluoride in the oral environment results in a gradual increase in mineral content, particularly near the tooth's surface. As such, the increase in hardness and elastic modulus of the old enamel with distance from the DEJ is expected to be attributed to a higher mineral content near the tooth's surface and is the result of more than one mechanism.

While there was no significant difference in the average properties between the two age groups, there were significant differences between the properties of young and old enamel near the tooth's surface as evident in Figure 4-6. No prior study has identified differences in the properties of enamel related to patient age. Considering all three regions of evaluation (cervical, cuspal and inter-cuspal regions) the elastic modulus and hardness of the old enamel were 16% and 12% greater than those properties for young enamel at the tooth's surface. Surprisingly, the increase in these properties with age was also accompanied by a reduction in property variation. The coefficient of variation (COV) for the elastic modulus and hardness measurements are shown as a function of normalized distance from the DEJ in Figure 5-1. Mechanical properties of the old enamel exhibited the lowest COV in all regions of evaluation. Furthermore, the COV for properties of the

old enamel was lowest near the tooth's surface, whereas in young enamel the variation was highest at the tooth's surface.

One of the most interesting aspects of property variations with normalized distance (Figure 5-1) is the comparatively higher variation midway between the DEJ and tooth surface (i.e. normalized distance is approximately 0.5) in the young enamel. This trend has never been reported before, is most distinct in the elastic modulus (Figure 5-1 (a)), and could result from the competing influences of two transport processes. Diffusion of mineral ions within enamel that originate from saliva undoubtedly decreases with increasing distance from the tooth's surface. Consequently, mineral changes would be expected to occur less rapidly within the inner enamel. However, there is also another potential route for diffusion from the tooth's interior through the dentin tubules. Due to the positive pulpal pressure and additional driving force posed by the oral pH, there is potential for diffusion of mineral ions from dentin to enamel, especially in young teeth. Lynch and Ten Cate [2006] recently found that remineralization of enamel lesions was accelerated by diffusion of dissolved dentin mineral, and that the process was largely dependent on the relative distance between the enamel and dentin. Therefore, the difference in enamel thickness within the cervical, cuspal and inter-cuspal regions changes the relative contribution of the two modes of diffusion, and their potential for causing an increase in mineralization. Longer paths within the cuspal (B-E) regions would be less likely to exhibit uniform property changes with distance than shorter paths within the cervical region (A, F). Therefore, the largest variation in properties for the three regions of evaluation would be expected to appear midway between the DEJ and the tooth's surface, and should be most evident when examined in terms of the normalized distance as identified in Figure 5-1. In the old enamel, the smallest property variations were evident at the tooth's surface. If the increase in the

elastic modulus and hardness of enamel result from a higher mineral content, then the combination of lower variation and significantly higher values in these properties at the tooth's surface suggests that the level of mineralization reaches a point of saturation after a specific age. Also of interest, according to the consistency in properties within the cervical, cuspal and inter-cuspal regions, the saturation appears to occur uniformly across the entire crown of the tooth.

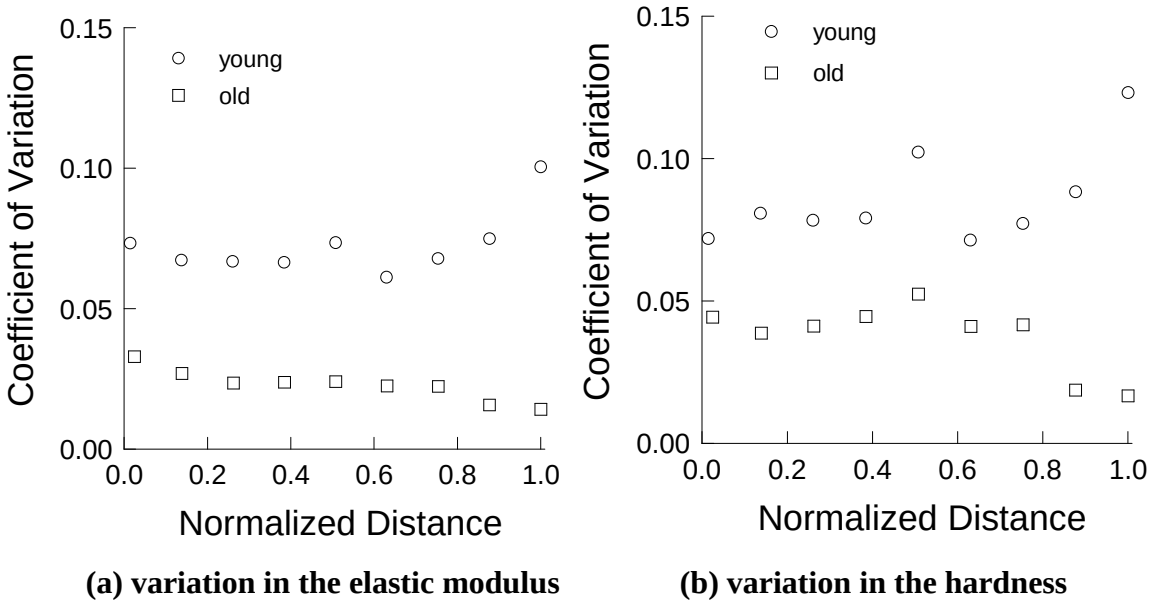

(a) variation in the elastic modulus **(b) variation in the hardness**

Figure 5-1. Coefficient of variation for the mechanical properties (elastic modulus and hardness) as a function of normalized distance from the DEJ.

It is expected that the increase in elastic modulus and hardness with age is at least partly associated with a reduction in the extent of interprismatic organic matrix. Previous studies have highlighted importance of the proteinaceous matrix on energy absorption, crack extension and the fracture toughness of this tissue. As a matter of fact, White *et al.* [2003] postulated that the larger fracture toughness of enamel in comparison to hydroxyapatite is associated with the unique mechanisms of toughening enabled by the organic matrix. If the increase in hardness and elastic modulus results from a reduction in the volume

concentration of the organic matrix, then there would be an expected decrease in the fracture toughness of enamel with age, as well.

5.2 Indentation Size Effect

Similar to other brittle materials, the enamel exhibited indentation size effects. Figure 5-2 presents the average Vickers hardness of the young and old enamel as a function of applied loads. A comparison of these two distributions shows that the Vickers hardness of both the young and old enamel is dependent on the indentation load and becomes constant beyond a specific magnitude of load. Contrary to results of the elastic modulus and hardness between the two age groups, there was no significant difference found in the indentation size effects. In both groups, the indents made with loads of less than 0.5 N or less (i.e. 0.1, 0.25 and 0.5 N) were associated with inelastic deformation, whereas indents made with loads of 0.5 N and greater underwent a combination of inelastic deformation and fracture through microcracks and well-defined cracks that developed along the periphery. Loads larger than 2 N were mostly associated with the development of well-defined cracks at the indentation corners as shown in Figure 4-8. It is important to highlight that the degree of microcracking and/or well-defined cracks was location dependent. Microcracking was more extensive near the DEJ (Figure 4-9) in the enamel from both age groups, but the development of well-defined cracks was most extensive in the outer enamel and particularly in the old enamel. It is believed that this behavior was the result of the organic sheath surrounding the prisms and the increases in organic proteins near the DEJ. The reduction in hardness of enamel with increasing load distinguishes that there is a change in the mechanistic response to concentrated contact loads. Overall, these results emphasize that human enamel does not exhibit a single hardness (for loads less than 2 N) and that

reported measurements in this study can reflect contributions from two different components of material behavior.

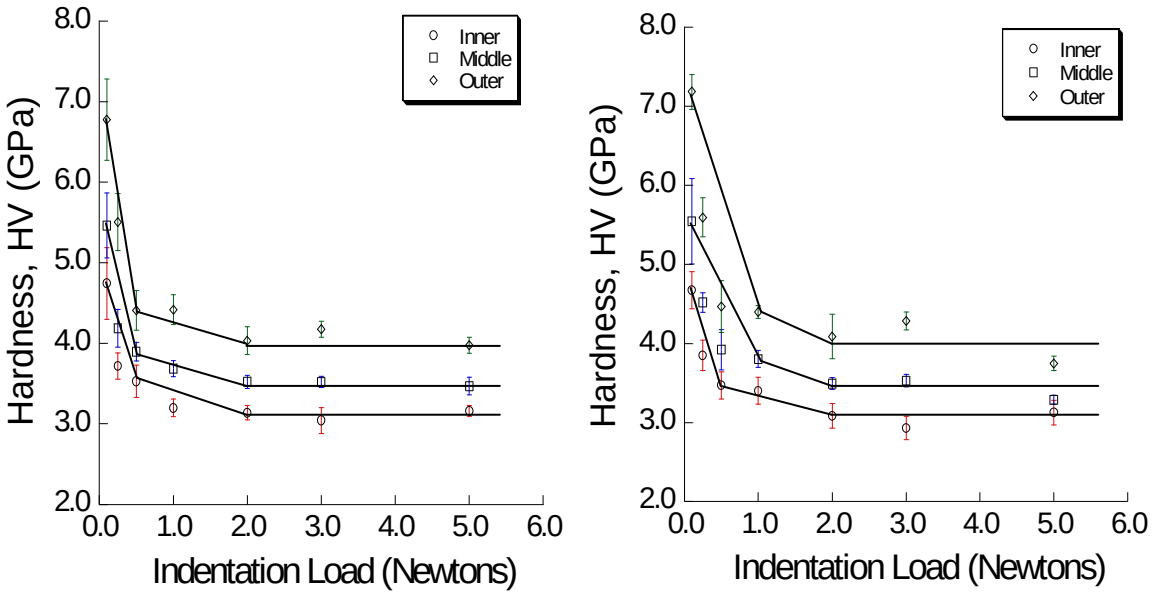

(a) young enamel **(b) old enamel**

Figure 5-2. Indentation size effects for young and old enamel. These results represent the average of all the Vickers hardness values for each age group.

Specifically, at indentation loads less than 0.5 N, the measurement reflects the enamel's ability to resist permanent deformation in the classical sense (i.e. through quasi-ductile dissipative mechanisms). Hardness measurements conducted between the aforementioned load range (0.5 N < P < 2 N) are influenced by a combination of dissipative processes, namely comprising deformation and fracture. At indentation loads equal to 2 N and larger, hardness measurements largely represent the tissue's resistance to indentation damage through the development of new surface area (i.e. brittle fracture). Despite the significance of this finding, only a single investigation [Collys *et al*., 1992] has addressed the potential for load dependence in the tissue's response. In that study all samples, including sound, demineralized human enamel and bovine enamel showed the load dependency in the hardness measurements. It was found that the Knoop hardness number (KHN) decreased

with an increase in the applied load. Apart from that investigation, no prior study has distinguished the indentation size effects in enamel and the mechanistic contributions to the mechanical behavior of this tissue. The literature is full of experimental studies that have evaluated the hardness of enamel after bleaching and whitening treatments. However, they rarely considered the load dependence in material response in their comparison of results with studies that used a difference indentation load. Results from the present study indicate that values of hardness obtained at different loads cannot be compared objectively, and that the measured hardness may not represent the aspect of material behavior that is of primary interest.

5.3 Indentation Fracture Toughness (IFT)

Earlier investigations have reported the fracture toughness of enamel and most investigations adopted the indentation method of evaluation due to the limited testing volume. According to complications associated with this method [Quinn and Bradt, 2007], it is considered more appropriate to call it 'Indentation Fracture Resistance', rather than fracture toughness. It is described here as the "apparent" fracture toughness in recognition of the concerns and contributions of earlier studies. Results for $K_{c(app)}$ for the young enamel (Table 4-2) are within 20% of that reported by Xu *et al*., [1998] and Caputo *et al*., [1981]. However, the closest agreement is obtained with the results presented by Marshall *et al*., [2000]. That group conducted the indentation fracture toughness test with applied loads of 6 and 8 N, which are at least twice the load used in the present study, but are obtained at loads which provide constant hardness (Figure 5-2). The estimated fracture toughness reported in their investigation ranges between 0.6 to 0.9 $MPa*m^{1/2}$, whereas in the present study this value ranges from 0.67 to 0.88 $MPa*m^{1/2}$ for the old enamel, and 0.88 to 0.95

$MPa*m^{1/2}$ for the young enamel. The consistency in the apparent fracture toughness with these earlier studies provides confidence in the method of measurement.

The apparent fracture toughness reported by Xu *et al*., [1998] and Caputo *et al*., [1981] were lower than those determined in the present study. Caputo *et al*., [1981] found that the apparent fracture toughness of enamel was dependent on the tooth type, prism orientation and the specific location evaluated. Again, differences in $K_{c(app)}$ between reported studies are not unexpected due to the experimental difficulties and limitations of the indentation fracture test. Quinn and Bradt [2007] addressed the primary drawbacks of the Vickers indentation fracture toughness test (IFT) and concluded that the processes of crack initiation and extension are not technically the same as that in the standardized/conventional fracture toughness tests. Also, there was some ambiguity in these earlier investigations as to whether the introduced crack in enamel had a Palmqvist or radial crack configuration. For example, Xu *et al*., [1998] and Marshall *et al*., [2000] assumed that the cracks in their investigations had a radial crack configuration, whereas Caputo *et al*., [1981] and the present study treated it as a Palmqvist configuration. That configuration was validated in Chapter 3. Assuming different crack configurations (either Palmqvist or median/radial) results in having to adopt different equations to calculate the fracture toughness, and this discrepancy in adopting an appropriate equation may cause differences in the measurement of apparent fracture toughness. Note, however, that despite using equivalent applied load, temperature, indentation duration time and sample preparation in the present study, the results from the two age groups were significantly different. The distinct difference in the estimated toughness indicates that the indentation fracture resistance test provided an objective evaluation, and served as a useful method to distinguish differences in fracture resistance that were attributed to the independent variables.

It is believed that the present study is the first investigation to distinguish that the apparent fracture toughness of the enamel becomes lower with increasing distance from the DEJ. Also, the apparent fracture toughness of the two age groups was significantly different near the occlusal surface; the average values of the young and old enamel near the occlusal surface were 0.96 MPa*$m^{1/2}$ and 0.64 MPa*$m^{1/2}$, respectively. In fact, the outer surface of the old enamel has the lowest apparent fracture toughness among the materials evaluated in this investigation (Table 4-2). The distribution in $K_{c(app)}$ at the tooth's surface over the entire age range evaluated is shown in Figure 5-3.

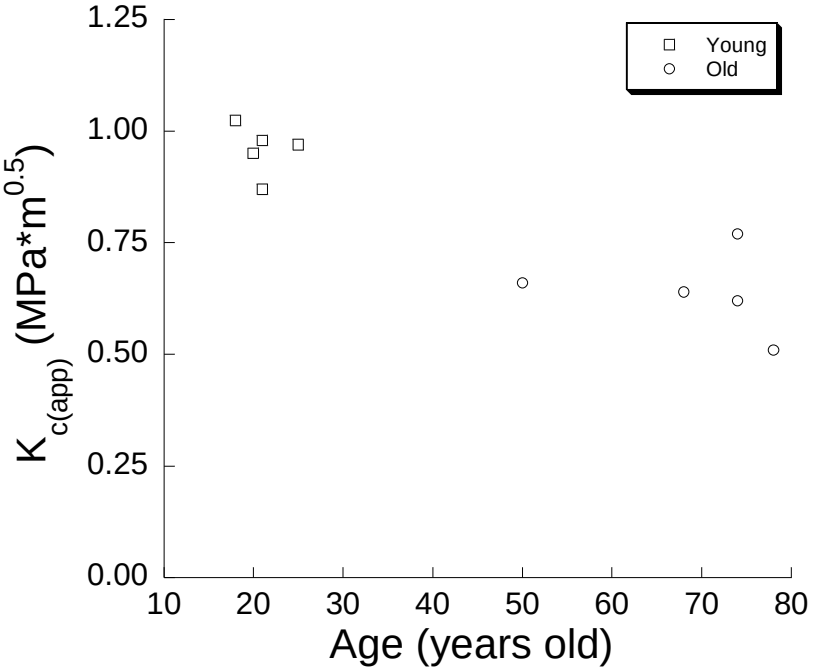

Figure 5-3. Apparent fracture toughness for the young and old enamel near the occlusal surface (outer region). Note that the young and old patient ranges from 18 to 25 years old and from 50 to 78 years old, respectively.

Interestingly, there appears to be a continuous decrease in the apparent toughness with increasing age. Using a linear estimation for the decrease, there is a reduction of approximately 0.1 MPa*$m^{1/2}$ every 10 years. Due to the longer period of exposure of

anterior teeth in comparison to 3rd molars, they may undergo an even greater decrease in toughness over the lifespan of an individual.

5.4 Brittleness

As described in Chapter 2, conventional properties, including the elastic modulus, hardness and fracture toughness, provide valuable measures for characterizing the mechanical behavior of a material. Yet, these mechanical properties are insufficient in accurately delineating a material's brittleness and brittleness is a critically important aspect of mechanical behavior for dental materials. Brittleness numbers estimated for the young and old enamel in this study exhibited distinct differences as shown in Figure 4-12 and Table 4-2. The brittleness numbers at the occlusal surface are presented as a function of the patient age in Figure 5-4. As evident in this figure, there is an increase in the brittleness with patient age. Specifically, the average brittleness number of the oldest enamel at the occlusal surface is more than three times greater than that of all young enamel evaluated.

As described in Section 5.2, there are two relevant age-related processes that may contribute to the observed differences; namely, there is a reduction of the interprismatic organic matrix and an increase in mineral content. Specifically, there is a reduction in the proteinaceous matrix residing along the prism boundaries as a result of natural maturation and oral conditions that lower the oral pH [Ten Cate, 1998]. In turn, prolonged exposure to mineral ions and fluoride within the oral environment can promote replacement of the organic material with fluoro-apatities [Robinson *et al*., 1995]. Therefore, the larger brittleness of the old enamel is expected to result from a reduction in the interprismatic

organic matrix and an increase in mineral content, both of which would reduce the resistance to cracking and brittle fracture.

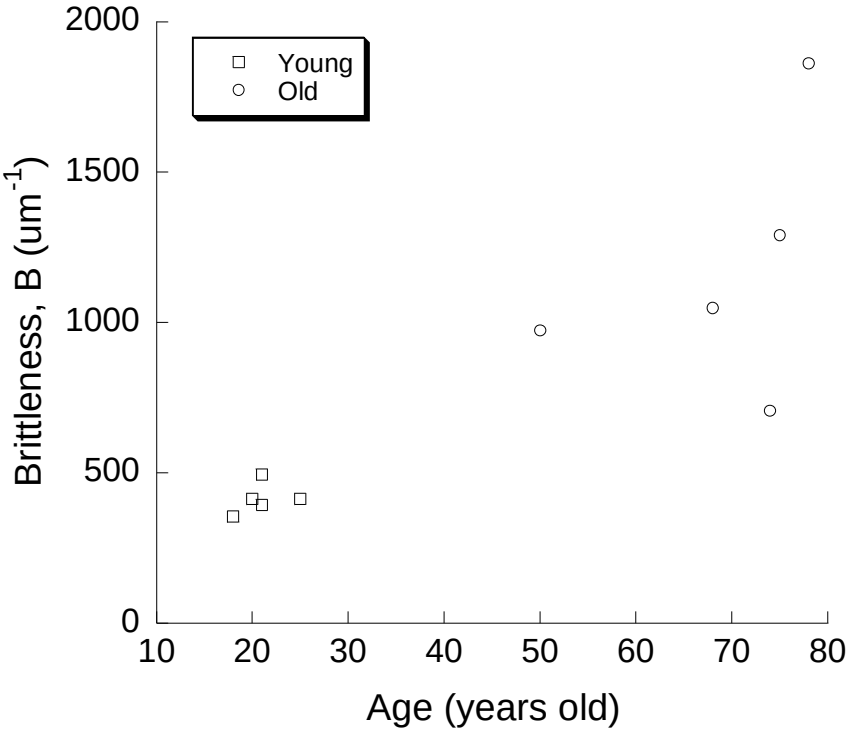

Figure 5-4. Brittleness numbers of the young and old enamel near the occlusal surface (outer region) with respect to the patient age. Note that the young patients range from 18 to 25 years old, whereas the old patients range from 50 to 78 years old.

Treatments that accelerate these processes could cause embrittlement of enamel. For example, tooth whitening releases contaminants from the enamel that bind to the interprismatic protein [Walton and Rotstein, 1996]. Bleaching removes these contaminants and causes the loss of a small degree of protein, as well. These regions are then "repaired" by the deposition of fluoroapatites, which cause an increase in the mineral content and could cause detrimental increases in the brittleness.

The importance of the interprismatic organic matrix on the mechanical behavior of enamel has received recent attention. In evaluations of the stress-strain characteristics and creep responses [He and Swain, 2007], it was reported that the enamel behaves more like a metal

than a ceramic, and that the protein content of the organic interprismatic enamel is the essential medium bestowing enamel with damage tolerance. A related study [He and Swain, 2007] also showed that the time-dependent behavior of enamel is lost when heated to temperatures that cause irreversible property changes to the organic matrix. It is believed that brittleness of the old enamel is greater than that of the young enamel due to changes in the material's capacity to undergo deformation and its propensity for fracture. Specifically, the microstructural changes cause a reduction in the energy dissipation by inelastic deformation and an increase in that via cracking and fracture. Overall, these results highlight that the interprismatic protein matrix may be more important to the initiation of cracks and brittle fracture of enamel than its contribution to elastic or inelastic deformation.

When compared to the young enamel, there is a marked increase in brittleness of the old enamel with distance from the DEJ, as well as a larger degree of variation in the brittleness numbers between the five samples. Yet, the old enamel is significantly more brittle than the examined dental materials and the young enamel, and particularly, at the occlusal surface. The comparatively high brittleness numbers of the old enamel distinguish that it becomes more likely to dissipate strain energy via fracture. These results forecast the potential problems that may arise in cyclic contact between enamel and dental materials in the teeth of senior patients. Dental restoratives have far lower brittleness numbers than the old enamel as evident in Table 4-2, which suggests that old enamel may be more likely to undergo the development of damage under cyclic contact than the restorative.

In application to dental materials, the brittleness index has several advantages. For example, brittleness numbers for the dissimilar ceramics (Table 4-2) underscored the qualitative differences between the brittle alumina and the tough zirconia that has been observed in

Hertzian contact studies [Peterson *et al*., 1998]. For the MGCs, the brittleness numbers range from approximately 50 to 300 μm^{-1} and increase with a reduction in mica platelet (grain) size. Previous studies on the contact damage resistance of MGCs have shown that coarse grain structures undergo substantial quasi-plastic deformation under Hertzian contact and thereby suppress the development of detrimental cone-cracks, while finer grain MGCs undergo a much greater degree of brittle contact damage [Peterson *et al*., 1998]. The brittleness numbers for the MGCs in Table 4-2 clearly distinguish the increase in brittleness with decreasing grain size. However, Yio *et al*., [2000] reported that MGCs with coarse grains have lower damage resistance under dynamic fatigue, despite their low brittleness. Thus, further investigations are necessary to understand the implications of the brittleness numbers determined for enamel on other aspects of the mechanical behavior.

5.6 Sources of Error

Although it is believed that this study has provided additional understanding of the mechanical behavior of human enamel, there are recognized limitations and potential sources of error that should be addressed. For example, the extracted teeth were stored at 2 ºC in HBSS for approximately three weeks prior to testing. The HBSS storage medium was used to maintain them in a hydrated condition and to avoid demineralization as this may cause property changes in the specimens. An earlier investigation [Habelitz *et al*., 2002] reported that there is no property change up to two weeks if a tooth is stored in HBSS. It is assumed that the longer storage period had minimal effects on the measured results as the pH of the solution is greater than 7. Another issue is that testing temperature was different from that of the oral environment. The specimens were tested at room temperature (around 21 ºC), while the oral temperature is approximately 37 ºC. It is

unknown whether or not the mechanical properties of enamel are influenced by these different temperatures. However, few earlier investigations [El Mowafy and Watts, 1986; Rasmussen *et al*., 1976] have reported that if a testing temperature is maintained between 0 and 60 ºC (0< T< 60 ºC), the temperature is not a significant factor on the fracture toughness and bonding strength of human dentin. Dentin has higher organic content than enamel. Thus, it would be a reasonable assumption that the estimated mechanical properties of the enamel are not affected by the lower testing temperature.

Results obtained from nanoindentation testing are greatly affected by the polishing quality since both the elastic modulus and hardness are calculated by the indentation contact area. Although each specimen was prepared with great care to maintain the same quality, the surface quality achieved for each specimen may not be uniform. To minimize variations on the surface roughness, each sample's surface was scanned to insure that a similar surface roughness was achieved (the surface roughness was approximately 0.01 µm ± 0.003). Consequently, the influence of surface texture on the property evaluation is expected to be minimal.

Recent evaluations have shown the importance of measurement parameters in quantifying properties of enamel using nanoindentation. The indentation load and depth could influence the relative contributions of the interprismatic matrix to the measured properties. All the indentations in the present study were introduced using the same load, which provided an objective and consistent basis for comparison. In nanoindentation testing, the applied load was 5 mN and was determined by considering the machine's capability and the measurement parameters used in previous investigations. Several preliminary tests were conducted to determine an optimal load. But as addressed previously, enamel

exhibits indentation size effects and applying a single load may lead to potential limitations. In spite of the indentation size effects in enamel, in the preliminary tests loads from 1000 to 9000 μN were applied and variations in the elastic modulus and hardness were within approximately 10%. Therefore, the use of a single load does not appear to be a necessity or substantial limitation to the nanoindentation evaluation.

The calibration and alignment of the testing machine plays a critical role on the accuracy of nanoindentation results. To prevent error due to poor calibration and alignment of the machine, calibration tests were conducted periodically and the alignment was inspected by the indentation geometry. For example, the calibration test was done on the reference sample (fused quartz) to ensure whether constants obtained from the tip area function test were acceptable or not. Measurement of the hardness and elastic modulus of the reference sample were within 2% of the accepted values. Also, most measures of E and K_c for the dental materials were not determined using indentation techniques. That could result in some bias in values of the brittleness calculated for these materials. Nevertheless, the variations in brittleness from differences in measurement technique are expected to be far smaller than the difference in brittleness associated with age.

The measurement resolution of the optical device used to measure indentation cracks was ±1 μm. Although careful attention and consistency was always practiced, crack length measurements were relatively subjective. Also, the crack tip was not always distinct, and due to this reason it was difficult to achieve completely objective crack length measurements. Nevertheless, it is believed that the overall result was not affected by these complications. Moreover, if errors are involved in the measurement of crack lengths, they would be distributed evenly in both age groups. Therefore, the influence of this error

would be minor and it would not be a critical contributor in estimating the apparent fracture toughness.

Lastly, enamel is structurally anisotropic. The orientation of the inorganic prism in enamel should affect the mechanical behavior, especially when measuring the indentation fracture toughness and brittleness numbers. However, a recent paper [Bradly *et al*., 2007] reported that in nanoindentation testing, the prism orientation of enamel is not a significant contributor to measures of the elastic modulus and hardness of enamel. Nevertheless, the prism orientation of enamel is expected to be a significant factor when measuring the apparent fracture toughness. Therefore, the measured apparent fracture toughness in the present study is limited to conditions where the indentation tip is parallel to the prism axis.

Despite these concerns and limitations, results of this experimental investigation have extended the current understanding of the mechanical behavior of human enamel and established that patient age is an important contributor to the mechanical properties.

Chapter 6

Conclusions and Future Research

An evaluation of the changes in mechanical properties of human enamel with aging was conducted. Fully erupted 3rd molars were acquired and divided into two groups corresponding to young ($18 \leq age \leq 30$) and old ($55 \leq age$) patients.

6.1 Conclusion

The hardness and elastic modulus were quantified using nanoindentation testing. Mechanical properties were examined as a function of distance from the DEJ and in three regions of the tooth (i.e. cervical, cuspal and inter-cuspal regions). The indentation fracture toughness and brittleness of human enamel and common crown replacement materials were estimated by microindentation testing. Also, indentation size effects of human enamel and selected dental restoratives were examined. According to results of the evaluation, the following conclusions were drawn:

1) The overall average elastic modulus of enamel from the young and old patients was 84.4 ±4.4 and 91.1±6.5 GPa, respectively. The overall average hardness from the young and old patients was 4.0 ± 0.3 GPa and 4.0 ± 0.5 GPa, respectively. There was no significant difference in the average properties between the young and old enamel.
2) The elastic modulus and hardness of enamel increased with distance from the DEJ for both age groups. When examined in terms of absolute distance from the DEJ, the gradient in hardness and elastic modulus was largest within the cervical region. However, when examined in terms of normalized distance from the DEJ, the properties distributions within each of the three regions were consistent.
3) The elastic modulus and hardness of the old enamel were 16% and 12% greater than those properties for young enamel at the tooth's surface. The differences in these properties between the two age groups were significantly different.
4) The Vicker's hardness of enamel was a function of the indentation load and exhibits indentation size effects. There was a decrease in hardness of enamel with increasing load. The hardness became load independent beyond a load of 2 N, which results from an increase in energy dissipation through the development of cracks and brittle fracture.
5) The average apparent fracture toughness $K_{c(app)}$ of the young enamel was 0.83 ± 0.09 MPa*$m^{0.5}$. No distinct trend in $K_{c(app)}$ of the young enamel was found with distance from the DEJ. Contrary to the young enamel, there was a decrease in the average $K_{c(app)}$ of the old enamel from the DEJ (0.88MPa*$m^{0.5}$) to the occlusal surface (0.67MPa*$m^{0.5}$). The difference in the average $K_{c(app)}$ between these age groups was significant at the occlusal surface ($p<0.001$), but not within the inner and mid the regions.

6) The average brittleness of the young enamel increased from 300 μm^{-1} at the DEJ to 400 μm^{-1} at the occlusal surface. The average brittleness of the old enamel increased from 310 μm^{-1} at the DEJ to nearly 900 μm^{-1} at the occlusal surface. At the DEJ there was no significant difference in brittleness between the young and old enamel. However, at the occlusal surface the brittleness of the old enamel was significantly greater ($p<0.02$) and between 2 to 4 times larger than that of young enamel.
7) The brittleness calculated for the porcelain, ceramic and micaceous glass ceramic restorative materials ranged between 50 and 400 μm^{-1}. Their comparatively low brittleness suggests that contact loading of the restoratives is more likely to promote either elastic or inelastic deformation than fracture, in comparison to enamel.
8) The enamel was the most brittle material of all those evaluated in this investigation and its brittleness increased with patient age. The brittleness index could serve as a useful scale in the design of materials used for crown replacement, as well as a quantitative tool for characterizing degradation in the mechanical behavior of enamel.

6.2 Future Research

It is clear that results from the present study contribute to our understanding of the mechanical behavior of human enamel and selected dental restoratives. However, there are still many topics that need to be explored. Further research is needed to provide additional understanding. Some recommendations of future research are listed below.

1) In the present study, only young and old enamel were examined. It is recommended that future work needs to be done to examine the properties over a more continuous age spectrum.
2) The present study did not couple measurements of the mechanical property distribution with a complementary examination of the enamel chemistry. Therefore, an investigation of differences in the chemical composition between young and old enamel will provide valuable data towards understanding their mechanical behavior.
3) This investigation did not perform an additional evaluation to determine whether the brittleness index correlates with a material's scratch and/or wear resistance. Consequently, the higher brittleness numbers for the old enamel cannot necessarily be used to indicate that it is more likely to fail through any one of the aforementioned modes without additional evidence. Further study should address these relationships.
4) The mechanical behavior of the interprismatic organic matrix has received recent attention. It is believed that a reduction in the volume concentration of the organic matrix with age results in a decrease in the fracture toughness of the enamel. Our preliminary test shows that the complex modulus of the enamel prisms and the interprismatic organic matrix can be examined using nanoindentation as evident in Figure 6-1. It would be valuable to verify that the changes in mechanical properties with patient age are attributed to loss of the interprismatic organic matrix or that the differences in organic content are responsible for the spatial variations in mechanical properties.

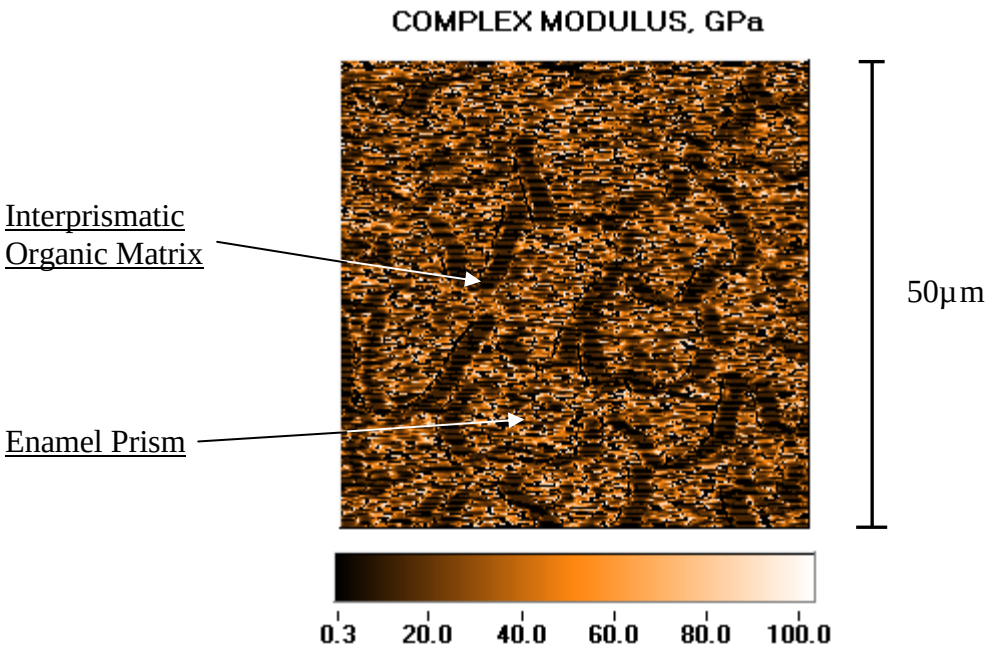

Figure 6-1. Complex modulus map of the enamel prism and interprismatic organic matrix at the occlusal surface in young enamel (23 years old).

Appendix A

Elastic Modulus and Hardness

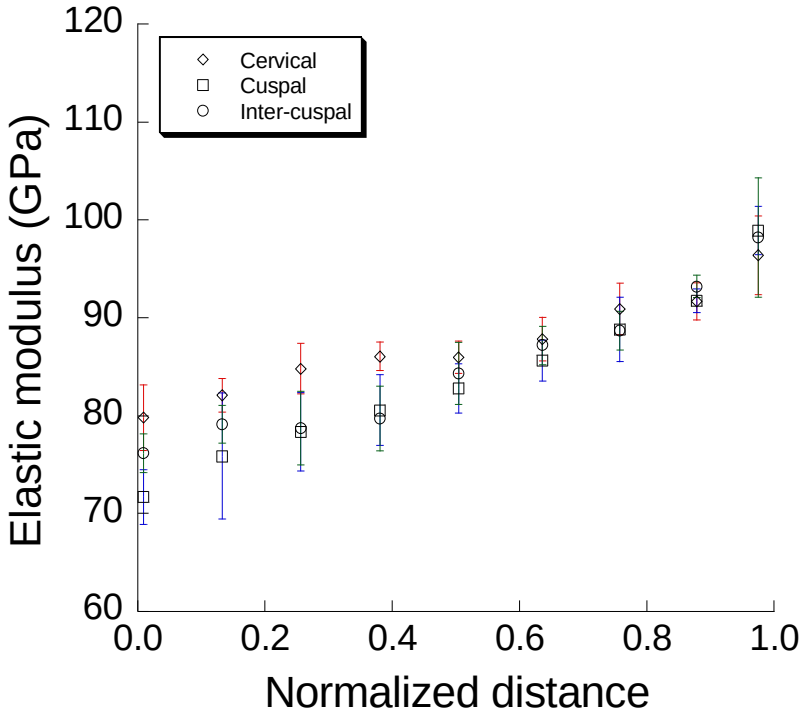

(a) Elastic modulus

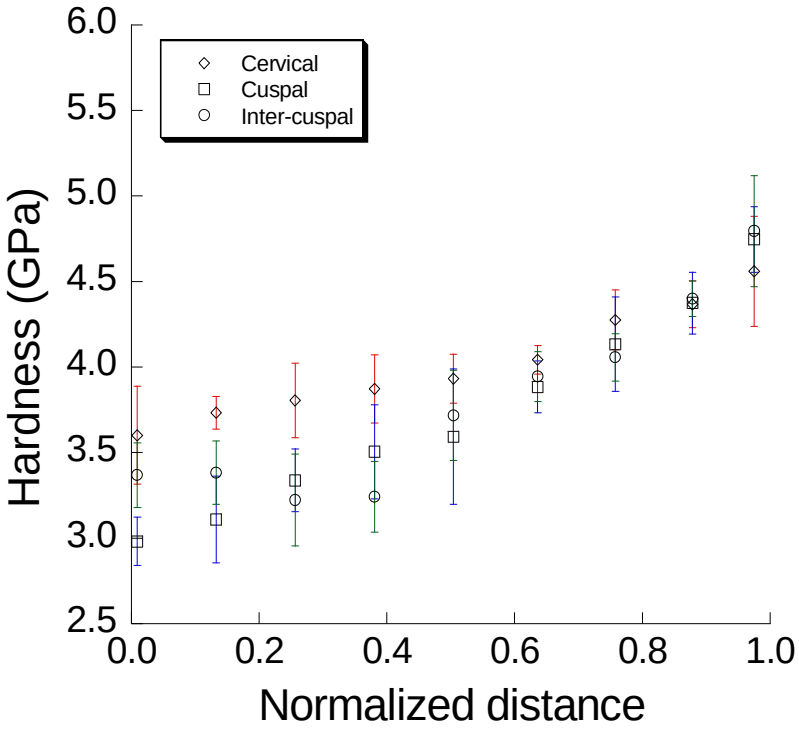

(a) Hardness

Figure A-1. Specimen #1 (60 years old, Male)

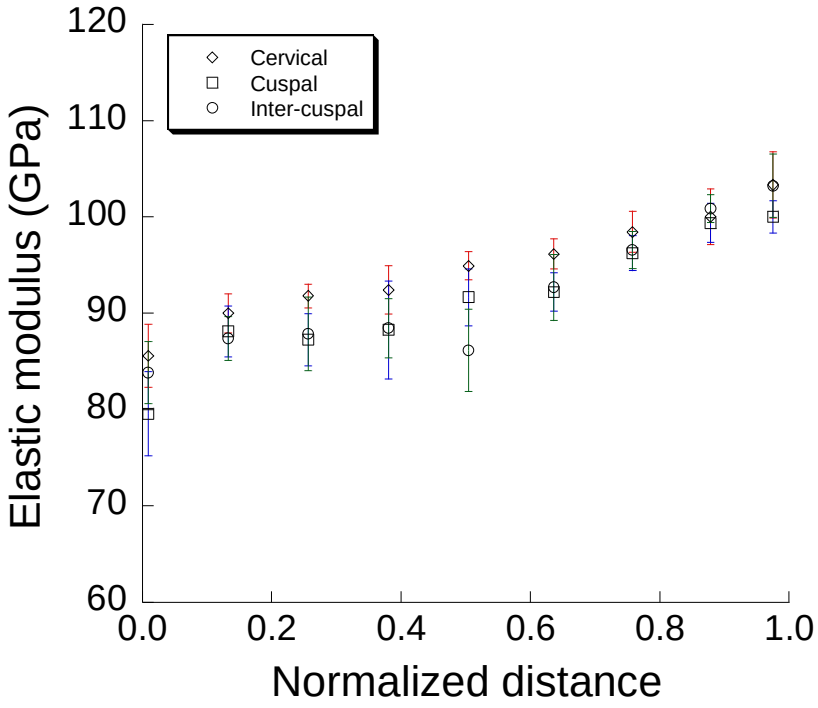

(a) Elastic modulus

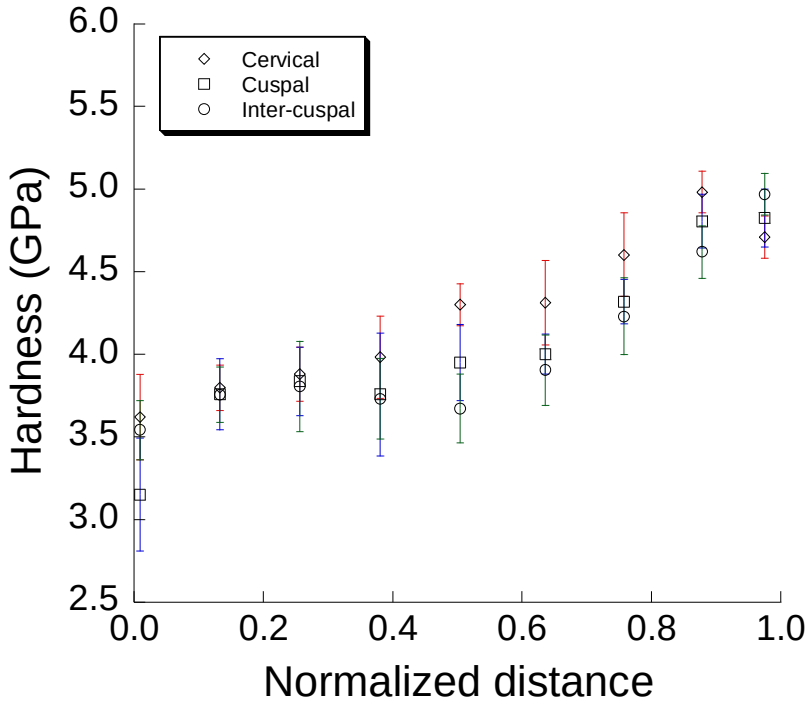

(b) Hardness

Figure A-2. Specimen #2 (92 years old, Female)

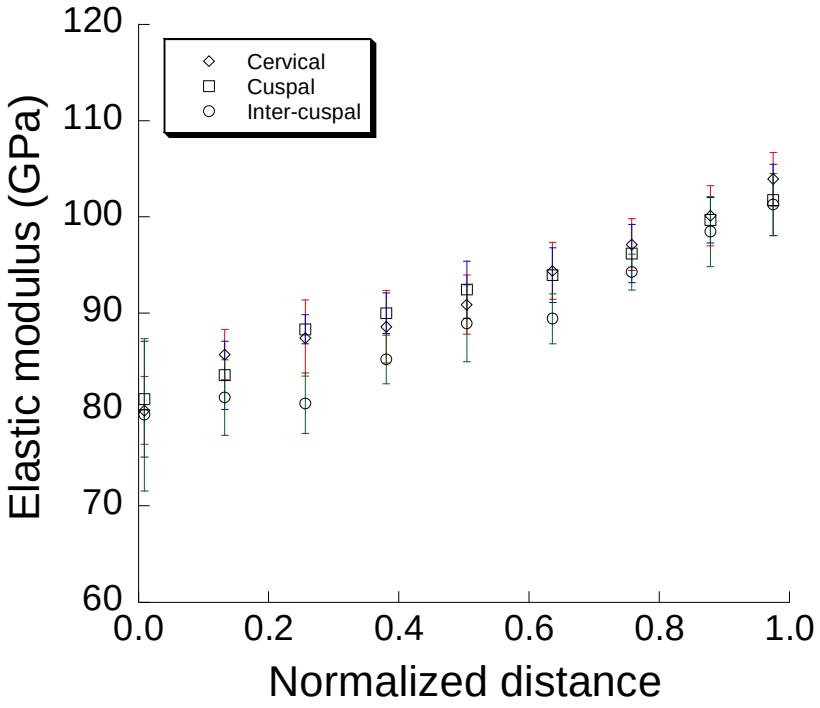

(a) Elastic modulus

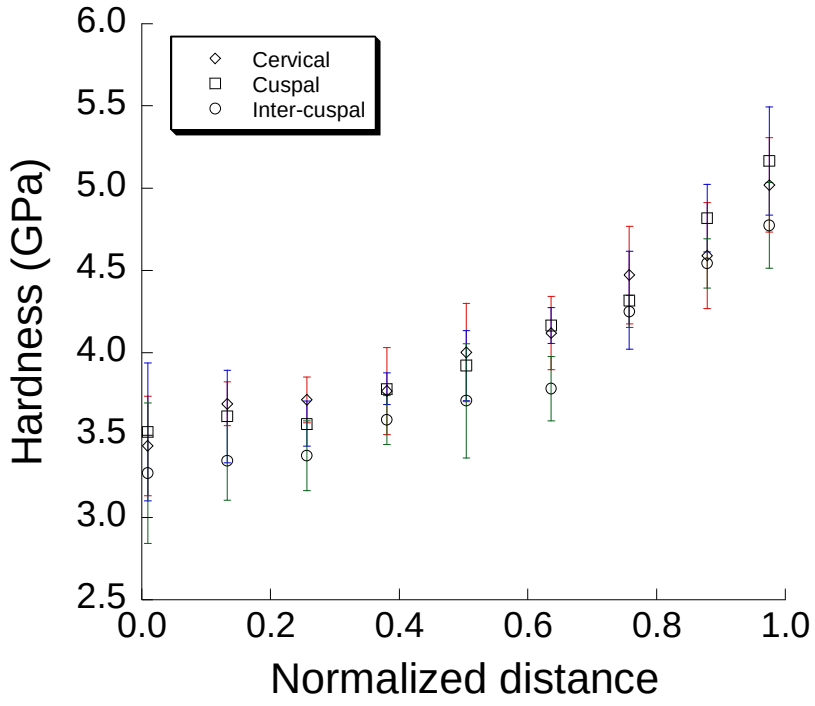

(b) Hardness

Figure A-3. Specimen #3 (57 years old, Female)

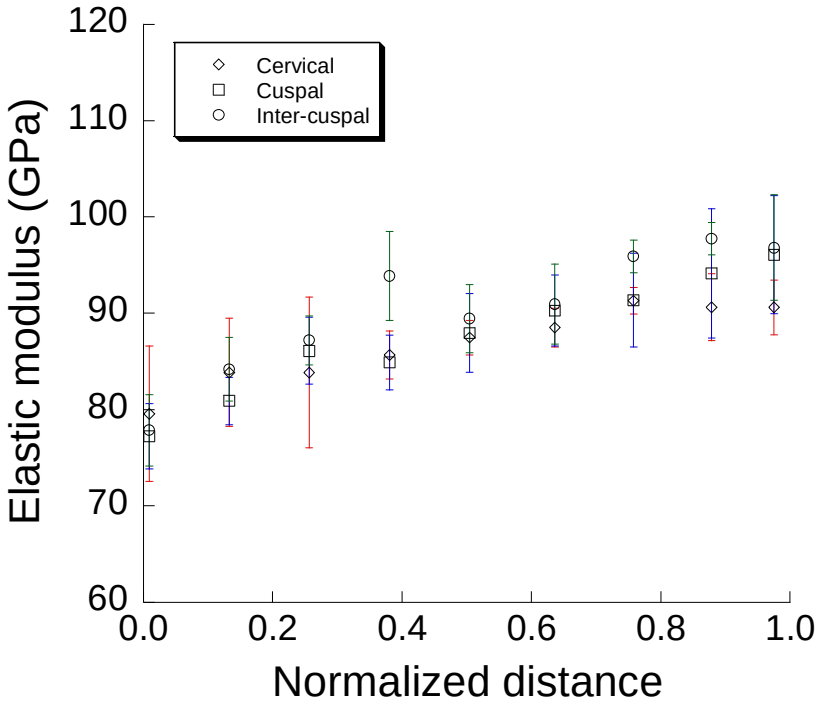

(a) Elastic modulus

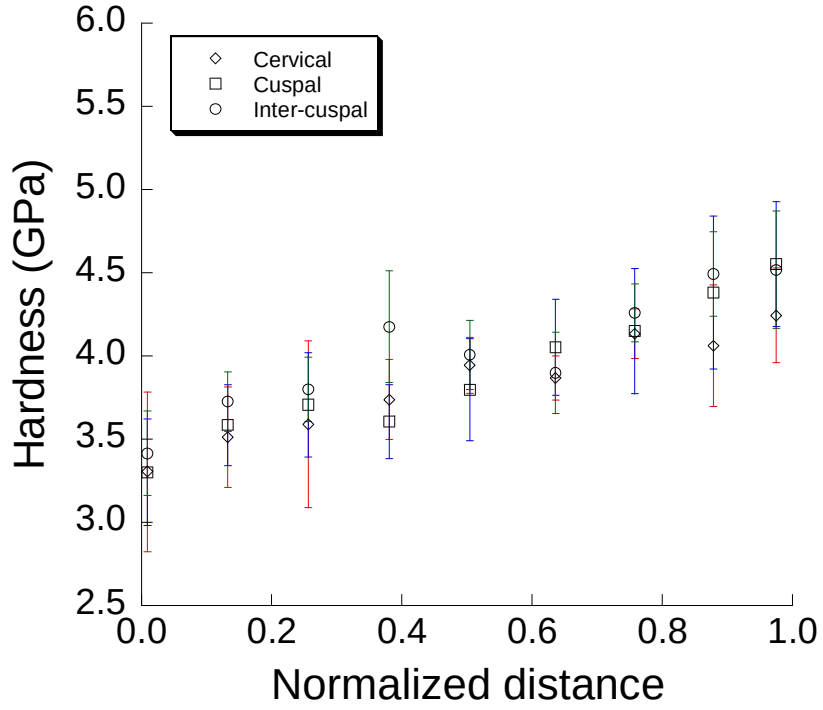

(b) Hardness

Figure A-4. Specimen #4 (59 years old, Male)

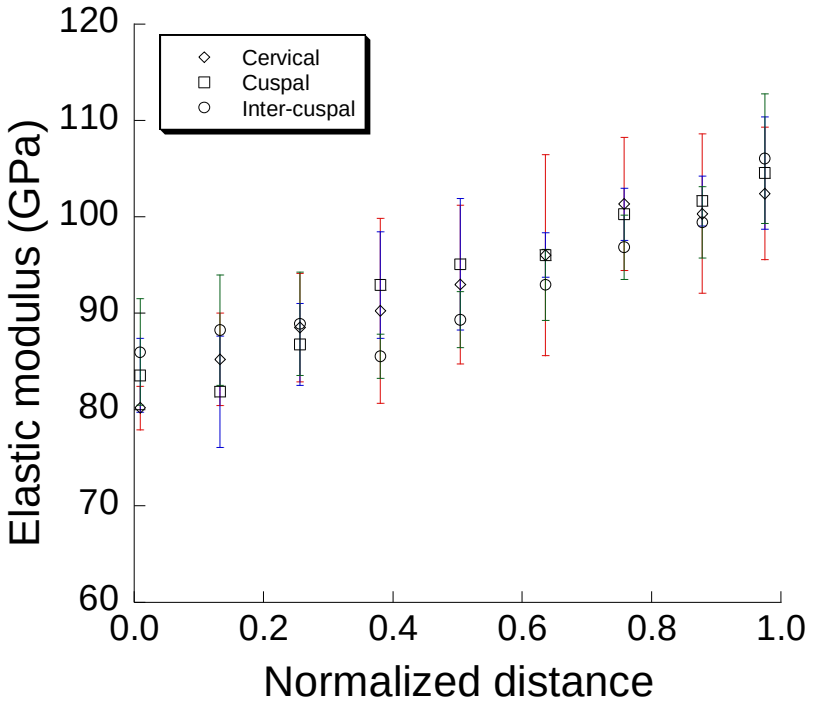

(a) Elastic modulus

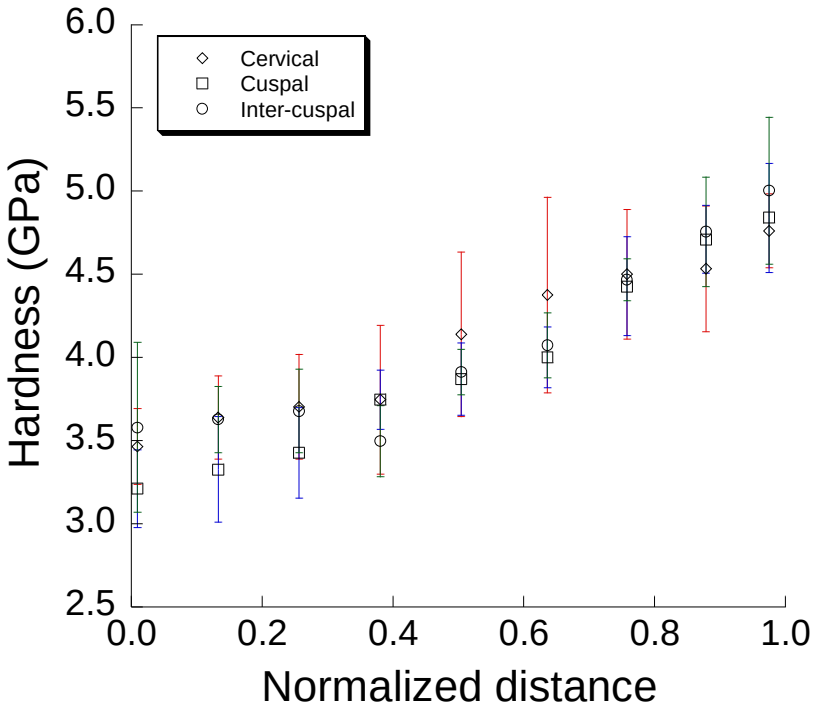

(b) Hardness

Figure A-5. Specimen #5 (92 years old, Female)

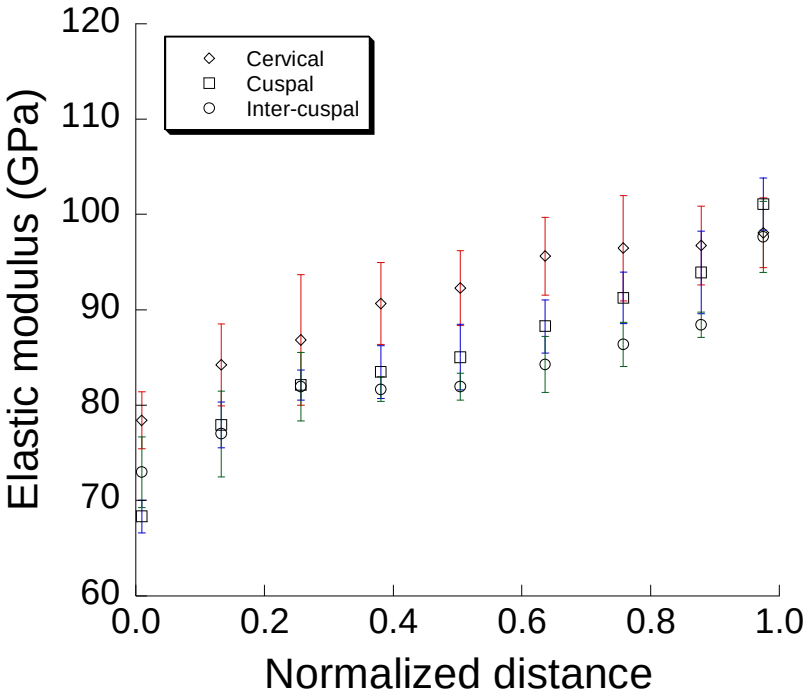

(a) Elastic modulus

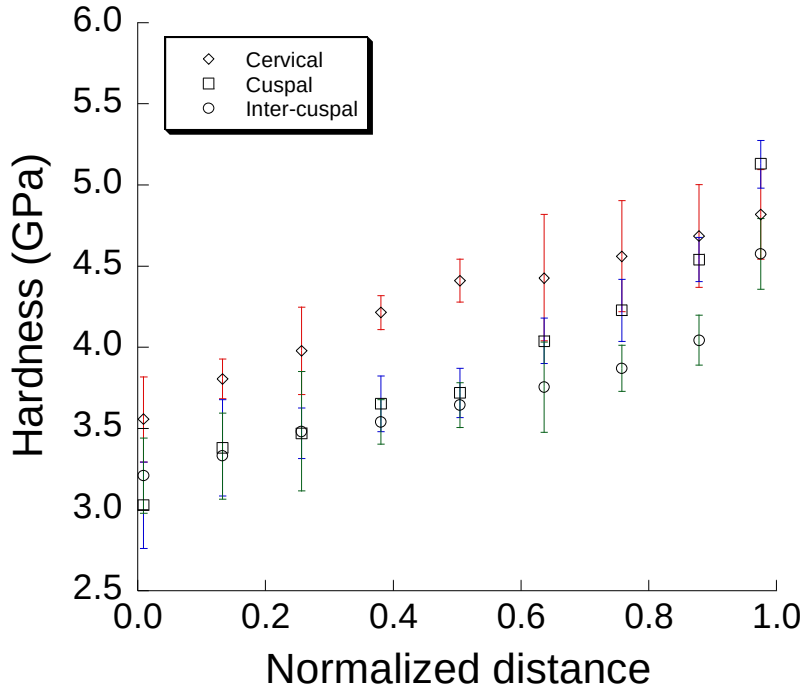

(b) Hardness

Figure A-6. Specimen #6 (81 years old, Male)

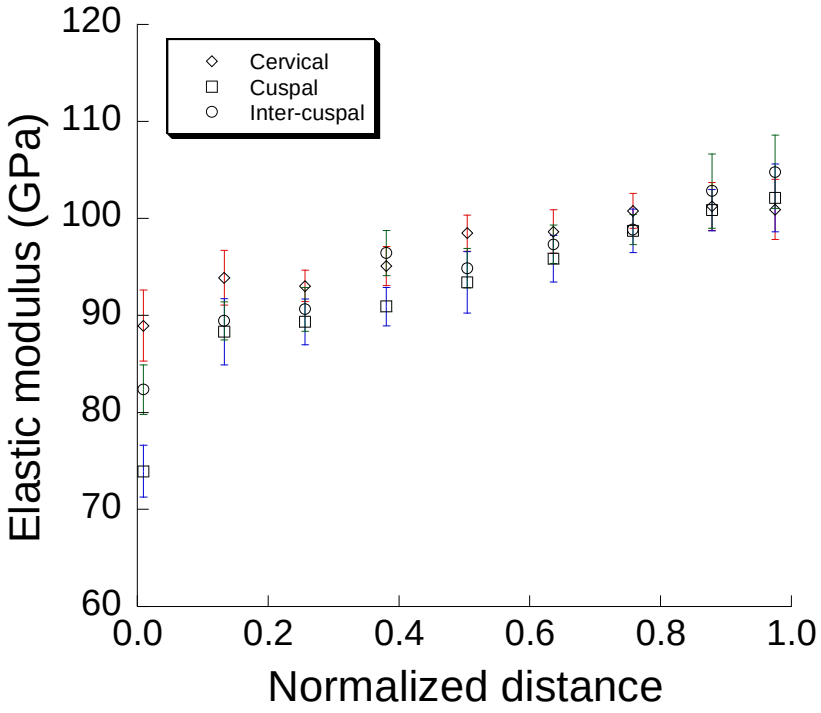

(a) Elastic modulus

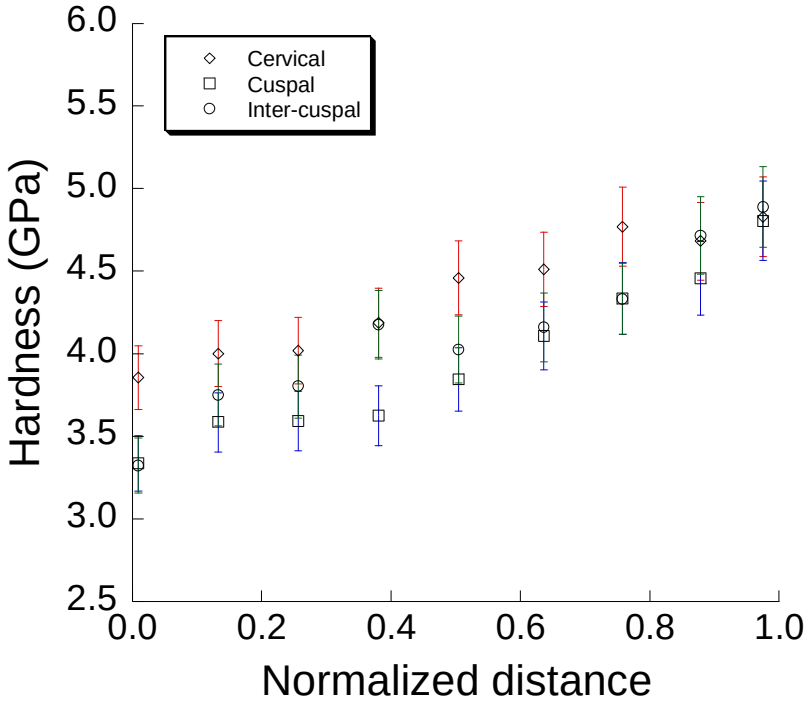

(b) Hardness

Figure A-7. Specimen #7 (68 years old, Male)

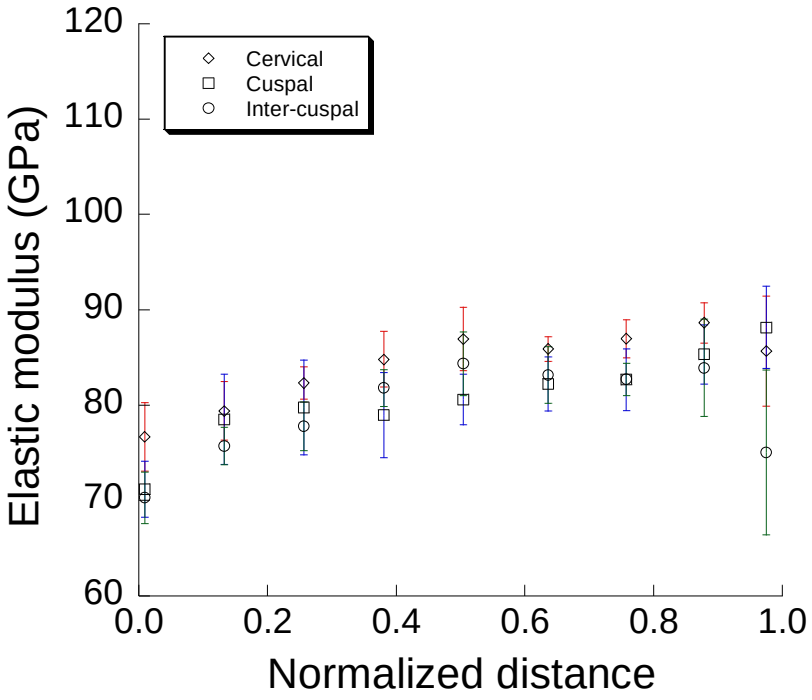

(a) Elastic modulus

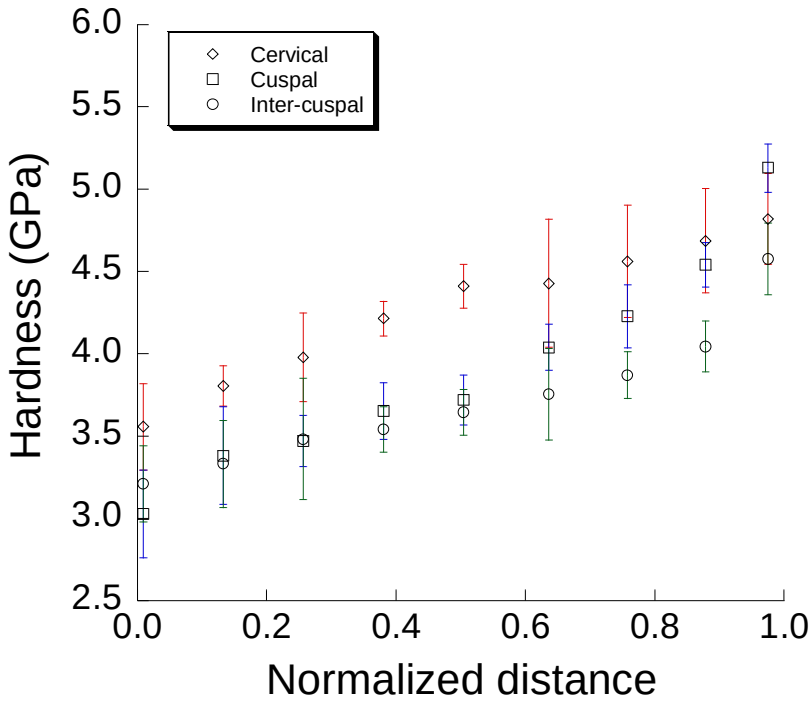

(b) Hardness

Figure A-8. Specimen #8 (18 years old, Male)

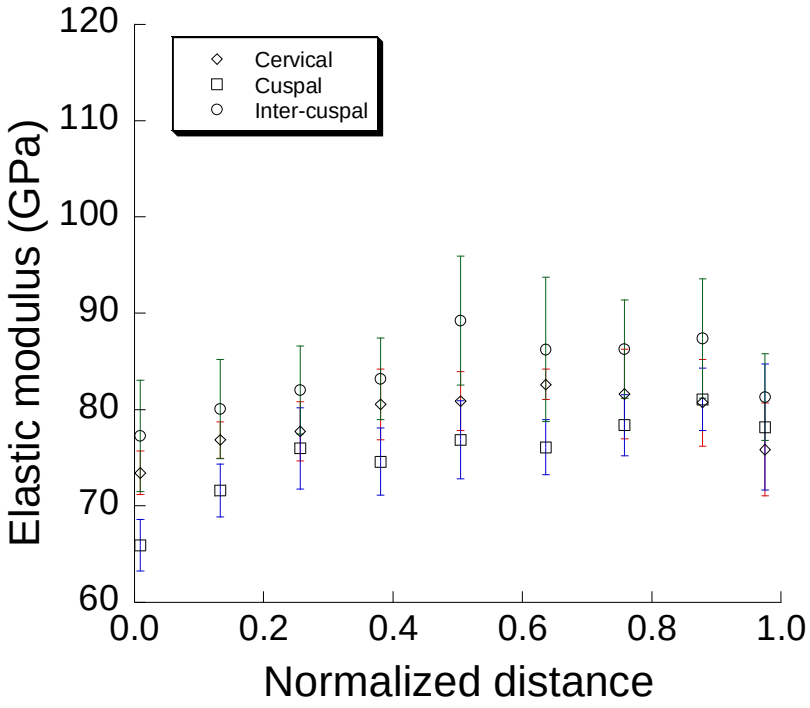

(a) Elastic modulus

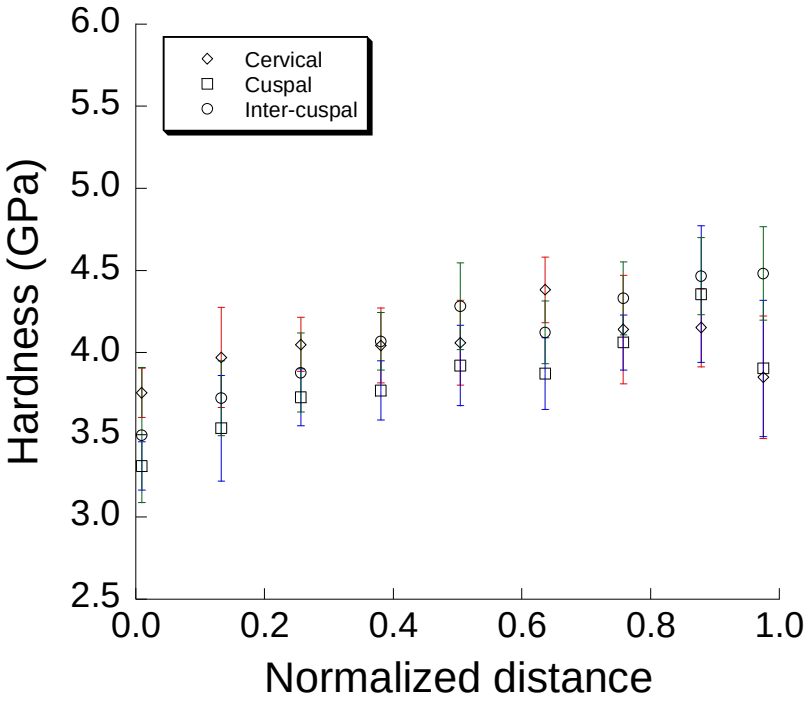

(b) Hardness

Figure A-9. Specimen #9 (19 years old, Female)

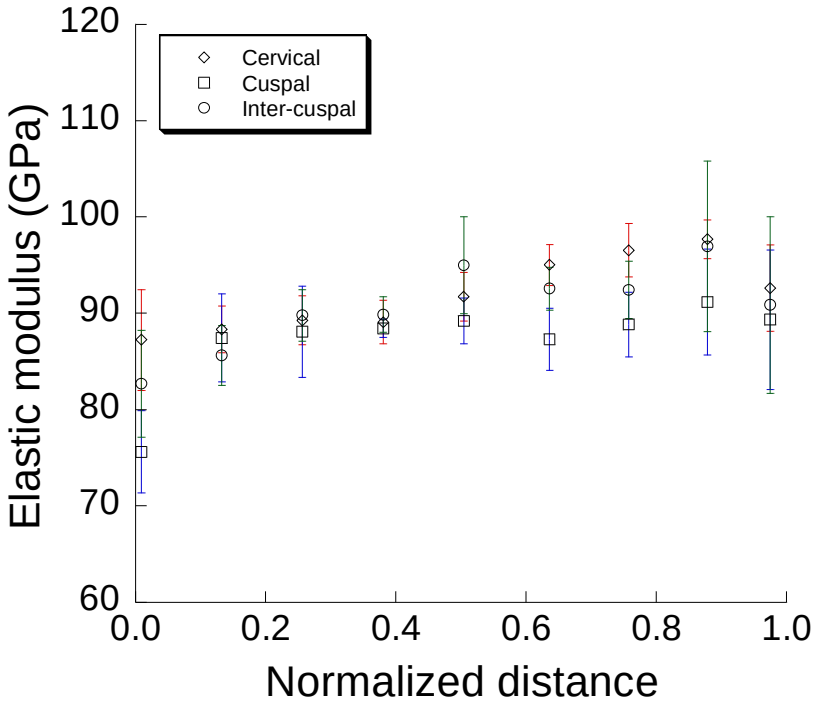

(a) Elastic modulus

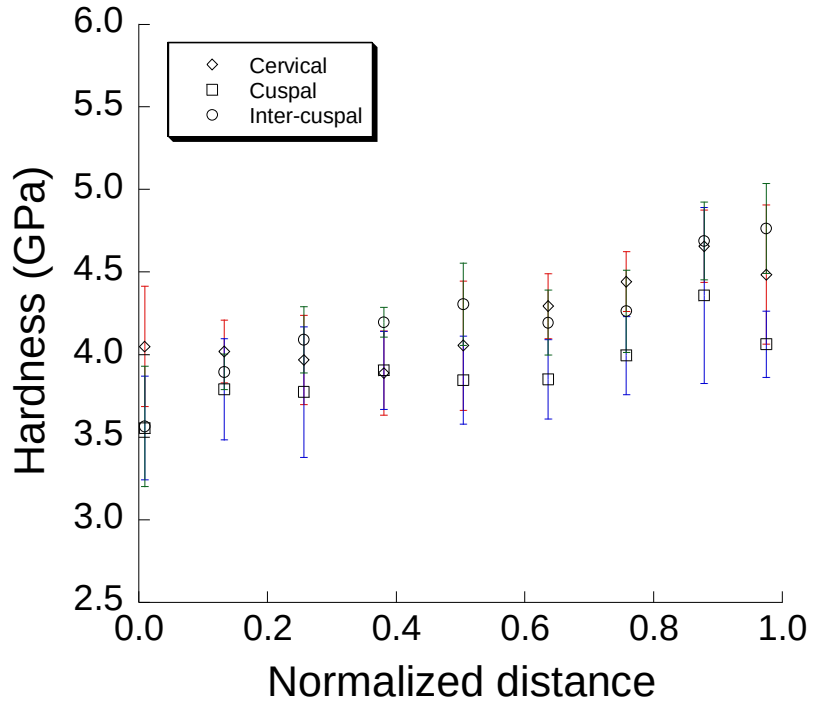

(b) Hardness

Figure A-10. Specimen #10 (22 years old, Female)

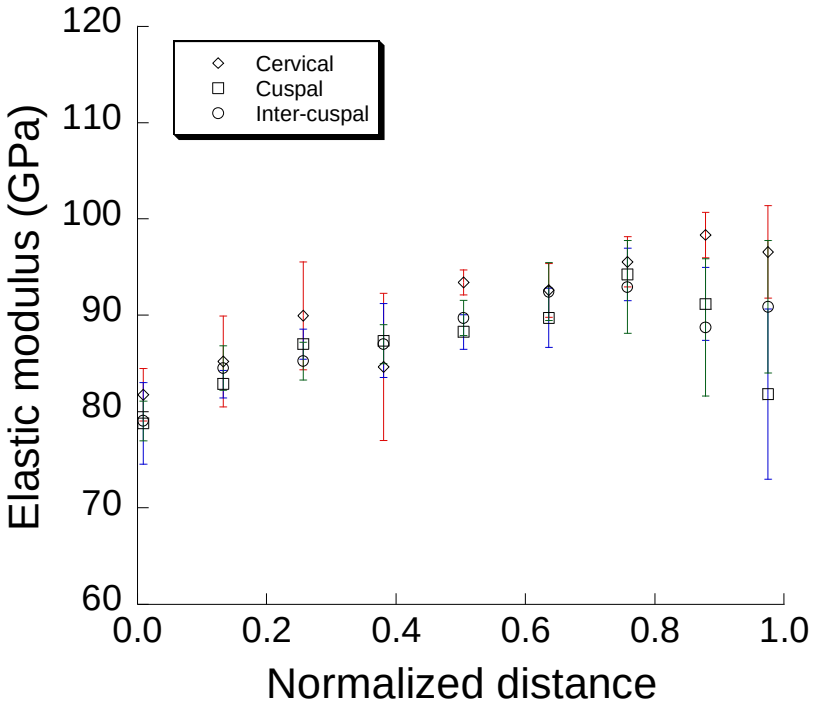

(a) Elastic modulus

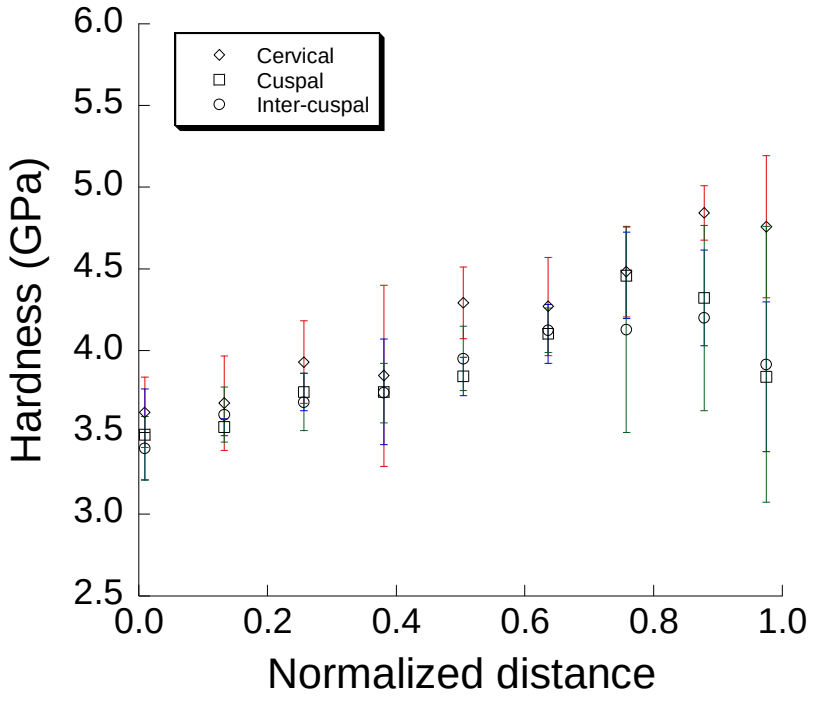

(b) Hardness

Figure A-11. Specimen #11 (23 years old, Male)

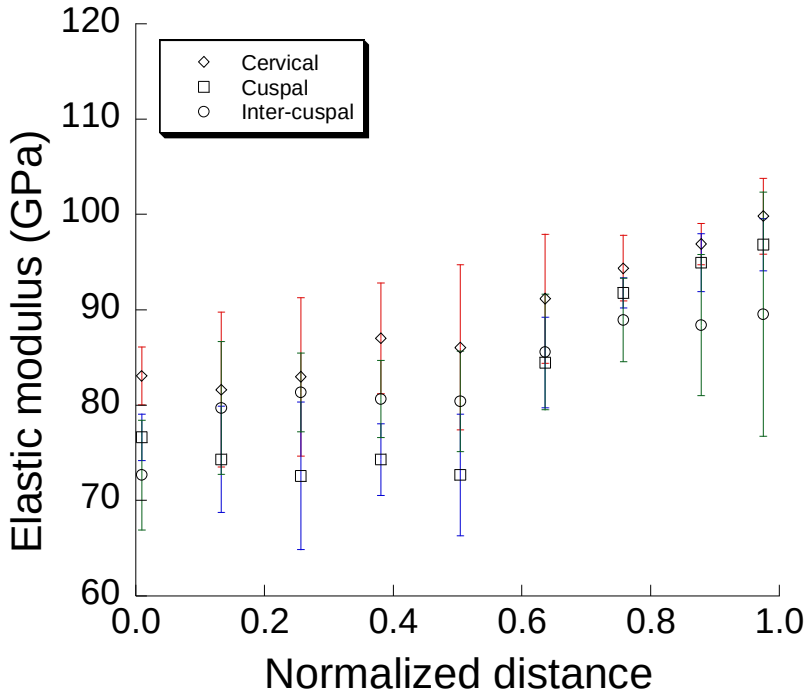

(a) Elastic modulus

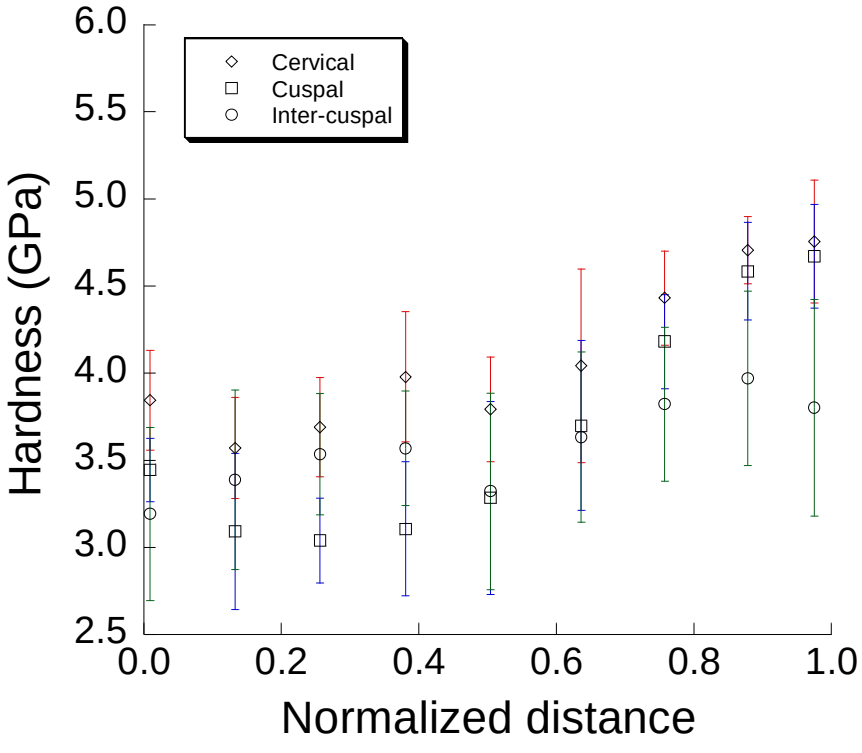

(b) Hardness

Figure A-12. Specimen #12 (21 years old, Female)

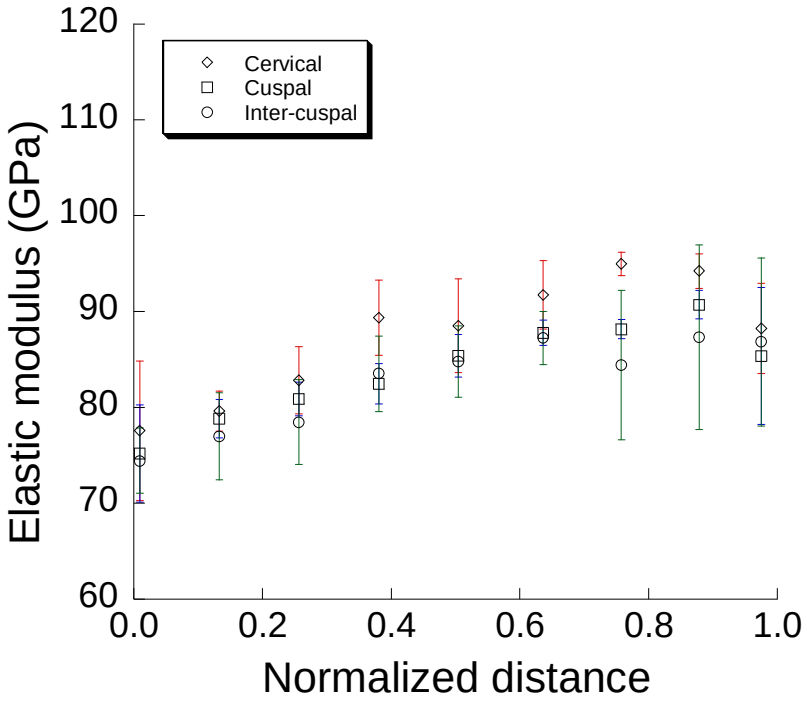

(a) Elastic modulus

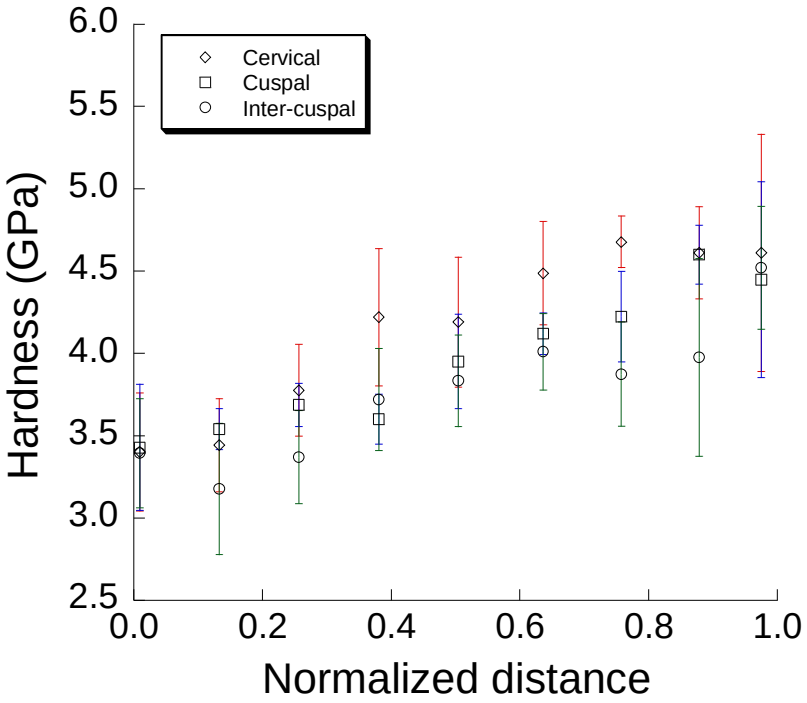

(b) Hardness

Figure A-13. Specimen #13 (27 years old, Male)

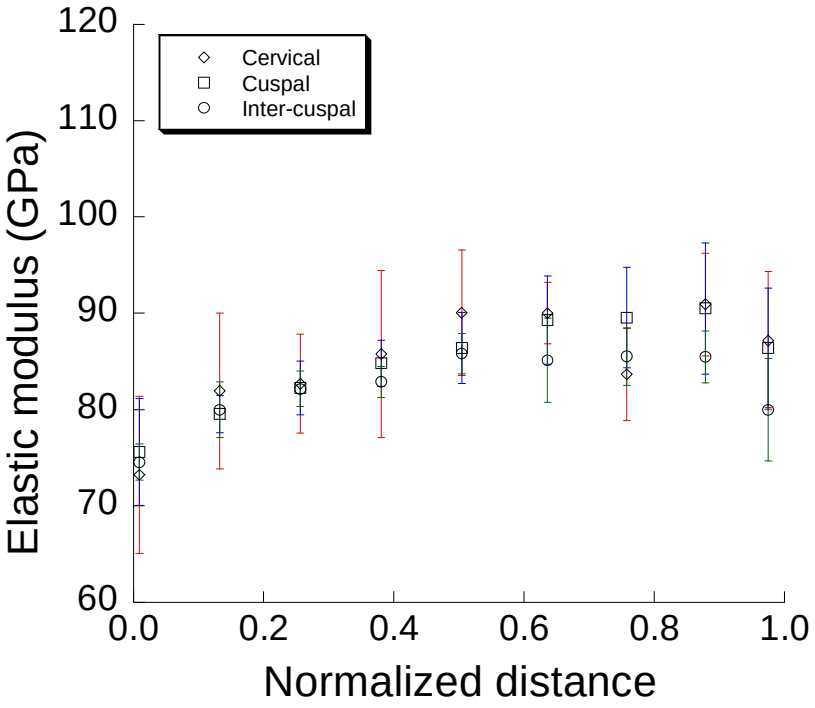

(a) Elastic modulus

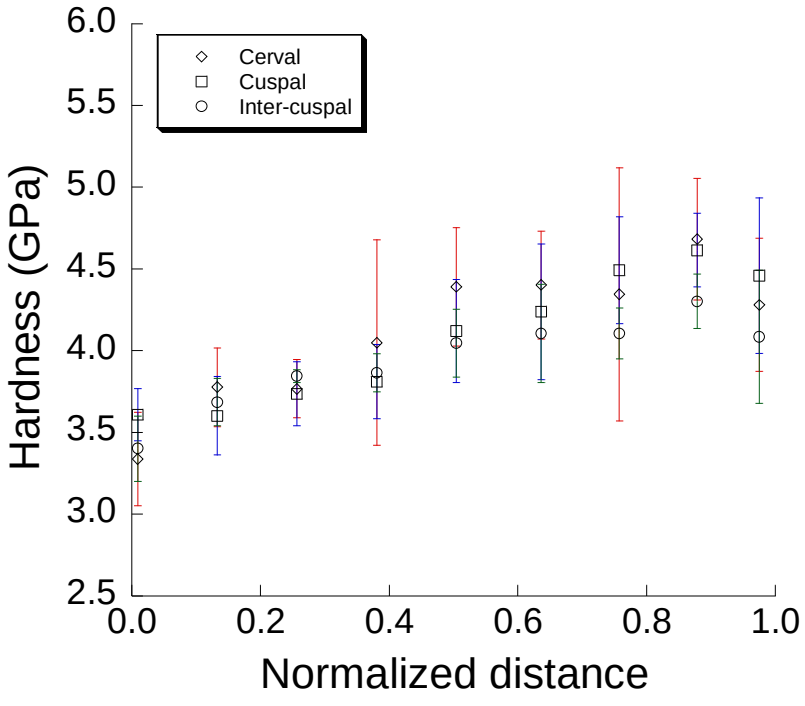

(b) Hardness

Figure A-14. Specimen #14 (29 years old, Female)

Appendix B

Apparent Fracture Toughness and Brittleness Number

N.D	A.F.T	S.T1	B.N	S.T2	c/L
0.03	0.80	0.05	355	47.60	0.85
0.15	0.82	0.09	369	84.71	0.80
0.27	0.80	0.05	411	50.24	0.89
0.38	0.78	0.04	455	45.06	0.83
0.50	0.83	0.09	430	94.80	0.78
0.62	0.87	0.03	405	22.95	0.73
0.74	0.87	0.04	428	40.47	0.76
0.85	0.74	0.04	619	57.00	0.99
0.97	0.87	0.00	444	0.00	0.60

Specimen #15 (21 years old, Male)

N.D	A.F.T	S.T1	B.N	S.T2	c/L
0.03	0.87	0.05	302	36.04	0.73
0.15	0.87	0.02	322	13.07	0.72
0.27	1.00	0.05	261	28.05	0.58
0.38	0.94	0.05	314	32.27	0.66
0.50	0.93	0.03	335	23.70	0.68
0.62	0.90	0.06	383	52.84	0.79
0.74	0.82	0.03	485	36.94	0.97
0.85	0.79	0.05	549	75.69	1.01
0.97	0.97	0.18	371	136.67	0.42

Specimen #16 (25 years old, Female)

N.D	A.F.T	S.T1	B.N	S.T2	c/L
0.03	0.88	0.05	292	29.76	0.57
0.15	0.79	0.02	394	25.24	0.75
0.27	0.78	0.02	427	17.57	0.80
0.38	0.69	0.03	573	40.76	1.03
0.50	0.76	0.03	498	46.43	0.88
0.62	0.75	0.05	545	73.03	0.92
0.74	0.78	0.07	544	96.86	0.92
0.85	0.83	0.04	500	53.95	0.77
0.97	1.02	0.04	319	23.76	0.35

Specimen #17 (18 years old, Male)

N.D	A.F.T	S.T1	B.N	S.T2	c/L
0.03	0.85	0.08	317	50.96	0.59
0.15	0.81	0.02	373	19.81	0.70
0.27	0.79	0.06	414	58.83	0.77
0.38	0.85	0.02	375	19.29	0.65
0.50	0.84	0.03	413	28.31	0.71
0.62	0.86	0.02	416	19.43	0.72
0.74	0.85	0.05	450	54.99	0.77
0.85	0.90	0.05	423	47.84	0.73
0.97	0.95	0.07	371	56.53	0.49

Specimen #18 (20 years old, Female)

N.D	A.F.T	S.T1	B.N	S.T2	c/L
0.03	0.97	0.09	246	47.48	0.60
0.19	0.95	0.06	274	30.97	0.59
0.34	0.89	0.02	343	17.58	0.64
0.50	0.86	0.11	414	125.39	0.79
0.66	0.88	0.04	398	33.21	0.70
0.81	0.85	0.04	462	45.83	0.82
0.97	0.98	0.11	354	82.52	0.45

Specimen #19 (21years old, Male)

N.D: Normalized Distance

A.F.T: Apparent Fracture Toughness

B.N: Brittleness Number

S.T1: Standard Deviation of A.F.T

S.T2: Standard Deviation of B.N

c/L: Ratio of Crack Length over Diagonal Length Indentation

N.D	A.F.T	S.T1	B.N	S.T2	c/L
0.03	0.76	0.05	398	49.20	1.08
0.16	0.85	0.03	346	22.15	0.77
0.30	0.76	0.04	477	46.90	0.94
0.43	0.75	0.02	549	35.46	1.01
0.57	0.79	0.04	534	54.07	0.90
0.70	0.82	0.05	546	63.24	0.87
0.84	0.80	0.02	628	40.09	0.92
0.97	0.75	0.03	636	46.87	0.90

Specimen #20 (74 years old, Female)

N.D	A.F.T	S.T1	B.N	S.T2	c/L
0.03	0.92	0.04	267	24.74	0.48
0.16	0.85	0.04	349	34.53	0.59
0.30	0.81	0.04	420	39.53	0.68
0.43	0.69	0.06	661	115.34	1.01
0.57	0.73	0.06	631	103.40	0.92
0.70	0.68	0.03	802	78.46	1.20
0.84	0.74	0.05	726	101.43	1.01
0.97	0.70	0.02	875	58.00	1.30

Specimen #21 (50 years old, Male)

N.D	A.F.T	S.T1	B.N	S.T2	c/L
0.03	0.82	0.02	334	14.53	0.78
0.19	0.79	0.03	410	33.87	0.89
0.34	0.78	0.04	470	47.94	0.95
0.50	0.70	0.05	654	96.65	1.15
0.66	0.64	0.11	924	297.23	1.40
0.81	0.66	0.11	951	296.97	1.43
0.97	0.66	0.17	1160	571.27	1.41

Specimen #22 (74 years old, Male)

N.D	A.F.T	S.T1	B.N	S.T2	c/L
0.03	0.83	0.06	334	50.97	0.59
0.16	0.84	0.10	365	99.52	0.68
0.30	0.83	0.05	406	52.22	0.73
0.43	0.81	0.05	474	73.35	0.81
0.57	0.81	0.08	515	99.87	0.79
0.70	0.77	0.05	666	13.87	0.85
0.84	0.75	0.04	719	93.01	0.92
0.97	0.68	0.06	943	171.82	1.19

Specimen #23 (68 years old, Male)

N.D	A.F.T	S.T	B.N	S.T	c/L
0.03	0.83	0.04	327	29.74	0.72
0.22	0.75	0.05	463	69.40	0.86
0.41	0.65	0.09	732	209.92	1.22
0.59	0.66	0.05	797	122.87	1.14
0.78	0.63	0.04	969	125.66	1.24
0.97	0.51	0.00	1674	0.00	2.00

Specimen #24 (78 years old, Male)

N.D: Normalized Distance

A.F.T: Apparent Fracture Toughness

B.N: Brittleness Number

S.T1: Standard Deviation of A.F.T

S.T2: Standard Deviation of B.N

c/L: Ratio of Crack Length over Diagonal Length Indentation

REFERENCES

Arola DD, Reprogel RK. Effects of aging on the mechanical behavior of human dentin. *Biomaterials*. 2005:26(18):4051-61.

Arola DD, Rouland JA, Zhang D. Fatigue and fracture of bovine dentin. *Experimental Mechanics*. 2002:42:380-88.

Bajaj D, Sundaram N, Nazari A, Arola D. Age, dehydration and fatigue crack growth in dentin. *Biomaterials*. 2006:27(11):2507-17.

Balooch G, Marshall GW, Marshall SJ, Warren OL, Asif SA, Balooch M. Evaluation of a new modulus mapping technique to investigate microstructural features of human teeth. *Journal of Biomechanics*. 2004:37(8):1223-32.

Barbour M.E, Parker D.M, Jandt K.D, Enamel dissolution as a function of solution degree of saturation with respect to hydroxyapatite: A nanoindentation study. *Journal of Colloid and Interface Science*. 2003:265:9-14

Berkey D, Berg R. Geriatric oral health issues in the United States. *International Dental Journal*. 2001:21:141-6

Bertacci A, Chersoni S, Davidson C.L, Prati C. In vivo enamel fluid movement. *European Journal of Oral Sciences*. 2007:115:169-73.

Blatz M. The faculty perspective. The clinical long-term success of ceramic restorations—Part II: posterior full-coverage crowns. *Practical Procedures Aesthetic Dentistry*. 2004:16(10):702.

Braly A, Darnell LA, Mann AB, Teaford MF, Weihs TO. The effect of prism orientation on the indentation testing of human molar enamel. *Archives of Oral Biology*. 2007:52: 856 – 60.

Bulman E. Tooth Decay Afflicts 4 Out Of 5. The Associated Press, GENEVA, Feb. 24, 2004.

Cameron C.E. Cracked tooth syndrome. *Journal of American Dental Association*. 1964:68:405-11.

Collys K, Slop D, Cleymaet R, Coomans D, Michotte Y. Load dependency and reliability of microhardness measurements on acid-etched enamel surfaces. *Dental Materials*. 1992:8(5):332-5.

Craig RG, Peyton FA. The microhardness of enamel and dentin. *Journal of Dental Research*. 1957:37(4):661-8.

Craig RG, Peyton FA, Johnson DW. Compressive properties of enamel, dental cements, and gold. *Journal of Dental Research*. 1961:40(5):936-45.

Cuy JL, Mann AB, Livi KJ, Teaford MF, Weihs TP. Nanoindentation mapping of the mechanical properties of human molar tooth enamel. *Archives of Oral Biology*. 2002:47(4):281-91.

El Mowafy OM, Watts DC, Fracture toughness of human dentin. *Journal of Dental Research*.1986:65:677-81.

Elderton RJ. The cause of failure of restorations: A literature review. *Journal of Dentistry*. 1976:14:257-62.

Ge J, Cui FZ, Wang XM, Feng HL. Property variations in the prism and the organic sheath within enamel by nanoindentation. *Biomaterials.* 2005:26(16):3333-9.

Habelitz S, Marshall G.W, Balooch M, Marshall SJ. Nanoindentation and storage of teeth. *Journal of Biomechanics*. 2002:35:995-8.

Habelitz S, Marshall SJ, Marshall GW Jr, Balooch M. Mechanical properties of human dental enamel on the nanometre scale. *Archives of Oral Biology*. 2001:46(2):173-83.

Hassan R, Caputo AA, Bunshah RF. Fracture toughness of human enamel. *Journal of Dental Research*. 1981:60(4):820-7.

He LH, Swain MV. Understanding the mechanical behavior of human enamel from its structural and compositional characteristics. *Journal of the Mechanical Behavior of Biomedical Materials*. 2008:1(1):18-29.

He LH, Swain MV. Influence of environment on the mechanical behaviour of mature human enamel. *Biomaterials*. 2007:28(30):4512-20.

He LH, Swain MV. Energy absorption characterization of human enamel using nanoindentation. *Journal of Biomedical Materials Research*. 2007:81(2):484-92.

He LH, Fujisawa N, Swain MV. Elastic modulus and stress-strain response of human enamel by nano-indentation. *Biomaterials*. 2006:27(24):4388-98.

Ichijo T, Yamashita Y, Terashima T. Observations on structural features and characteristics of biological apatite crystals. 7. Observation on lattice imperfection of human tooth and bone crystals II. The Bulletin of Tokyo Medical and Dental University. 1993:40(4):193-205.

Imbeni V, Kruzic J.J, Marshall GW, Marshall SJ, Ritchie RO. The dentin-enamel junction and the fracture toughness of human teeth. *Nature Materials*. 2005:4(3):229-32.

Issac M, Ori I. Engineering Mechanics of Composite Materials,2nd ed., Oxford University Press, Inc., 2006.

Kim JW, Bhowmick S, Chai H, Lawn BR. Role of substrate material in failure of crown-like layer structures. *Journal of Biomedical Materials Research, Part B: Applied Biomaterials*. 2007:81(2):305-11.

Kinney JH, Nalla RK, Pople JA, Breunig TM, Ritchie RO. Age-related transport root dentin: mineral concentration, crystallite size, and mechanical properties. *Biomaterials*. 2005:26:3363-76.

Koester KJ, Ager JW 3rd, Ritchie RO. The effect of aging on crack-growth resistance and toughening mechanisms in human dentin. *Biomaterials*. 2008:29(10):1318-28.

Kolker JL, Damiano PC, Armstrong SR, Bentler SE, Flach SD, Caplan DJ, Warren JJ, Kuthy RA, Dawson DV, Jones MP. Natural history of treatment outcomes for teeth with large amalgam and crown restorations. *Operative Dentistry*. 2004:29(6):614-22.

Lester KS, Boyde A. Relating developing surface to adult ultrastructure in chiropteran Enamel by SEM. *Advances Dental Research*. 1987:1(2):181-90.

Low IM, Duraman N, Mahmood U, Mapping the structure, composition and mechanical properties of human teeth. *Materials Science and Engineering*. 2008:28:243-7.

Lynch RJM, Ten Cate JM. The effect of adjacent dentine blocks on the demineralisation and remineralization of enamel in vitro. *Caries Research*. 2006:40(1):38-42.

Mahoney E, Holt A, Swain M, Kilpatrick N. The hardness and modulus of elasticity of primary molar teeth: An ultra-micro-indentation study. *Journal of Dentistry*. 2000:28:589-94.

Marshall GW, Balooch M, Gallagher RR, Gansky SA, Marshall SJ. Mechanical properties of the dentinoenamel junction: AFM studies of nanohardness, elastic modulus, and fracture. *Journal of Biomedical Materials Research*. 2001:54:87-95.

Moore D, Stewart J. Prevalence of defective dental restoration. *Journal of Prosthetic Dentistry*. 1967:17:372-8.

Meredith N, Sherriff M, Setchell DJ, Swanson SA. Measurement of the microhardness and Young's modulus of human enamel and dentine using an indentation technique. *Archives of Oral Biology*. 1996:41(6):539-45.

National Institutes of Health (U.S.). Diagnosis and management of dental caries throughout life. NIH Consensus Statement. 2001:18:1-23.

Niihara K, Morena R and Hasselman DPH. Evaluation of KIC of brittle solids by the indentation method with low crack to indent ratios. *Journal of Materials Science Letters.*1982:1:13-6.

Oliver WC and Pharr GM. An improved technique for determining hardness and elastic modulus using load and displacement sensing indentation experiments. *Journal of Materials Research.* 1992:**7**(6):1564-83.

Peterson IM, Wuttiphan S, Lawn BR, Chyung K. Role of microstructgure on contact damage and strength degradation of micaceous glasspceramics. *Dental Materials*. 1998:14(1):80-9.

Peterson IM, Pajares A, Lawn BR, Thompson VP, Rekow ED. Mechanical characterization of dental ceramics by hertzian contacts. *Journal of Dental Research.* 1998:77(4):589-602.

Quinn GD and Bradt RC. On the Vickers indentation fracture toughness test. *Journal of American Ceramic Society*. 2007:90(3):673–80.

Quinn JB, Quinn GD, Kelly JR, Scherrer SS. Fractographic analyses of three ceramic whole crown restoration failures. *Dental Materials*. 2005:21(10):920-9.

Quinn JB, Sundar V and Lloyd IK. Influence of microstructure and chemistry on the fracture toughness of dental ceramics. *Dental Materials*. 2003:19:603-11.

Quinn JB and Quinn GD. Indentation brittleness of ceramics: a fresh approach. *Journal of Materials Science*. 1997:32(16): 4331-46.

Quinn JB and Quinn GD. On the hardness and brittleness of ceramics. *Key Engineering Materials*. 1997:132-136:460-3.

Rasmussen ST, Patchin RE, Scott DB, Heuer AH. Fracture properties of human enamel and dentin. *Journal of Dental Materials*. 1976:55:154-64.

Ritchie, RO, Kinney, JH, Kruzic, JJ, Nalla, RK. A fracture mechanics and mechanistic approach to the failure of cortical bone. *Fatigue & Fracture of Engineering Materials & Structures*. 2005:28(4):345-71.

Robinson C, Kirkham, J, and Brookes SJ, and Shore RC. Chemistry of mature enamel. In Dental Enamel: Formation to Destruction. ed. C. Robinson, J. Kirkham and R. Shore, CRC Press. 1995:167-91.

Scherrer SS, Quinn JB, Quinn GD, Kelly JR. Failure analysis of ceramic clinical cases using qualitative fractography. *International Journal of Prosthodontics*. 2006:19(2):185-92.

Schwartz RS, Summitt JB, Robbins JW. Fundamental of operative dentistry: A contemporary approach. Quintessence Publishing Co. Inc., Chicago, 1996.

Skobe Z, Stern S. The pathway of enamel rods at the base cusps of human teeth. *Journal of Dental Research*. 1980:59(6):1026-32.

Spears I.R. A three-dimensional finite element model of prismatic enamel: a re-appraisal of the data on the Young's modulus of enamel. *Journal of Dental Research*.1997:76(10):1690-7.

Staines M, Robinson WH, and Hood JAA. Spherical indentation of tooth enamel. *Journal of Material Science.* 1981:16(9):2551-6.

Stanford J.W, Paffenbarger G.C, Kumpula J.W, Sweeney W.T, Determination of some compressive properties of human enamel and dentin. *The Journal of the American Dental Association*. 1958:57:487-96.

Summitt JB, Robbins JW, Schwartz R. Fundamental of operative dentistry: A contemporary approach, 2nd edition. Quintessence Publishing Co. Inc., Chicago, 2001.

Ten Cate, AR. Oral Histology: Development, Structure, and Function, 5th edition, Saint Louis: Mosby-Year Book. 1998.

Walton RE, Rotstein I, "Bleaching of discoloured teeth: Internal and external. In: Walton R.E, Torabinejad M. (Eds.), Principles and Practice of Endodontics, 2nd edition. W.B. Saunders, Philadelphia. 1996:385-400.

Waters NE. Some mechanical and physical properties of teeth. In: Vincent J, Curry J, editors. The mechanical properties of biological materials. Cambridge University Press: 1980:99-134.

White B, Albertini T, Brown L, Larach-Robinson D, Redford M, Selwitz R. Selected restoration and tooth conditions: United States. *Journal of Dental Research.* 1996:75:661-671.

White SN, Luo W, Paine ML, Fong H, Sarikaya M, Snead ML. Biological organization of hydroxyapatite crystallites into a fibrous continuum toughens and controls anisotropy in human enamel. *Journal of Dental Research*. 2001:80(1):321-6.

Willems G, Celis JP, Lambrechts P, Braem M, Vanherle G. Hardness and Young's modulus determined by nanoindentation technique of filler particles of dental restorative materials compared with human enamel. *Journal of Biomedical Materials Research*. 1993:27(6):747-55.

Wilson NH, Burke FJT, Mjor IA. Reasons for placement and replacement of restorations of direct restorative materials by a selected group of practitioners in the UK. *Quintessence International*. 1997:28(4):245-8.

Xu HH, Smith DT, Jahanmir S, Romberg E, Kelly JR, Thompson VP, Rekow ED. Indentation damage and mechanical properties of human enamel and dentin. *Journal of Dental Research*. 1998:77(3):472-80.

Yio JG, Lee KS and Lawn BR. Role of microstructure in dynamic fatigue of glass-ceramics after contact with spheres. *Journal of American Ceramic Society*. 2000:83(6):1545-7.

Zhou J, Hsiung L.L. Depth-dependent mechanical properties of enamel by nanoindentation. *Journal of Biomedical Materials Research*. 2007:Part A.81 A(1):66-74.

Zhang Y, Lawn BR, Malament KA, Van Thompson P, Rekow ED. Damage accumulation and fatigue life of particle-abraded ceramics. *International Journal of Prosthodontics*. 2006:19(5):442-8.

Zhang Y, Song JK, Lawn BR. Deep-penetrating conical cracks in brittle layers from hydraulic cyclic contact. *Journal of Biomedical Materials Research, Part B: Applied Biomaterials*. 2005:73(1):186-93.